



Pacemaker Channels and the Chronotropic Response in Health and Disease

Konstantin Hennis¹, Chiara Piantoni¹, Martin Biel, Stefanie Fenske^{1*}, Christian Wahl-Schott^{1*}

ABSTRACT: Loss or dysregulation of the normally precise control of heart rate via the autonomic nervous system plays a critical role during the development and progression of cardiovascular disease—including ischemic heart disease, heart failure, and arrhythmias. While the clinical significance of regulating changes in heart rate, known as the chronotropic effect, is undeniable, the mechanisms controlling these changes remain not fully understood. Heart rate acceleration and deceleration are mediated by increasing or decreasing the spontaneous firing rate of pacemaker cells in the sinoatrial node. During the transition from rest to activity, sympathetic neurons stimulate these cells by activating β -adrenergic receptors and increasing intracellular cyclic adenosine monophosphate. The same signal transduction pathway is targeted by positive chronotropic drugs such as norepinephrine and dobutamine, which are used in the treatment of cardiogenic shock and severe heart failure. The cyclic adenosine monophosphate-sensitive hyperpolarization-activated current (I_h) in pacemaker cells is passed by hyperpolarization-activated cyclic nucleotide-gated cation channels and is critical for generating the autonomous heartbeat. In addition, this current has been suggested to play a central role in the chronotropic effect. Recent studies demonstrate that cyclic adenosine monophosphate-dependent regulation of HCN4 (hyperpolarization-activated cyclic nucleotide-gated cation channel isoform 4) acts to stabilize the heart rate, particularly during rapid rate transitions induced by the autonomic nervous system. The mechanism is based on creating a balance between firing and recently discovered nonfiring pacemaker cells in the sinoatrial node. In this way, hyperpolarization-activated cyclic nucleotide-gated cation channels may protect the heart from sinoatrial node dysfunction, secondary arrhythmia of the atria, and potentially fatal tachyarrhythmia of the ventricles. Here, we review the latest findings on sinoatrial node automaticity and discuss the physiological and pathophysiological role of HCN pacemaker channels in the chronotropic response and beyond.

Key Words: action potentials ■ autonomic nervous system ■ heart rate ■ myocytes, cardiac ■ sinoatrial node

A regular and rhythmic heartbeat is one of the most fundamental processes of life. Around embryonic day 36, the developing heart starts beating and the heartbeat does not stop until the person dies. Remarkably, the rhythmicity of cardiac contractions is controlled with high precision, making the normal heartbeat almost perfectly regular on palpation, with physiological baseline fluctuations known as heart rate variability.¹ This regularity persists even if the heart rate (HR) changes due to respiration or a change in activity level. The body's need for blood supply varies depending on physical exertion or emotional activity. To meet such varying demands,

cardiac output is mainly regulated by adjusting the HR, which, in turn, is controlled by the autonomic nervous system (ANS): increased activation of the sympathetic nervous system accelerates, while increased activation of the parasympathetic nervous system slows down the heart. This mechanism is termed chronotropic effect and enables smooth changes in HR, without rapid fluctuations or rhythm disturbances. Three components are associated with the chronotropic response, which are (1) the actual HR, (2) the variability of HR at a given time, and (3) the initiation site of pacemaker activity (Figure 1). When the activity state changes from rest to physical

Correspondence to: Stefanie Fenske, PhD, Department of Pharmacy, Center for Drug Research, Pharmacology for Natural Sciences, Ludwig-Maximilians-Universität München, Butenandtstr. 7, 81377 Munich, Germany, Email stefanie.fenske@cup.uni-muenchen.de; or Christian Wahl-Schott, MD, Institute of Cardiovascular Physiology and Pathophysiology, Biomedical Center Munich, Ludwig-Maximilians-Universität München, Großhaderner Str. 9, 82152 Munich, Germany, Email christian.wahlschott@med.uni-muenchen.de

*S. Fenske and C. Wahl-Schott contributed equally.

For Sources of Funding and Disclosures, see page 1370.

© 2024 The Authors. *Circulation Research* is published on behalf of the American Heart Association, Inc., by Wolters Kluwer Health, Inc. This is an open access article under the terms of the [Creative Commons Attribution Non-Commercial-NoDerivs](https://creativecommons.org/licenses/by-nc-nd/4.0/) License, which permits use, distribution, and reproduction in any medium, provided that the original work is properly cited, the use is noncommercial, and no modifications or adaptations are made.

Circulation Research is available at www.ahajournals.org/journal/res

Nonstandard Abbreviations and Acronyms

AC	adenylyl cyclase
AC1	adenylyl cyclase isoform 1
ADRB2	beta(2)-adrenergic receptor
ANS	autonomic nervous system
AP	action potential
CaM	calmodulin
CaMKII	Ca ²⁺ /calmodulin-dependent protein kinase II
cAMP	cyclic adenosine monophosphate
CDR	cyclic adenosine monophosphate-dependent regulation
CHF	chronic heart failure
HCN channel	hyperpolarization-activated cyclic nucleotide-gated cation channel
HR	heart rate
LCR	local calcium release
MDP	maximum diastolic potential
NCX1	sodium-calcium exchanger 1
PDE	phosphodiesterase
PKA	protein kinase A
SAN	sinoatrial node
SDD	slow diastolic depolarization
SK	small-conductance
SND	sinus node dysfunction
SR	sarcoplasmic reticulum

activity and back, all 3 parameters are changed by the ANS and need to be considered.

Another remarkable characteristic of cardiac physiology is the automaticity of the heart. The autonomous heartbeat is generated by specialized cardiac tissue in the heart itself, without the need for external stimulation. In this process, the sinoatrial node (SAN) acts as the primary pacemaker (Figure 1A and 1B). It is located in the right atrium of the heart,² with the central part (or head) of the node being localized caudally to the orifice of the superior caval vein (right superior caval vein in rodents). Laterally, it is limited by the crista terminalis, and, medially, it extends toward the interatrial septum. From the head region, the peripheral SAN (or tail) extends toward the inferior caval vein. The longitudinal axis of the SAN can be identified by the SAN artery, which runs in an axial direction through the head and tail and supplies blood to the SAN. The blood supply to the SAN is independent from that of the neighboring atrium and constitutes a selective blood-SAN barrier between the artery and the node. Functionally, the SAN contains specialized cardiomyocytes called pacemaker cells that spontaneously generate rhythmic action potentials (APs). These APs are also called pacemaker potentials (Figure 1D) and serve as the source of strictly timed electrical discharges that

propagate along the cardiac conduction system and ultimately trigger the contraction of all atrial and ventricular myocardial cells.³ The special ability of SAN pacemaker cells to generate spontaneous APs is enabled by slow diastolic depolarization (SDD; Figure 1D). During this phase of the pacemaker cycle, ion channels and transporters carry net inward currents that slowly depolarize the membrane until the voltage threshold for the next AP is reached. The slope of SDD, which is altered during the chronotropic response, and the repolarization velocity and AP duration determine the chronotropic state of the SAN and regulate the frequency of the heartbeat.^{4,5}

Intuitively, one would assume that all pacemaker cells in the SAN fire simultaneously and at the same frequency to generate a common network rhythm. However, recent research has shown that there are subdivisions of pacemaker cell regions within the SAN characterized by different firing rates.⁶ The region with the fastest firing frequency has been termed the leading pacemaker region of the SAN.^{7,8} The presence of a leading pacemaker region has been confirmed in the SAN of the mouse,⁹ rabbit,¹⁰ dog,¹¹ and human.¹² During HR acceleration on increased activation of the sympathetic nervous system, the leading pacemaker region shifts upwards, while during deceleration of HR on increased activation of the vagus nerve, it shifts downwards toward the atrioventricular junction^{7,8} (Figure 1B). Thus, the fastest HR is generated in a leading pacemaker region in the upmost part of the SAN, while the slowest HR arises in lower parts of the SAN. This observation has even led to the conclusion that instead of being described as the head and tail region of the SAN; at least in rats and humans, there are 2 competing right atrial pacemakers located near the superior vena cava (superior SAN) and near the inferior vena cava (inferior SAN)¹³ coinhabiting the SAN. This conclusion is further supported by a recent publication demonstrating that in mice, the microvasculature of the superior central SAN is more densely organized with more and closer contacts of capillaries to SAN pacemaker cells than the inferior peripheral SAN.⁶ Moreover, there is a sharp transition within the blood supply, which marks the border between the 2 parts of the SAN. This difference in the architecture of the microvasculature is also paralleled by the differential anatomy of autonomic inputs.¹⁴ There is evidence that in humans¹⁵⁻¹⁷ and goats,¹⁸ the SAN is surrounded by an extensive paranodal area with properties of both nodal and atrial tissues. This paranodal area has been proposed to adopt a role in pacemaking, which could explain the widespread distribution of the leading pacemaker site (wandering pacemaker) in the human right atrium as observed in clinics. Alternatively, it could facilitate the exit of APs from the SAN to the atrial muscle.¹⁷ To date, functional studies are lacking, and, therefore, the function of this area remains unclear.¹⁷ In addition to the SAN and possibly as part of the paranodal area, in rats,^{19,20} dogs,^{21,22} and humans²³ an

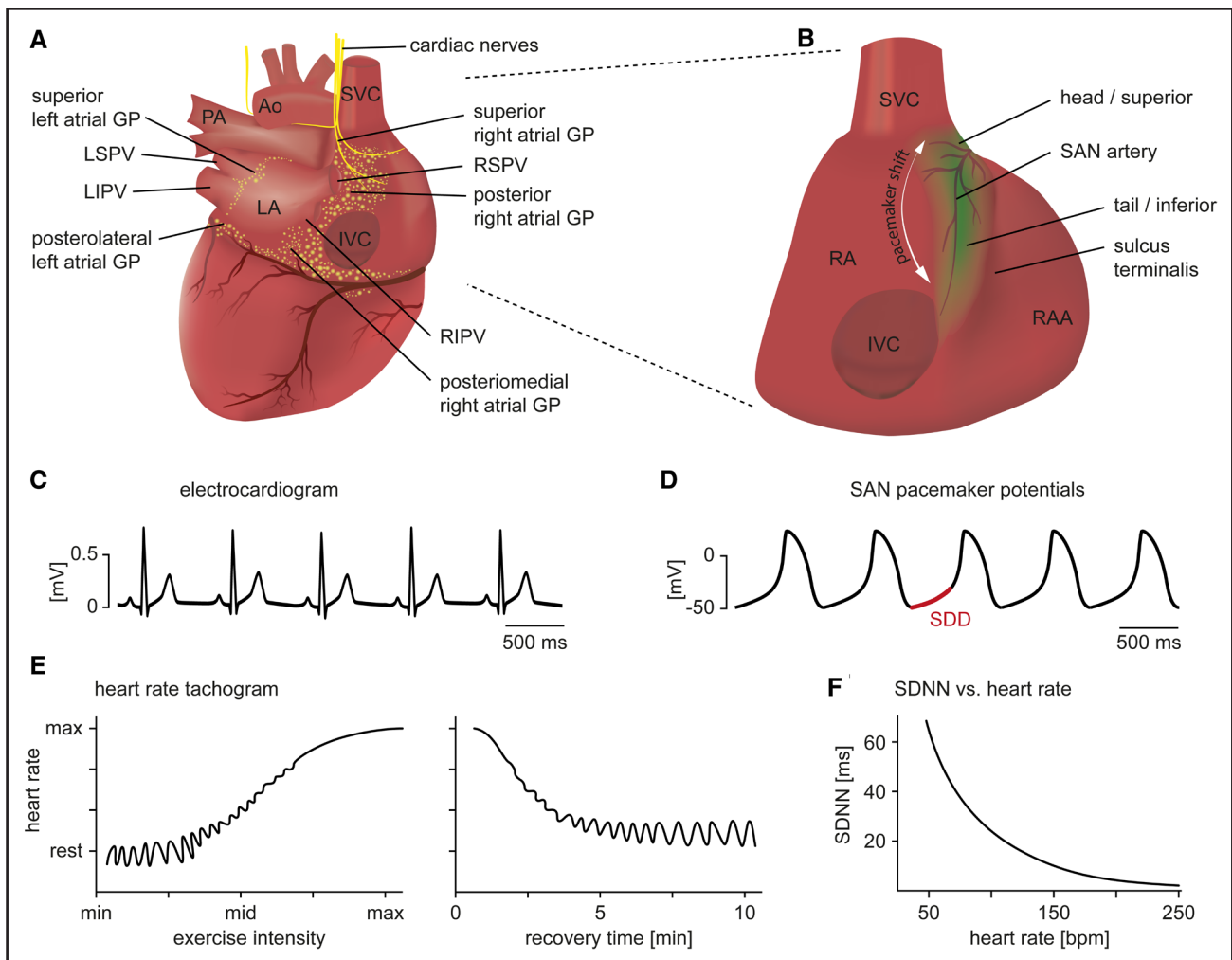


Figure 1. Three components of the chronotropic effect are controlled by the autonomic nervous system (ANS).

A, The sinoatrial node (SAN) is densely innervated by the sympathetic and parasympathetic nervous system (see text for details). **B**, Inset of (**A**) depicting the localization and anatomy of the SAN. Upon changes in ANS input, the leading pacemaker region shifts between the head (superior SAN) and the tail (inferior SAN). **C** and **D**, Schematic human ECG (**C**) and SAN pacemaker potential (**D**) recordings. **E**, Heart rate (HR) tachograms visualizing the changes in absolute HR and HR variability (HRV) during exercise (**left**) and recovery (**right**). Variability is relatively high at lower HRs (during rest) and decreases when HR is accelerated (during exercise). **F**, Relation between HRV (represented as SD of NN intervals [SDNN]) and absolute HR. GP indicates ganglionated plexus; IVC, inferior vena cava; LIPV, left inferior pulmonary vein; LSPV, left superior pulmonary vein; NN interval, normal RR interval (ie, interbeat intervals from which artifacts have been removed); RAA, right atrial appendage; RIPV, right inferior pulmonary vein; RSPV, right superior pulmonary vein; SDD, slow diastolic depolarization; and SVC, superior vena cava.

anatomically and functionally confined subsidiary atrial pacemaker has been described; it is located superior to the inferior vena cava and inferior to the crista terminalis. The subsidiary atrial pacemaker region is characterized by its own leading pacemaker region, which is independent of the SAN and gives rise to slower HR than the SAN.

Interestingly, even in the leading pacemaker region of the SAN, there is heterogeneity with respect to firing behavior.^{24,25} This includes nonfiring or dormant pacemaker cells, which have only lately become better characterized experimentally^{6,25–31} (Table 1). Most recent studies revealed that nonfiring pacemaker cells fulfill important physiological functions in the SAN and

are necessary to ensure smooth HR transitions during the chronotropic response.^{4,25,32,33} Understanding the mechanisms that regulate firing behavior and the transition between firing and nonfiring is of great physiological and pathophysiological importance and represents an increasingly upcoming research topic in cardiac cellular electrophysiology.

This review is dedicated to the role of pacemaker channels in the chronotropic response in health and disease. It is based on an analysis of >230 *in vivo* and *in vitro* studies in different mammalian species (178 references) and humans (50 references) and also modeling studies (17 references). In each section, special emphasis is placed on demonstrating the relationships between

the physiology and pathophysiology of humans and other mammals and formulating conclusions that are generally valid for humans. To this end, we will outline how the ANS innervates the SAN to initiate the chronotropic response (Figure 1). We then will introduce the hyperpolarization-activated cyclic nucleotide-gated cation channel (HCN channel) family (Figure 2) as the molecular correlate of the pacemaker current (I_p) and present the cellular mechanisms by which these channels, together with other transmembrane ion channels and Ca^{2+} handling proteins, interact to generate the autonomous firing of pacemaker cells at the single cell level (Figure 3). Further on, we will introduce the concept of nonfiring cells in the SAN and review the mechanisms underlying the nonfiring mode (Figures 4 and 5). This is followed by a discussion of how pacemaker channels regulate the chronotropic response in the heart. The focus will be on the 3 components associated with this response, the actual HR, the variability of HR at a given time, and the anatomic site of the leading pacemaker region. Then, 2 models will be presented, which explain the interaction between firing and nonfiring cells in the SAN network (Figure 6), and how HCN channels contribute to this interaction and, thereby, regulate the chronotropic response. Finally, we will discuss how diseases affect the pacemaking of the heart.

CHOLINERGIC AND ADRENERGIC NEURONS OF THE ANS INITIATE THE CHRONOTROPIC RESPONSE

The SAN is densely innervated by the ANS^{34,35} (Figure 1A). Cell bodies of preganglionic cardiac parasympathetic neurons are primarily residing in the nucleus ambiguus within the brain stem. Reportedly, only a minority of cardiac parasympathetic neurons are located in the dorsal motor nucleus of the vagus and these neurons control ventricular inotropy and excitability, but not HR. Axons from neurons in the nucleus ambiguus form the cardiac branches of the vagus nerve, which bilaterally innervate cholinergic neurons in the cardiac ganglia located on the epicardial surface. Postganglionic fibers arising from these ganglia in turn densely innervate the SAN,³⁶ atrioventricular node, and myocardial tissue. The parasympathetic nervous system regulates HR on a fast time scale of milliseconds,^{25,37–42} allowing for beat-to-beat control of HR.

The cell bodies of preganglionic cardiac sympathetic neurons are located in the intermediolateral cell columns of the upper 4 to 7 thoracic segments of the spinal cord.³⁴ These neurons receive input from forebrain centers.^{34,36} Axons arising from these neurons project to the superior cervical, cervicothoracic, and thoracic ganglia. The axons from these postganglionic neurons form the sympathetic cardiac nerves on both sides, which project to cardiac plexuses and also directly to the SAN. In contrast to the

parasympathetic nervous system, the sympathetic nervous system controls HR on a slower time scale, within seconds.^{37–42}

Furthermore, intrinsic cardiac ganglia located around the pulmonary veins modulate the activity of ANS (Figure 1). In the mouse, it has been reported that cholinergic neurons in the inferior pulmonary vein-ganglionated plexus and noradrenergic neurons in the craniomedial part of the right stellate ganglion project to the SAN.⁴³ Furthermore, vagal afferents have been shown to enhance parasympathetic and reduce sympathetic efferent outflow to the heart via central mechanisms. In pig and human hearts, the right atrial ganglionated plexus mediates primarily bilateral vagal inputs to exert profound functional control of the SAN and the leading pacemaker region.⁴⁴

The balance between the 2 branches of the ANS can be estimated by comparing the resting HR in vivo (basal HR)⁴⁵ and the HR in the absence of autonomic input (intrinsic HR, measured in the denervated heart or with pharmacological inhibition of the ANS).^{45–48} In small animals, the basal HR is high, for example, around 500 bpm in mice.^{49–51} By contrast, the intrinsic HR in mice is substantially lower than the basal HR. This indicates a significant sympathetic tone in the mouse and other small animals.⁵¹ In humans and also dogs, the basal HR is much lower, for example, around 60 to 100 bpm in humans. In those species, basal HR arises under pronounced vagal tone,⁵¹ and pharmacological blockade of autonomic input significantly accelerates the HR.

When the ANS stimulates SAN pacemaker cells to increase or decrease their firing rate, this is achieved by changing the duration of the pacemaker cycle, in particular by changing the SDD rate, as well as the repolarization velocity and AP duration. These effects are mainly caused by altering the intracellular concentration of the second messenger cyclic adenosine monophosphate (cAMP), which is the central element to determine the chronotropic state of the SAN. Increased activation of the sympathetic nervous system leads to the release of the neurotransmitter noradrenaline from nerve terminals in the SAN. Noradrenaline binds to G_s protein-coupled beta-1 adrenergic receptors (β_1 adrenoceptors/*ADRB1*) at the surface of pacemaker cells, causing the G_{α_s} subunit to activate adenylyl cyclases (ACs). Subsequently, ACs catalyze the production of cytosolic cAMP, which, in turn, activates a plethora of downstream targets (Figure 3), many of which are involved in the SAN pacemaker process. Conversely, increased activation of the parasympathetic nervous system causes the release of acetylcholine that binds to G_i protein-coupled M_2 muscarinic receptors (*CHRM2*), thereby inhibiting cAMP synthesis by ACs. The possible mechanisms by which these changes in cytosolic cAMP ultimately accelerate or decelerate the heart⁵² include direct cAMP effects and PKA (protein kinase A)- and CaMKII (Ca^{2+} /calmodulin-dependent

protein kinase II)-dependent phosphorylation of downstream targets and will be discussed in the ANS Initiates the HR Increasing or Decreasing Effect of the Chronotropic Response section.

SAN PACEMAKER MECHANISMS ARE THE BASIS OF THE CHRONOTROPIC RESPONSE

The chronotropic response is the result of changes in the SAN pacemaker process, which itself is based on a multitude of subcellular mechanisms (Figure 3). In this section, we highlight the mechanisms that control the 2 modes of sinoatrial pacemaker cells, that is, the firing mode characterized by spontaneous pacemaker potentials and the nonfiring mode, which is required for stabilizing the HR, especially during chronotropic responses. To make the mechanisms underlying spontaneous firing more comprehensible, a concept of 2 interconnected clocks has been established.⁵³ In this concept, the term membrane clock refers to cyclic activation and deactivation/inactivation of ionic currents generated by ion channels and transporters in the cell membrane, whereas the term calcium clock describes subcellular periodic uptake and release of Ca^{2+} from the sarcoplasmic reticulum (SR).^{53–55} However, because there are proteins that can be assigned to both clocks, for example, the NCX1 (sodium-calcium exchanger 1), and because the 2 clocks influence each other as coupled oscillators, it would be more precise to speak of a coupled clock system.^{56,57} Nevertheless, for reasons of conformity with the relevant literature, we will use the traditional terms membrane clock and calcium clock in this review.

The Membrane Clock Is the Motor of the Pacemaker Potential

To achieve spontaneous firing, a complex sequence of ion movements across the cell membrane is required, which together determine the pacemaker potential composed of the SDD, the AP upstroke, and the repolarization phase.^{45,33} HCN channels (Figure 2) represent a central element of the membrane clock and are considered key drivers of SDD. The channels pass a non-inactivating mixed Na^+/K^+ current (I_f)⁵⁸ and remain open throughout the pacemaker cycle.⁵⁹ Beginning at the maximum diastolic potential (MDP), I_f initiates slow depolarization of the membrane.^{5,58,60,61} In mammals, there are 4 HCN channel isoforms, termed HCN1–4.^{5,58,62,63} The distinctive feature of these channels is their activation by membrane hyperpolarization. Moreover, HCN channel activity is regulated by cAMP (see ANS Initiates the HR Increasing or Decreasing Effect of the Chronotropic Response section),⁶⁴ and the 4 HCN isoforms differ in

their activation and deactivation kinetics and in their sensitivity to cAMP.^{32,62} HCN4 (hyperpolarization-activated cyclic nucleotide-gated cation channel isoform 4) is highly expressed in SAN pacemaker cells^{65,66} and is characterized by the slowest kinetics and highest cAMP sensitivity among the 4 subtypes.^{62,67} Throughout the human SAN, HCN4 is the main isoform and is evenly distributed alongside HCN1 and HCN2,⁶⁸ while no clear evidence of HCN3 expression has been reported.¹⁶ Similarly, in mice, HCN4 is the predominant isoform expressed in the entire SAN.^{25,69} HCN1, however, is almost exclusively present in the head region of the murine SAN,⁶⁹ and the expression profiles of HCN2 and HCN3 have not yet been conclusively clarified. In addition to enabling spontaneous firing, HCN channels are involved in functional intercellular crosstalk between pacemaker cells of the SAN³² (see HCN Channels Stabilize SAN Function During the Chronotropic Response section). Moreover, HCN channels are expressed in secondary pacemaker structures further downstream in the cardiac conduction system.^{65,66} In the subsidiary atrial pacemaker region of the rat, transcripts of HCN1, HCN2 and HCN4 have been reported^{19,70} with higher levels of HCN2 and HCN1 and similar levels of HCN4 compared with the SAN.^{19,70} In the human paranodal area, transcript levels of HCN1 and HCN4 have been reported to be lower and transcripts of HCN2 higher compared with the SAN.¹⁶ In the murine atrioventricular node, similar to expression in the SAN, HCN4, HCN1, and (with restriction to few individual cells) HCN2 have been detected.⁶⁵ Interestingly, 2 mouse studies with an inducible heart-specific knockout of HCN4⁷¹ or conditional silencing of complete cardiac I_f ⁷² report severe impairment of atrioventricular conduction up to complete atrioventricular block. While this indicates an important role of HCN4 in atrioventricular node function, no changes in atrioventricular conduction are reported in other HCN4 mouse models.^{25,73–76} Furthermore, HCN channels seem to be involved in the generation of escape rhythms below the atrioventricular node.⁷⁷ In the bundle of His, HCN4 appears to be the only isoform expressed,⁶⁵ while in the bundle branches and Purkinje fibers, HCN4, HCN1, and small amounts of HCN2 are expressed.^{65,78,79} In this review, we specifically focus on HCN channels in the SAN and mechanisms relevant to the chronotropic effect. For further reading on HCN channels in secondary pacemaker structures, please refer to references^{65,80–83}.

During SDD in SAN cells, the mainly HCN4-mediated I_f (Figure 3A through 3C) depolarizes the membrane to a range sufficient for activation of voltage-gated T-type and L-type Ca^{2+} channels^{5,84,85} (Figure 3). $\text{Ca}_v3.1$ (*CACNA1G*) is the predominant T-type Ca^{2+} channel isoform in the adult mammalian SAN and, together with $\text{Ca}_v3.2$ (*CACNA1H*), constitutes I_{CaT} that activates at negative voltages around -60 mV⁸⁶ (Figure 3D). At more positive voltages, L-type Ca^{2+} channels are concomitantly activated

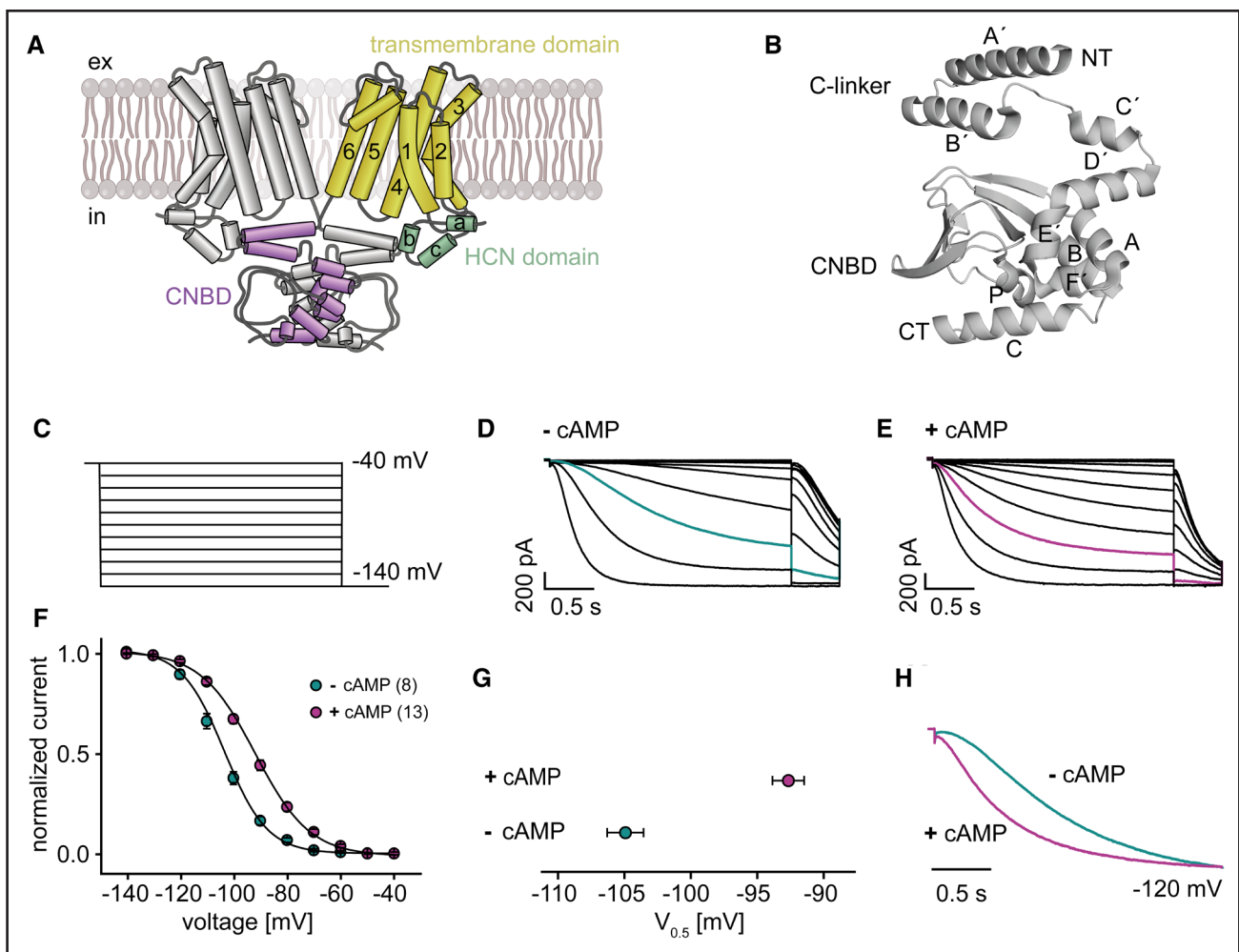


Figure 2. Structure and biophysical properties of HCN4 (hyperpolarization-activated cyclic nucleotide-gated cation channel isoform 4) channels.

A, Each of the 4 subunits of the tetrameric hyperpolarization-activated cyclic nucleotide-gated cation channel (HCN channel) complex consists of 6 alpha-helical transmembrane segments (yellow), the intracellular N terminus including the HCN domain (cyan), and the C terminus (magenta). For clarity, only 2 of the 4 subunits are depicted. **B**, Structure of the C terminus composed of the C-linker and cyclic nucleotide-binding domain (CNBD). **C**, Hyperpolarizing voltage step protocol to evoke HCN currents in patch-clamp experiments. **D** and **E**, Representative current traces recorded in whole-cell configuration at room temperature in HEK293 cells expressing HCN4 channels, without (–) and with (+) cyclic adenosine monophosphate (cAMP, 100 $\mu\text{mol/L}$) in the intracellular solution. **F**, Activation curves of HCN4 in the absence (cyan) and presence of cAMP (magenta). The binding of cAMP to the CNBD induces a shift of the activation curve toward more positive potentials, thereby increasing the open probability in the physiological voltage range. **G**, Half-maximal activation voltage ($V_{0.5}$) in the absence (cyan) and presence of cAMP (magenta). **H**, Enlargement of HCN current traces from (**D**) and (**E**) at -120 mV, highlighting the acceleration of activation kinetics in the presence of cAMP. All data shown in (**D**–**H**) are representative data measured in our laboratory. N numbers are given in parentheses. Data are represented as mean \pm SEM.

and contribute to the late SDD and AP upstroke phase (Figure 3E). I_{CaL} is comprised of $\text{Ca}_v1.3$ (*CACNA1D*) and $\text{Ca}_v1.2$ (*CACNA1C*)-mediated currents that are activated one after the other due to their distinct activation thresholds (test potential at which 50% of the maximum current is activated⁸⁷) of -45 and -25 mV, respectively.^{84,88,89} In addition, SAN cells express voltage-gated Na^+ channels that have been shown to play a role in pacemaking and impulse conduction (Figure 3F). The presence of tetrodotoxin-sensitive (neuronal) $\text{Na}_v1.1$ (*SCN1A*) and $\text{Na}_v1.3$ (*SCN3A*) channels⁹⁰ and the tetrodotoxin-insensitive (cardiac) $\text{Na}_v1.5$ (*SCN5A*) isoform⁹¹ has

been reported in the mouse. In the human SAN, $\text{Na}_v1.6$ (*SCN8A*) is additionally expressed and contributes to intranodal conduction.⁹² Furthermore, a sustained inward Na^+ current (I_{st}) has been found in SAN cells.^{93–96} This current is activated at negative membrane potentials and persists throughout the range of SDD, bearing the possibility of a functional contribution to pacemaking. Only recently, the L-type $\text{Ca}_v1.3$ channel was identified as an obligatory molecular component of I_{st} in SAN cells.^{94,97,98} In the next phase of the pacemaker cycle, the positive membrane potential causes both inactivation of voltage-gated Na^+ and Ca^{2+} currents and activation

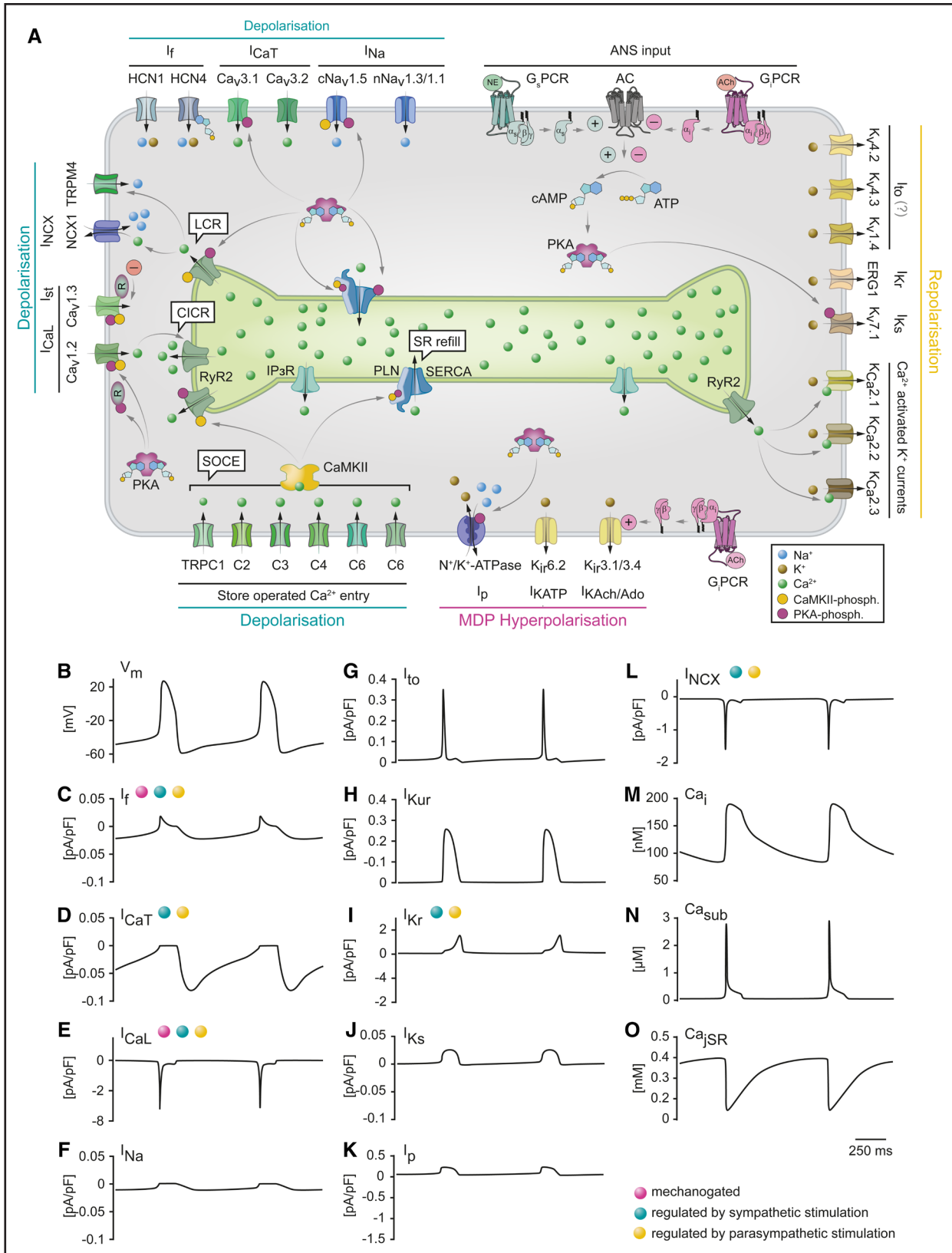


Figure 3. Membrane clock and calcium clock mechanisms underlie sinoatrial node (SAN) cell automaticity and are regulated by the autonomic nervous system (ANS).

A, Schematic illustration of a human SAN pacemaker cell depicting the ion channels and transporters of the membrane clock and the molecular components of the calcium clock. Together, the respective currents are responsible for generating the depolarization, repolarization, and hyperpolarization/maximum diastolic potential (MDP) of the pacemaker potential (see text for details). The signal transduction pathways of the ANS for triggering the chronotropic response are included. Sympathetic activity stimulates, whereas parasympathetic activity (Continued)

of voltage-gated K^+ currents, which are responsible for membrane repolarization and return to the MDP (Figure 3G through 3J). There are 3 distinct voltage-gated K^+ currents, that is, the rapidly activating (I_{Kr}) and slowly activating (I_{Ks}) delayed rectifier K^+ currents and the transient outward current (I_{to}).⁵ In the SAN, I_{Kr} is generated by channels composed of the ERG1 α subunit (*KCNH2*),⁹⁹ possibly in interaction with its accessory subunit MiRP1 (*KCNE2*). I_{Ks} channels consist of the $K_v7.1/KvLQT1$ α subunit (*KCNQ1*) in combination with minK (*KCNE1*).¹⁰⁰ However, the expression of both I_{Kr} and I_{Ks} seems to underlie profound species-dependent differences. I_{to} expression is variable across the SAN and appears to be more important for AP repolarization in peripheral than in central regions.¹⁰¹ While $K_v4.2$ (*KCND2*) and $K_v4.3$ (*KCND3*), as well as $K_v1.4$ (*KCNA4*), have been suggested to be possible candidates encoding I_{to} in the SAN,^{101–103} the actual subunit composition is not yet known. After reaching the MDP, the time- and voltage-dependent decay of K^+ currents allows the inward currents to initiate membrane depolarization and can, thus, be described as another key mechanism of early SDD.¹⁰⁴ In addition, SAN cells express several inwardly rectifying K^+ channels responsible for $I_{K_{ACh}}/I_{K_{A\text{do}}}$, $I_{K_{ATP}}$ (Figure 3A), and I_{K_1} . $I_{K_{ACh}}/I_{K_{A\text{do}}}$ is based on the expression of the G protein-coupled K^+ channels GIRK1 and GIRK4, which are composed of $K_{ir}3.1$ (*KCNJ3*) and $K_{ir}3.4$ (*KCNJ5*), respectively.^{5,84,105} Upon activation of G_i protein-coupled M_2 muscarinic receptors or A1R and A3R adenosine receptors, these channels are directly opened by binding of the $G_{\beta\gamma}$ subunit to the channel complex.^{105,106} The corresponding outward K^+ current significantly hyperpolarizes the MDP and slows down the firing rate of SAN cells during parasympathetic activity.^{107,108} $I_{K_{ATP}}$ in the SAN is generated by channels consisting of the pore-forming $K_{ir}6.2$ (*KCNJ11*)¹⁰⁹ or $K_{ir}6.1$ (*KCNJ8*) subunit¹¹⁰ and the regulatory SUR2A (*ABCC9*) subunit that is important for the channel's reactivity to the metabolic state of the cell.¹¹¹ K_{ATP} channels are blocked by ATP and open when intracellular ATP concentrations drop. The current is, thus, activated when the metabolic rate is low, leading to a slowdown of pacemaker activity that potentially protects the heart from ischemic damage.^{109,110} The background K^+ current I_{K_1} is mainly generated by $K_{ir}2.1$ (*KCNJ2*) and $K_{ir}2.3$ (*KCNJ4*) channels.¹⁶ It is small or absent in human SAN¹⁶ but moderately expressed in murine SAN cells,^{5,30} although at significantly lower densities than in the working myocardium. In ventricular and atrial cardiomyocytes, I_{K_1} is considered to stabilize the

resting membrane potential and counteract spontaneous firing, thereby generating the driving force for inward Na^+ and Ca^{2+} currents during the AP. The greatest influence on the resting membrane potential of excitable cells is exerted by the sodium-potassium pump (Na^+/K^+ -ATPase), which is also significantly involved in setting the MDP of SAN cells to the range of -60 mV^{5,112} (Figure 3K). This is achieved by carrying a steady-state net outward current (I_p). However, also a voltage-dependent behavior of I_p has been described, which, together with its intrinsic Na^+ dependency, could cause a periodic change in I_p , possibly contributing to SAN cell automaticity.^{5,113} More recently, the family of Ca^{2+} -activated K^+ channels (K_{Ca}) has been suggested to influence pacemaking in the SAN⁸⁴ (Figure 3A). These channels are categorized into voltage-independent small-conductance (SK) and intermediate-conductance channels, as well as voltage-dependent big-conductance channels. K_{Ca} channels have distinct sensitivities to Ca^{2+} conferred by the interaction of CaM (calmodulin) with SK and intermediate-conductance channels^{114,115} or by direct binding of Ca^{2+} to big-conductance channels.^{116,117} The 3 SK channel isoforms, SK1 ($K_{Ca}2.1/KCNN1$), SK2 ($K_{Ca}2.2/KCNN2$), and SK3 ($K_{Ca}2.3/KCNN3$),^{118,119} as well as the intermediate-conductance channel (SK4, $K_{Ca}3.1/KCNN4$)¹²⁰ and big-conductance channel ($K_{Ca}1.1/KCNMA1$),¹²¹ are expressed in the SAN and translate changes in intracellular Ca^{2+} into repolarizing currents, thereby affecting the AP duration, MDP, and SDD of pacemaker cells.¹²² Another protein regulated by intracellular Ca^{2+} is the sodium-calcium exchanger 1 (NCX1/*SLC8A1*), a transporter located in the cell membrane whose activity is indispensable for SAN automaticity.^{31,123,124} NCX1 transports 1 Ca^{2+} ion and 3 Na^+ ions in opposite directions. The reversal potential of NCX in cardiac myocytes is around -20 mV,^{125,126} thereby facilitating the outward transport of Ca^{2+} coupled with inward transport of Na^+ (forward mode) in the diastolic range of membrane potentials, which is more negative than -20 mV. Consequently, NCX1 activity causes a net inward current (I_{NCX}) during late SDD that increases when subsarcolemmal Ca^{2+} is elevated (Figure 3L). Moreover, members of the superfamily of transient receptor potential channels are expressed in the SAN^{84,127} (Figure 3A). TRPC channels are involved in store-operated Ca^{2+} entry,^{128,129} whereas TRPM4 activity directly contributes to the baseline firing rate^{130–132} and TRPM7 indirectly influences pacemaking by regulating the expression of HCN4.^{127,133}

Figure 3 Continued. inhibits cyclic adenosine monophosphate (cAMP) synthesis by adenylyl cyclases (ACs). This regulates the phosphorylation of membrane clock and calcium clock proteins by PKA (protein kinase A) and CaMKII (Ca^{2+} /calmodulin-dependent protein kinase II) as indicated by arrows and magenta (PKA) or yellow circles (CaMKII). **B**, Time course of human SAN pacemaker potentials. **C** through **L**, Time course of a selection of ionic currents normalized to membrane capacitance in units of pA/pF. **M** through **O**, Time course of Ca^{2+} dynamics contributing to the pacemaker potential. All traces in (**B–O**) are adapted from the mathematical model of a human SAN pacemaker cell by Fabbri et al.³³⁶ Mechanosensitivity and autonomic regulation are indicated by color coding. ACh indicates acetylcholine; CICR, calcium-induced calcium release; GPCR, G protein-coupled receptor; LCR, local calcium release; NE, norepinephrine; SOCE, store-operated Ca^{2+} entry; and SR, sarcoplasmic reticulum.

Different groups have recently demonstrated that several components of the membrane clock, and, consequently, the HR are regulated by stretch (for review see¹³⁴). In large mammals with inherently slow HR, stretch increases HR, while in smaller mammals such as the mouse and rat with resting HR of ≥ 500 bpm, SAN stretch can increase or decrease the beating rate.^{134–137} Stretch-induced changes in beating frequency occur in isolated hearts,^{138,139} isolated right atria,^{140–142} SAN tissue,¹³⁷ and individual SAN cells,¹⁴³ all of which lack autonomic innervation. These and other experiments (for details, please see reference¹³⁴) suggest that the chronotropic response of the heart to stretch is, at least in part, intrinsic to the SAN.^{134,144} The response of the SAN to stretch occurs faster than and complementary to the positive chronotropic response induced by the ANS and occurs on a beat-to-beat time scale. The cellular mechanisms that elicit the chronotropic response to SAN stretch involve stretch-activated ion channels and have been summarized recently.^{134,145} Some of these channels are closed under baseline conditions and require a stretch to be activated (CIC2, CIC3, SWELL1, PIEZO1/2, TREK-1).¹⁴⁴ Others are integral components of the membrane clock, and their mechanosensitivity additionally modulates the contribution of these channels to SDD. For example, the activation, deactivation, and amplitude of the currents generated by HCN2 pacemaker channels in heterologous expression systems have been shown to be altered by mechanical stimulation.^{146,147} In addition, many other ion channels and transporters in the heart have been shown to be mechanosensitive, including I_{NCX} , I_{CaL} , I_{CaT} , I_{Kr} , and I_{Ks} .¹⁴⁸ Thus, mechanosensitive gating of ion channels supports the pacemaker function to adapt to changes in hemodynamic load on a beat-to-beat basis, which intrinsically occur on a fast time scale.^{134,144} Finally, there is also evidence of an interaction between the control of HR by the ANS and the mechanosensitivity of the SAN. Specifically, when the vagus nerve is stimulated, the SAN stretch-induced increase in beating rate is greater than without nerve stimulation. Conversely, the decrease in beating rate in response to vagus nerve stimulation is attenuated following SAN stretch in both SAN tissue preparations and whole animals.^{149,150}

The Calcium Clock Supports Pacemaking by the Membrane Clock

In addition to the membrane clock, periodically occurring subcellular Ca^{2+} dynamics of the calcium clock play an important role in cardiac pacemaking^{26,28,56} (Figure 3A and 3L through 3O). During diastole, the opening of ryanodine receptor 2 (RyR2/RyR2) generates rhythmic local calcium release (LCR) from the SR,^{151–153} resulting in a periodic increase in the subsarcolemmal Ca^{2+} concentration. The question of whether LCRs are triggered by I_{CaL} or occur independently has been investigated

experimentally.^{153–157} In permeabilized rabbit SAN cells and in intact rabbit SAN cells under acute voltage-clamp conditions, it has been shown that rhythmic LCRs occur spontaneously and do not require membrane currents per se.^{153,157} In contrast, an important role of I_{CaL} in generating RyR2-dependent Ca^{2+} release was demonstrated in murine pacemaker cells.^{154–156} Regardless of the basic requirements for the occurrence of LCRs, there is evidence that the kinetics of membrane currents and intracellular Ca^{2+} cycling are coupled to each other and are synchronized during changes in HR across different species.¹⁵⁸ Functionally, RyR2-mediated LCRs have an impact on the pacemaker cycle via NCX1. When subsarcolemmal local Ca^{2+} is elevated (Figure 3N), more Ca^{2+} is extruded from the cell and the net inward current I_{NCX} increases. In this way, I_{NCX} translates LCRs into changes in membrane potential and significantly contributes to depolarization during the late (exponential) phase of SDD⁵⁶ (Figure 3L). In SAN cells, LCRs are strictly regulated, and their timing and magnitude are influenced by the amount of Ca^{2+} stored in the SR. During the AP, intracellular Ca^{2+} increases (Figure 3M) due to calcium-induced calcium release. The SR/endoplasmic reticulum Ca^{2+} -ATPase (SERCA2a/ATP2A2) contributes to removing Ca^{2+} from the cytosol after AP termination, thereby refilling the SR Ca^{2+} stores and enabling LCRs during the next pacemaker cycle.¹⁵⁹ SERCA activity is, in turn, regulated by phospholamban (PLN/PLN), a small pentameric protein, which, when unphosphorylated, directly binds to and inhibits SERCA¹⁶⁰ (Figure 3A). In addition, reverse NCX activity (Ca^{2+} entry coupled with Na^{+} extrusion) at positive membrane potentials during the AP has been suggested to influence the SR Ca^{2+} content and, hence, the calcium clock function.¹⁶¹ Furthermore, intracellular calcium dynamics are influenced by the Ca^{2+} -mobilizing second messenger inositol-1,4,5-triphosphate.^{162–164} Type II inositol-1,4,5-triphosphate receptor ($\text{IP}_3\text{R2}/\text{ITPR2}$) is the predominant isoform located on the SR of murine SAN cells^{163,164} and releases Ca^{2+} when inositol-1,4,5-triphosphate is present (Figure 3A). This has been shown to have a direct effect on pacemaker function, possibly through activation of NCX1, other Ca^{2+} -dependent currents, or stimulation of Ca^{2+} -activated ACs.¹⁶² In addition, pacemaking depends on the function of calsequestrin 2 (CASQ2/CASQ2), the main Ca^{2+} binding protein in the SR of SAN cells. CASQ2 has been shown to be important for ensuring robust diastolic Ca^{2+} release, which is necessary for maintaining a normal resting HR and regular rhythmicity.¹⁶⁵ Whether the proteins of the calcium clock—just like their counterparts of the membrane clock—are regulated by stretch is currently under investigation and debate. While some studies do not report that calcium clock proteins are activated by stretch,¹⁴⁴ others do.^{134,136,166}

Given that the mechanisms of the membrane clock and calcium clock all influence SDD and, thereby, the

pacemaker activity, the question arises as to how important the individual contributions are. At least for the membrane clock and calcium clock, this issue was investigated on the transcript and protein level. Using high-resolution mass spectrometry, a recent study identified 7000 proteins in the SAN and the neighboring atrial myocardium. Strikingly, the expression of 575 proteins differs between the 2 tissues. Using single-nucleus RNA sequencing of sinus node biopsies, measured protein abundances could be attributed to specific cell types. The data reveal significant differences between the SAN and the atrial myocardium in ion channels responsible for the membrane clock, but not in calcium clock proteins. Furthermore, the expression of PKA and CaMKII was more abundant in the atrial muscle, and the PDEs (phosphodiesterases) detected were either uniformly expressed (PDE1A) or more highly expressed (PDE3A and PDE5E) in the atrial muscle compared with the SAN. Together, these findings suggest that specific ion channels of the membrane clock are primarily responsible for pacemaking.¹⁶⁷

Nonfiring Cells Are Important Players in SAN Pacemaking

Given the broad knowledge about how autonomic firing at the single cell level is generated, it came as a surprise that single pacemaker cells can enter a nonfiring state and switch back and forth between firing and nonfiring (Figures 4 and 5). In the following, we provide the results of a comprehensive analysis of the literature and a detailed comparison of studies in which nonfiring pacemaker cells have been reported (Tables 1 through 3). The baseline for the discovery of nonfiring cells is the observation that acute preparations of single SAN cells are typically heterogeneous, morphologically and functionally, with only a fraction of around 10% to 30% of cells spontaneously beating with visible contractions or firing.^{168,169} Only recently, researchers have started to closely investigate cells without apparent automaticity (Table 1). The respective studies report the characterization of quiescent pacemaker cells isolated from guinea pig SAN,^{26,29} arrested human SAN cells,²⁸ and dormant²⁷ and nonfiring²⁵ murine cells. Importantly, nonfiring pacemaker cells were not only found in single-cell preparations but also in intact tissue explants containing the whole SAN region.^{24,25} Together, these observations strengthen the suggestion that rather than being experimental artifacts, these cells have an important physiological function in the SAN.^{4,25,32,33}

Continuously firing SAN cells (Figure 4A) usually have a stable and hyperpolarized MDP of -50 to -70 mV. The membrane potential of dormant cells, however, varies substantially between the different studies. In addition, some results show initially firing cells with intermittent episodes of nonfiring, whereas, in others, the cells

are initially dormant and need to be stimulated to show rhythmic firing. By comparing the characteristics of the respective cells, 3 different groups could be identified.

The first group comprises initially firing cells that spontaneously and reversibly switch to nonfiring (Figures 4B and 5A). Before entering the nonfiring mode, the MDP of firing cells slowly hyperpolarizes by ≈ 8 mV until firing ceases.²⁵ During nonfiring episodes, the membrane potential remains at hyperpolarized values in the range of -60 mV.²⁵ This is accompanied by a slow membrane depolarization until firing is reinitiated. Under baseline (unstimulated) conditions, the transition to nonfiring is rare but can be augmented by the application of the muscarinic receptor agonist carbachol (Figure 4C). Likewise, nonfiring is completely abolished when cells are stimulated with the beta-adrenoceptor agonist isoproterenol.²⁵ This confirms the crucial role of ANS input in controlling the firing behavior of SAN cells. Similar to this observation, burst-firing cells with long silent periods at hyperpolarized membrane potentials, interrupted by short periods of high-frequency AP firing, have been reported.⁶ The possible biophysical mechanisms underlying hyperpolarized nonfiring cells will be described in HCN Channels Stabilize SAN Function During the Chronotropic Response section.

The second group of cells is initially dormant, has a relatively depolarized membrane potential of -30 to -40 mV, and develops rhythmic firing only on hyperpolarization during sustained beta-adrenergic stimulation^{27,29} (Figure 4D). Such cells were found in wild type (WT) preparations from mice and guinea pigs^{27,29} (Table 1). Similar observations were made in human cells although the responder rate to isoproterenol stimulation was considerably lower.²⁸ Importantly, viability is clearly confirmed because tonic firing can be induced in responding cells by application of isoproterenol (100 nmol/L– 1 μ mol/L). The cellular mechanism underlying the depolarized membrane potential during nonfiring has not been investigated. It is possible that ion conductances with a more positive reversal potential around -35 mV become dominant during nonfiring. In line with this, a background current has been postulated (reviewed in reference⁵⁴) with an equilibrium potential between -30 and -40 mV. The selective activation of this current could explain depolarized nonfiring pacemaker cells. Another explanation would be that the integrity of these pacemaker cells is compromised.

The third group comprises depolarized dormant cells that do not show changes in membrane potential and fail to elicit APs during beta-adrenergic stimulation (non-responder; Figure 4E).^{28,29} While these cells still generate LCRs under baseline conditions and show increased membrane current densities (I_{CaL} , I_K , and I_f) during isoproterenol application,²⁹ it is not clear why automaticity cannot be restored. Therefore, they may have been damaged during cell isolation so that (in the words of the

Table 1. Nonfiring pacemaker cells in different species

WT, different species	Recording technique (perforated or whole-cell patch-clamp, calcium imaging)	Initial state (firing or dormant)	Initial membrane potential	Measurement duration (reported or determined from figures)
Fenske et al ²⁵ PMID: 33144559 (mouse) Classification: group 1	Perforated (ampho) and calcium (Fluo-4)	Only initially firing cells were investigated (WT rarely switched between firing/nonfiring)	Firing, -57 mV Hyperpolarized during nonfiring: $MDP \pm 10$ mV	Up to 1 h (minimum 5 min)
Grainger et al ⁶ PMID: 34250490 (mouse) Classification: group 1 (burst firing)	Perforated (ampho) and calcium (Fluo-4)	43%–75% firing (tonic, irregular, burst) 17%–36% subthreshold oscillations 8%–21% electrically silent	Firing ≈ -56 mV Silent, NA	5 s shown
Louradour et al ²⁷ PMID: 35406677 (mouse) Classification: group 2 (groups 1 and 3 in supplement)	Perforated (β -escin) and calcium (CAL-520)	33% of cells firing 66% of cells dormant	Firing, -55 mV Dormant, -30 mV (few cells dormant -70 mV)	Few seconds shown before ISO
Tsutsui et al ²⁸ PMID: 29895616 (human) Classification: groups 2 and 3	Perforated (ampho) and Calcium (Fluo-4)	50% of cells firing 25% dormant, responding to ISO 25% dormant, nonrespond to ISO	Firing, -50 mV Dormant, -35 mV	Few seconds shown before ISO
Tsutsui et al ²⁹ PMID: 33897445 (guinea pig) Classification: groups 2 and 3	Perforated (ampho) and calcium (Fluo-4)	33% of cells firing 66% of cells dormant	Firing, -58 mV Dormant, -40 mV	1 min shown before ISO/ cAMP
Kim et al ²⁶ PMID: 30092494 (guinea pig) Classification: NA	Calcium transients (Fluo-4)	Dormant cells (Ca^{2+} transients induced by ISO)	NA	30–90 s shown
Bychkov et al ²⁴ PMID: 32819526 (mouse) Classification: NA	Calcium transients (Fluo-4) and microelectrodes (intact tissue)	Heterogeneous Ca^{2+} signals in intact SAN tissue explants, including dormant cells	Firing, -60 mV Dormant, NA	2–4 s shown
Groenke et al ³¹ PMID: 24278453 (mouse) Classification: NA	Whole cell and calcium (Fura-2)	71% of cells firing	Firing, -70 mV Silent, NA	Minimum 5 min
Cho et al ³⁰ PMID: 12879867 (mouse) Classification: NA	Whole cell	$\approx 2\%$ of cells spontaneously beating	Firing, -57 mV Dormant, NA	0.5 s shown

cAMP indicates cyclic adenosine monophosphate; ISO, isoprenaline; MDP, maximum diastolic potential; NA, not available; SAN, sinoatrial node; and WT, wild type.

authors) arrested cells may represent SANCs that have lost functional clock coupling, possibly because of the cell isolation procedure.²⁸

Technical Requirements for Recording and Classifying Pacemaker Cell Activity

To ensure reliable characterization of nonfiring cells, certain experimental quality criteria need to be fulfilled. In the first group of cells, the switch between the 2 modes happens at a slow time scale. Therefore, spontaneous activity must be recorded over a long period to reliably detect, investigate, and characterize nonfiring. Moreover, it is essential to ensure that cytosolic cAMP is kept close to physiological levels during measurements by performing current-clamp experiments with the perforated patch-clamp method. To this end, a pore-forming compound (Figure 4F) is used, which provides electrical access to the intracellular compartment without breaking the membrane patch. Consequently, the integrity of the cytoplasm is largely preserved by preventing dilution of the intracellular milieu, washout of cellular

factors including cAMP, and also marked rundown of ion channel currents. In this respect, amphotericin B is superior to other compounds such as beta-escin due to the considerably smaller pore size. Beta-escin pores are significantly larger, resulting in the permeation of even high-molecular-weight compounds.^{170,171} In future experiments, firing and nonfiring need to be exactly monitored and documented over long time periods with several cycles covered in one recording. Such sufficiently long recordings should confirm that the cells can switch back and forth between the 2 modes spontaneously or pharmacologically triggered, thereby confirming cell viability.

Altogether, these recent data suggest that there may be different manifestations of nonfiring in SAN cells, characterized by depolarized versus hyperpolarized membrane potentials and by stimulated versus spontaneous switch to rhythmic firing (Figure 4). To minimize selection bias and optimize validity, future studies should consider the different behaviors of SAN cells, clearly specify the population studied, and ideally use consistent nomenclature for the different modes.

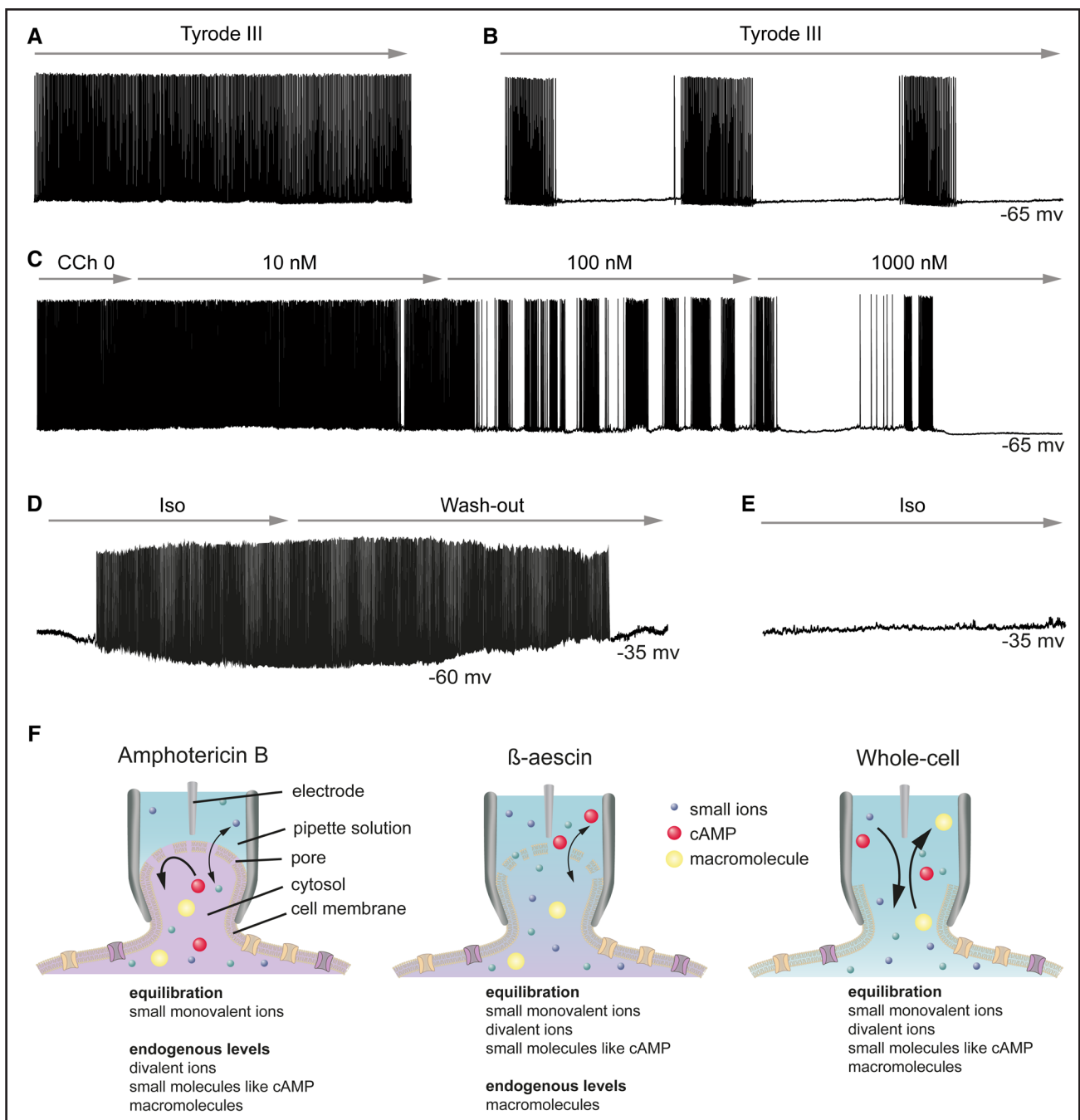


Figure 4. Characteristics of nonfiring and dormant pacemaker cells in current-clamp recordings.

A, Action potential recording of a continuously firing pacemaker cell under baseline conditions (superfusion with physiological tyrode III solution²⁵ as control). **B**, Recording of an initially firing cell that spontaneously switched between firing and nonfiring several times. During nonfiring, the membrane potential remained relatively hyperpolarized (group 1, see text for details). **C**, Recording of an initially firing cell during superfusion with increasing concentrations of carbachol (CCh). High concentrations of CCh induced nonfiring at hyperpolarized membrane potentials. **D**, Action potential (AP) recording of an initially dormant cell that generated rhythmic APs only during superfusion with isoproterenol (ISO). When being dormant, the membrane potential was relatively depolarized (group 2, see text for details). **E**, Recording of a nonresponding cell that remained dormant and relatively depolarized during superfusion with ISO (group 3, see text for details). The traces in (**A–C**) are adapted from Fenske et al²⁵ and are original AP recordings of murine sinoatrial node (SAN) cells. **D** and **E**, Schemes representing firing behavior in guinea pig SAN cells and are adapted from Tsutsui et al.²⁹ **F**, Experimental conditions of patch-clamp measurements with amphotericin B (**left**), β -escin (**middle**), and in whole-cell configuration (**right**). Differences in the mobility of monovalent ions, divalent ions, small molecules, and macromolecules between the cytosol and pipette solution are highlighted.

THE ANS INITIATES THE HR INCREASING OR DECREASING EFFECT OF THE CHRONOTROPIC RESPONSE

Traditional View of the Chronotropic Effect

The second messenger cAMP is the key determinant of the chronotropic state of the SAN, and it is used to be generally believed that cAMP-dependent regulation (CDR) of HCN4 is the primary mechanism for mediating the frequency aspect of the chronotropic response.^{60,61,64,175} However, besides HCN channels, several cAMP receptors have been identified in the SAN, including other proteins of the membrane clock and calcium clock (Figure 3). HCN4 is activated by membrane hyperpolarization and carries a depolarizing inward current during SDD. Furthermore, the channel contains a cyclic nucleotide-binding domain in its intracellular C-terminus¹⁷⁶ that makes it directly responsive to cytosolic cAMP levels (Figure 2). The traditional concept assumes that when the activity of the sympathetic nervous system increases, cAMP-binding to the cyclic nucleotide-binding domain of HCN4 and subsequent increase in I_f would be responsible for accelerating SDD, thereby increasing the firing frequency of pacemaker cells and, consequently, increasing HR (positive chronotropic effect). On the other hand, a reduction in HCN4 activity due to reduced cytosolic cAMP caused by parasympathetic signaling would be responsible for slowing down SDD and, thereby, reducing HR (negative chronotropic effect). This theory became widely accepted in cardiac physiology but did not remain undisputed. Although recent data from isolated single cells support the view that the increase in I_f following beta-adrenergic stimulation is responsible for at least part of the concomitant increase in firing rate¹⁷⁷ in vitro, this concept has never been conclusively confirmed in vivo. In fact, during the past 20+ years, different research groups have been investigating the cardiac function of several mouse models targeting HCN4^{25,71–76,172,178} (Table 2). The results demonstrate that despite the lack of responsiveness to cAMP or the complete absence of HCN4, the adult animals still showed a normal increase in HR, clearly refuting the longstanding textbook knowledge of HCN4 function as the main driver of the chronotropic response in the SAN. This implies that although changes in intracellular cAMP regulate HCN4 activity and I_f , this particular regulation is not the cause of altering SDD and mediating HR transitions but must serve a different purpose. Only recently, it was discovered that CDR of HCN4 plays an important role in controlling the firing and nonfiring mode of pacemaker cells, which is crucial for stabilizing the HR and leading pacemaker region, and dampening ANS input during the chronotropic response.^{4,25,32,33} In HCN Channels Stabilize SAN Function During the Chronotropic

Response section, we will propose a model explaining the underlying mechanism.

Alternative ANS Targets to Mediate HR Regulation

If CDR of HCN4 is not the main mechanism underlying ANS-induced changes in HR, frequency regulation must be controlled by other ion channels and transporters in pacemaker cells. Beta-adrenergic signaling increases cytosolic cAMP and, thereby, activates PKA,¹⁷⁹ which, in turn, phosphorylates and activates a variety of proteins of the membrane clock and calcium clock (Figure 3). These downstream targets of PKA include voltage-gated T-type $Ca_v3.1$ channels,^{180,181} L-type $Ca_v1.3$ ¹⁸² and $Ca_v1.2$ channels,^{183,184} $Na_v1.5$ channels,^{185,186} RyRs,¹⁸⁷ PLN,^{159,188} Na^+/K^+ -ATPase,¹⁸⁹ and delayed rectifier K^+ channels.^{190,191} While I_{Ks} is clearly augmented by PKA-dependent phosphorylation, there is no agreement on the beta-adrenergic modulation of I_{Kr} .¹⁹¹ Moreover, it was recently discovered that the mechanism by which PKA positively regulates I_{CaL} in ventricular myocytes during the inotropic response is based on phosphorylation of the small G protein Rad and subsequent disinhibition of $Ca_v1.2$.¹⁹² It is, therefore, possible that members of the RGK GTPase family such as Rad or Rem are also essential to the chronotropic effect by regulating $Ca_v1.2$ and $Ca_v1.3$ channels in SAN cells.^{193,194} In parallel, sympathetic activity stimulates CaMKII,^{195–197} subsequently activating L-type $Ca_v1.3$ ¹⁸² and $Ca_v1.2$ channels,^{174,183} $Na_v1.5$ channels,^{185,186} PLN,¹⁹⁸ SERCA,¹⁹⁹ and RyR2.¹⁹⁸ Moreover, the resulting elevated diastolic Ca^{2+} levels positively regulate TRPM4,^{131,132} K_{Ca} channels,^{118,120,121} NCX1,^{56,200,201} and Ca^{2+} -activated ACs (AC isoform 1 [AC1] and AC8).^{173,202,203} When studied individually, these proteins have all been shown to influence the firing rate of pacemaker cells and play a role in the chronotropic response. However, it is evident that there is a high degree of redundancy or mutual cooperation involved in this process, and the relative contribution of each mechanism to efficient autonomic regulation of HR remains to be determined.

HCN CHANNELS STABILIZE SAN FUNCTION DURING THE CHRONOTROPIC RESPONSE

Besides the increasing or decreasing effect on HR by the ANS, 2 more components of the chronotropic response need to be considered (Figure 1): the stability of the HR at a given time point, which is characterized by a specific variability or fluctuation over time (heart rate variability), and the stability of the anatomic position of the leading pacemaker region within the SAN. Together, the 3 components of the

chronotropic response are independently regulated by the ANS. The main function of HCN channels is to dampen and stabilize the electrical activity of the SAN network in time and at a given anatomic position within the SAN at basal conditions and during modulation by the ANS. Thereby, HCN channels ensure smooth changes in HR without rapid fluctuations or even rhythm disturbances in time and with regard to anatomic localization. The detailed mechanisms underlying these HCN channel functions and, in particular, the mechanisms by which these channels

regulate the nonfiring and firing of SAN pacemaker cells are presented in a model (Figure 5).

Mode Shifts of HCN Channels Can Induce Cyclic Changes Between Firing and Nonfiring

The finding that during sufficiently long current-clamp recordings, a substantial fraction of murine WT cells shows transient episodes of nonfiring before returning to rhythmic firing²⁵ (Figure 5A) can be explained by dynamic mode shifts that can specifically be induced

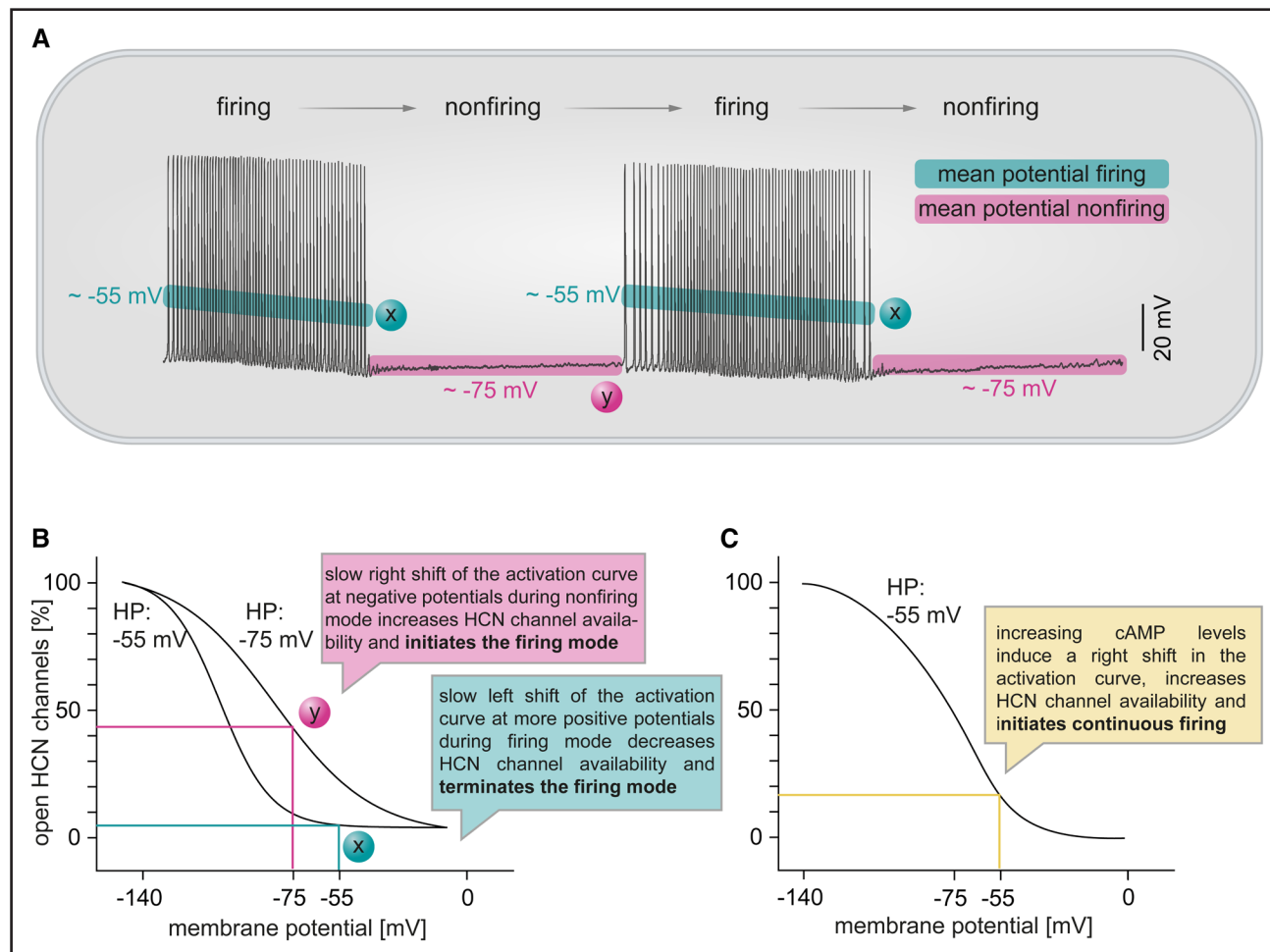


Figure 5. Hysteresis in voltage-dependent activation of hyperpolarization-activated cyclic nucleotide-gated cation channels (HCN channels) may regulate firing and nonfiring.

A, Representative current-clamp recording of a pacemaker cell that spontaneously switched between firing and nonfiring (original action potential [AP] recording of a murine sinoatrial node (SAN) cell adapted from Fenske et al²⁵). The mean membrane potential during firing (cyan) and nonfiring (magenta) is indicated, and the values were corrected for liquid junction potential. The abrupt changes in mean membrane potential at the beginning and end of nonfiring slowly induce dynamic mode shifts in HCN channels (see text for details). **B**, Qualitative model to describe the transition of voltage dependence of HCN4 (hyperpolarization-activated cyclic nucleotide-gated cation channel isoform 4) in SAN cells during firing and nonfiring. Activation curves of HCN4 channels measured in HEK293 cells at 2 different holding potentials (HPs). The HPs of -55 and -75 mV were chosen to reflect the mean membrane potentials during firing and nonfiring, respectively. The relatively positive HP of -55 mV (mimicking firing) induces a slow shift of the activation curve to the left (mode x, cyan) so that fewer HCN channels are open at a given membrane potential. Conversely, the relatively negative HP of -75 mV (mimicking nonfiring) induces a slow shift of the activation curve to the right (mode y, magenta) so that more HCN channels are available. The concomitant changes in I_f are expected to regulate the switch between firing and nonfiring in SAN cells. **C**, Cyclic adenosine monophosphate (cAMP) has an additional effect on the position of the activation curve and determines the amount of open HCN channels. In this way, the autonomic nervous system is expected to regulate the number of nonfiring pacemaker cells in the SAN. The activation curves in **(B and C)** were adapted from Fenske et al.²⁵.

Table 2. Firing and nonfiring pacemaker cells in HCN4 mouse models

HCN4 mouse models	Recording technique (perforated or whole-cell patch-clamp, calcium imaging)	Initial state (firing or dormant)	Initial membrane potential	Measurement duration (reported or determined from figures)
Herrmann et al ⁷³ PMID: 17914461 Inducible global KO	Perforated (ampho)	89% of cells are silent (firing induced by ISO)	Silent, −60 mV	Few seconds before ISO, total recording of 1 min
Hoesl et al ⁷⁴ PMID: 18538341 Inducible cardiac conduction system-specific KO	Perforated (ampho)	55% firing, but then switched to nonfiring 45% silent	Firing, −55 mV Silent, −65 mV	1 min shown during transition to nonfiring
Baruscotti et al ⁷¹ PMID: 21220308 Inducible heart-specific KO	Whole cell	Firing (rate reduced)	Firing, −60 mV	2–4 s shown
Mesirca et al ⁷² PMID: 25144323 Dominant-negative hHCN4-AYA	Perforated (escin)	Firing (arrhythmic, DADs, and rate reduced)	Firing, −64 mV	≈4 s shown
Kozasa et al ⁷⁵ PMID: 29315578 Conditional HCN4 Oex or KD	Whole cell	Oex: firing (normal rate)	Firing, −60 mV	1–2 s shown before ACh
		KD: firing (arrhythmic and rate reduced) Quiescent cells excluded from analysis	Firing, −60 mV	1–2 s shown before ACh
Harzheim et al ¹⁷² PMDI: 18219271 cAMP-insensitive HCN4R669Q, embryonic hearts per cells	Whole cell	Firing (rate reduced)	Firing, −83 mV	≈5 s shown
Alig et al ⁷⁶ PMID: 19570998 cAMP-insensitive hHCN4-573X (conditional, heart-specific)	Perforated (β-escin)	11% firing 61% firing/nonfiring 28% quiescent	Firing, −51 mV Quiescent, NA	1 min shown before ISO, 3 min in total
Fenske et al ²⁵ PMID: 33144559 cAMP-insensitive HCN4FEA (global KI)	Perforated (ampho)	Only initially firing cells were investigated (mutant frequently switched between firing/nonfiring)	Firing, −57 mV Hyperpolarized during nonfiring: MDP ±10 mV	Up to 1 h (minimum 5 min)

ACh indicates acetylcholine; DAD, delayed afterdepolarization; HCN4, hyperpolarization-activated cyclic nucleotide-gated cation channel isoform 4; ISO, isoprenaline; KD, knockdown; KO, knockout; MDP, maximum diastolic potential; NA, not available; and Oex, overexpression.

in HCN channels.^{4,25,32,33} Mode shifts are the cause of voltage-dependent changes in the position of the activation curve: depolarized membrane potentials induce a leftward shift of the activation curve toward more negative voltages (mode x) and hyperpolarized membrane potentials induce a rightward shift of the activation curve toward more positive voltages^{4,25,32,33,204–208} (mode y; Figure 5B). Because in HCN4 channels, these mode shifts occur slowly, the mechanism could drive the slow alternations between firing and nonfiring in the following way.

The different membrane potentials during firing and nonfiring (Figure 5A) have a long-lasting effect, meaning that the cell changes its firing behavior in a history-dependent fashion. An important prerequisite for this scenario is that the activation and deactivation kinetics of HCN4 are substantially slower than the duration of the pacemaker cycle. When the cell is firing, I_h can, therefore, be considered almost constant during the pacemaker potential with only minor oscillations around a constant mean. Consequently, both voltage-dependent activation

and dynamic mode shifts are determined by the mean membrane potential, which suddenly changes at the beginning and end of nonfiring (Figure 5A). During nonfiring, the relatively hyperpolarized membrane potential increases the activation of HCN channels, slowly driving the cell back toward firing. This effect is potentiated by an additional slow shift of the activation curve toward the right (mode y in Figure 5B) so that more HCN channels are open at a given membrane potential and the cell membrane can be depolarized faster. At a critical point, the threshold is reached and the cell returns to rhythmic firing. The effect persists for a while during depolarization (firing) until it slowly declines, the activation curve shifts back toward the left (mode shift to mode x in Figure 5B), fewer HCN channels are open at a given membrane potential, and the MDP slowly hyperpolarizes, eventually leading to the next nonfiring episode. In addition, the binding of cAMP influences the position of the activation curve and facilitates channel opening (Figure 5C). This means that the intrinsic biophysical effect is further

Table 3. Alternative targets linked to nonfiring pacemaker cells

Other mouse models or pharmacological intervention	Recording technique (perforated or whole-cell patch-clamp, calcium imaging)	Initial state (firing or dormant)	Initial membrane potential	Measurement duration (reported or determined from figures)
Ren et al ¹⁷³ PMID: 36509290 AC1 KO	Perforated (ampho) and calcium (Fluo-4)	Initially firing cells, spontaneous switch between firing/nonfiring	Firing \approx -60 mV Hyperpolarized during nonfiring	90 s shown
Groenke et al ³¹ PMID: 24278453 Atrial-specific NCX1 KO	Whole cell	4% firing (sparse/irregular) 96% silent but excitable	KO, -58 mV (WT, -70 mV)	Minimum 5 min
Vinogradova et al ¹⁷⁴ PMID: 11055979 CaMKII inhibition	Perforated (β -escin)	Only initially firing cells were investigated AIP (peptide inhibitor): 75% arrested KN-93 (low dose): 66% arrested KN-93 (high dose): 100% arrested	AIP \approx -40 mV KN-93 \approx -55 mV (ctrl, -66 mV)	\approx 10 sec shown
Vinogradova et al ¹⁵⁷ PMID: 16424365 PKA inhibition	Perforated (β -escin) and calcium (Fluo-3)	Only initially firing cells were investigated PKI (peptide inhibitor): 100% arrested H-89: 100% arrested	PKI \approx -30 mV H-89, NA (ctrl \approx -60 mV)	Few seconds shown

AIP indicates autacamide-2 inhibitory peptide; KO, knockout; NA, not available; PKA, protein kinase A; PKI, autacamide-2 inhibitory peptide; and WT, wild type.

regulated and superimposed by the ANS, which, thereby, controls the cell's firing behavior through sympathetic and parasympathetic signaling.

Quiescent/dormant/nonfiring SAN cells have only recently been identified in WT preparations (Table 1), most likely because nonfiring occurs rarely in the WT, or because experimenters did not further investigate a pacemaker cell, which was nonfiring. In contrast, nonfiring pacemaker cells have been reported before in the context of genetic mouse models, including knockout and loss-of-function mutations in HCN4 (Table 2). Interestingly, intermittent or permanent nonfiring due to impaired or absent HCN4 function was typically accompanied by hyperpolarized membrane potentials,^{25,73,74,76} which could reflect a more frequent occurrence and exaggeration of the spontaneous nonfiring described in WT cells. I_p , thus, provides a depolarization reserve in SAN cells that prevent overshooting hyperpolarization and keep the membrane potential in a range in which diastolic depolarization and tonic firing are, in principle, possible.⁷³ Within this range of membrane potentials, mode shifts in HCN4 cause the voltage-dependent hysteresis that could induce the alternations between firing and nonfiring (Figure 5A and 5B). In addition, the effect is further fine-tuned by the CDR of HCN4 and, thereby, controlled by the ANS. Activation of HCN4 by cAMP contributes to terminating nonfiring episodes (Figure 5C) and maintaining cellular automaticity, while a reduction in HCN4 activity promotes nonfiring. In line with this, transient episodes of nonfiring are heavily increased when the CDR of HCN4 is missing.²⁵ Similar effects were observed in AC1 knockout mice.¹⁷³ AC1 is an important downstream target of beta-adrenergic signaling and forms functional microdomains with HCN4. It is, therefore, well possible that AC1 provides cAMP required for the regulation of HCN4. In addition, dysfunction of several other proteins

has been associated with quiescent SAN cells. Some prominent examples include CaMKII,¹⁷⁴ PKA,¹⁵⁷ $Ca_v1.3$,²⁷ and NCX1³¹ (Table 3).

Interactions Between Firing and Nonfiring Cells Tonicly Entrain and Synchronize the SAN

The main function of the SAN is to ensure a rhythmic heartbeat and to enable smooth HR transitions. This raises the important question of how firing and nonfiring cells interact with each other and how the fraction/number of nonfiring cells is controlled to obtain a stable rhythm in the network of the SAN. The intact SAN is a heterogeneous tissue composed of various cell types connected to each other and embedded in an extracellular matrix of connective tissue, mainly consisting of elastin and collagen fibers.^{17,209} The different cell types include pacemaker cells and atrial myocytes,²¹⁰ sympathetic and parasympathetic neurons,²¹¹ and nonexcitable cells such as fibroblasts²¹² and macrophages.²¹³ Recently, additional components (telocytes and peripheral glia cells), which also belong to the group of nonexcitable cells and further increase the heterogeneity of the SAN, have been discovered.^{14,24} This heterogeneity has even led to the comparison of the SAN with brain-like structures^{33,57,214} or networks, composed of neuron-like cellular components.^{215,216} Within this network, pacemaker cells are weakly electrically coupled to each other via gap junctions. In the central SAN, gap junctions are formed by the connexins Cx30.2 and Cx45 (low conductance), while there is no expression of Cx43 (intermediate conductance) and only little expression of Cx40 (high conductance). In the periphery of the SAN at the border to the surrounding atrial myocardium, Cx43 and Cx45 are expressed.²¹⁷ Through the weak electrical coupling, a mutual and long-lasting interaction process

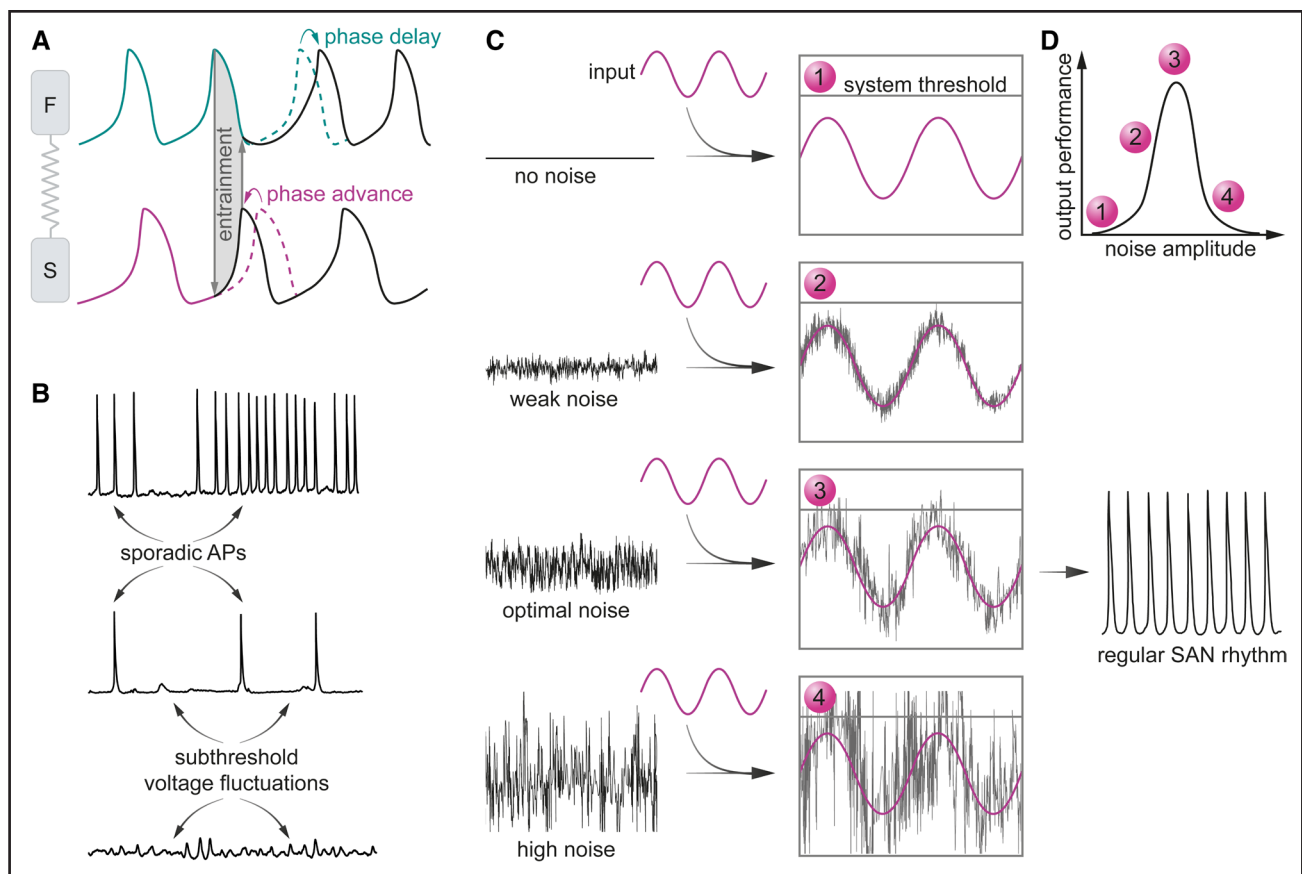


Figure 6. Current models for synchronization of the sinoatrial node (SAN).

A, Mutual entrainment model. Schematic drawings of spontaneous pacemaker potentials of a fast (F) and slow (S) firing cell connected by a high-resistance gap junction. All-or-none action potentials (APs) are conducted through gap junctions. The high coupling resistance attenuates conducted potentials, so they reach the acceptor cell as subthreshold potentials that only evoke subthreshold depolarizations in this cell. Subthreshold potentials shorten or prolong the following pacemaker potential depending on the timing in the cycle, leading to the synchronization of cells to a common network rhythm. For details, see text. **B** through **D**, Stochastic resonance model. **B**, Subthreshold fluctuations in membrane potential are attenuated by gap junctions and add up to subthreshold stochastic voltage noise (shown in **C**). Subthreshold voltage fluctuations may or may not be triggered by intracellular Ca^{2+} signals (not shown). In a realistic situation, in regions close to the superior SAN, large subthreshold voltage signals at the natural frequency of the firing cells would be generated (corresponding to sinusoidal input in **C**), while in the inferior SAN, only small amplitude subthreshold voltage fluctuations with rare pacemaker potentials would be generated, which only contribute to stochastic noise. For details, see text. **C**, **Left**, Addition of noise of increasing amplitude to an arbitrary subthreshold sinusoidal input signal. **Right**, Noise-performance relationship of pacemaker activity. At low noise levels, the threshold is not reached efficiently (1). At successively increasing noise levels, the threshold is reached more efficiently (2) and the performance reaches a peak at the resonance point (3) and then successively decreases as noise levels are further increased (4). **D**, The resonance curve is obtained from analog experiments as shown in **C**. For details, see text. **(A)** was adapted from Michaels et al.²² The voltage traces and APs in **(B and C)** are original current-clamp measurements of murine SAN cells recorded in our laboratory. The noise and sinusoidal input are schematic representations adapted from van der Groen et al.³⁷

between neighboring firing and nonfiring cells will take place, which has been termed tonic entrainment.^{4,25,32,33} Nonfiring cells are more hyperpolarized and will electrotonically draw flows of cations, including Ca^{2+} , from more depolarized firing cells to which they are coupled via gap junctions. As a result, nonfiring cells will slightly depolarize and neighboring firing cells will slightly hyperpolarize. When a new equilibrium is reached, the common firing rate will be decreased and a bradycardic network rhythm will emerge.^{25,33} In this way, nonfiring cells may function as brakes in the SAN network and, continuously, inhibit the activity of surrounding firing cells. In addition, tonic inhibition appears to increase during vagal activity and decrease during beta-adrenergic stimulation,

probably because more cells switch to the nonfiring or firing mode, respectively.^{4,25} While this process is important for setting the baseline HR and stabilizing SAN network activity, it is not involved in changing HR, that is, mediating the frequency aspect of the chronotropic effect.^{4,25,32,33} Like in neuronal networks, inhibitory control of excitability may be essential in the SAN to ensure a robust function of the pacemaker process but requires a stable balance between nonfiring cells (inhibition) and firing cells (excitation). Under physiological conditions, this balance is controlled by the CDR of HCN4, which is particularly important to dampen and fine-tune the HR-lowering effect of the parasympathetic nervous system.^{25,75} In contrast, when activation of HCN4 by cAMP is

missing or disturbed, the fraction of nonfiring pacemaker cells strongly increases. As a consequence, impulse formation in the central SAN and propagation to the atrial myocardium are delayed. Such overshooting inhibition is responsible for SAN dysfunction and secondary arrhythmia, which predominantly occurs during chronotropic responses.²⁵ Taken together, the newly discovered role of HCN4 in the SAN is to regulate the number of nonfiring cells, which is critical for stabilizing the network rhythm and protecting the SAN during ANS-induced HR transitions.^{4,25,32,33} At the same time, the stabilizing action of HCN channels will also stabilize the leading pacemaker region in a given anatomic location.

As pointed out above, nonfiring cells with depolarized membrane potential seem to be present in the SAN. Initially, the existence of such cells in the sinus node has been postulated, and their role has been investigated in computer simulation studies of the sinus node.²¹⁸ Subsequently, depolarized nonfiring pacemaker cells have been experimentally confirmed (Table 1). In addition, nonexcitable cells characterized by depolarized membrane potential such as fibroblasts or macrophages have been described, which could also interact with SAN pacemaker cells via gap junctions in the SAN network. Regardless of whether excitable or nonexcitable, in an intact SAN network a depolarized nonfiring cell, if connected via gap junctions, would induce analog current flow from nonfiring to firing cells as described above, but in the reverse direction, thereby depolarizing firing cells and hyperpolarizing the particular nonfiring cell. This would be expected to accelerate and also to stabilize the network rhythm. The described scenario for tonic entrainment between depolarized nonfiring and neighboring firing cells needs to be experimentally confirmed in future experiments.

In addition to tonic entrainment, a phasic entrainment mechanism has been postulated,^{32,219–222} and experimental evidence has been provided.²²³ Phasic entrainment is faster than tonic entrainment; it contributes to synchronizing spontaneous firing on a beat-to-beat time scale.^{32,219–221} The process is illustrated in Figure 6A in which 2 hypothetical pacemaker cells interact with each other. It is assumed that 1 fast-firing cell (marked with F in Figure 6A) is weakly coupled to a slow-firing cell (marked with S in Figure 6A) and both cells fire all-or-none suprathreshold pacemaker potentials. With weak coupling between cells (solid traces), pacemaker potential firing of 1 cell is conducted to the other but attenuated by high-resistance gap junctions so it produces only subthreshold membrane depolarizations in the other cell. In turn, these subthreshold depolarizations either accelerate or delay the next firing of that cell, depending on timing.²²¹ For example, if the second pacemaker potential of the faster firing cell F occurs at a phase close to the middle of the intrinsic period of S, it induces a shortening of the next pacemaker potential of S, accelerating the firing of this cell. Similarly, this second pacemaker potential of cell S

occurs at an early phase of cell F and induces a prolongation of the next pacemaker cycle of F, slowing down the firing of cell F. The model predicts that by similar interactions as outlined for the 2 cells in Figure 6A, the entire SAN including all pacemaker cells can be entrained to operate at one and the same frequency. The common network frequency would lie in between the frequency that the fastest and slowest cells would generate if they were isolated cells. The model would furthermore predict that phase shifts would arise between individual cells, which would mimic the classical propagation of excitation. However, rather than sequentially activating one cell after the other, there would be apparent conduction resulting from phase shifts between cells. The role of HCN channels in phasic entrainment would be to contribute to synchronization by dampening depolarizing or hyperpolarizing influences and stabilizing the membrane potential in the subthreshold diastolic voltage range.^{32,58,69,224}

Recently, it was shown that some assumptions of the concept of phasic entrainment are not met in the SAN network, and, therefore, the model had to be modified. For example, the cellular heterogeneity of the SAN is considerably higher than initially postulated.^{14,24} There even might be at least 2 separate weakly coupled independent meshworks of HCN4⁺/Cx43⁻/F-actin⁻ cells on the one hand and Cx43⁺/F-actin⁺/HCN4⁻ cells on the other hand.²⁴ In addition, not all pacemaker cells of the SAN fire with the same frequency, rather there are several clusters with differing frequencies giving rise to multicentric SAN activation.^{225,226} In line with this, anatomically distinct subdivisions such as the superior and inferior SAN can be distinguished,^{6,13} which could provide an explanation for pacemaker shifts on activation of the SAN by the parasympathetic or sympathetic nervous system.^{13,226} Further insight into the entrainment process was provided in a recent study, using elaborated imaging techniques.^{14,24} This study postulated that not only suprathreshold all-or-none pacemaker potentials can induce the entrainment process but also subthreshold fluctuations in membrane potential differing in amplitudes, frequency, and kinetics. The subthreshold fluctuations in membrane potential could either arise from LCRs from the SR, which lead to subthreshold Ca²⁺ signals, which, in turn, are transformed into corresponding depolarizing inward currents by the NCX, thereby inducing subthreshold oscillations in membrane potential. In addition, there is evidence for subthreshold fluctuations in membrane potential that are not triggered by local intracellular Ca²⁺ signals.⁶ Regardless of the underlying mechanism, subthreshold fluctuations in membrane potential could become integrated and, eventually, reach the threshold for firing in this particular cell or induce firing in neighboring cells by entrainment.²⁴ In conclusion, the classical entrainment model and also its modification have in common that regular pacemaking results from the reduction of electrical heterogeneity present at the level of single cells.

Interestingly, an alternative conceptual model, termed the stochastic resonance model,^{227,228} postulates exactly the opposite of the entrainment model, that is, that electrical heterogeneity of single pacemaker cells is the motor of regular pacemaking. According to this model, pacemaker cells, in addition to firing suprathreshold APs (firing mode), produce stochastic low-amplitude voltage fluctuations in a range of 4 to 17 mV⁶ (noise; Figure 6B), which, on their own, cannot trigger firing. In the network of the SAN, where firing and nonfiring cells are weakly connected to each other via gap junctions, voltage noise could add to and thereby amplify weak signals (periodic oscillations) at their peaks and increase the probability of crossing the threshold for firing (Figure 6C). It would be expected that successively increasing noise would increase the firing frequency up to a resonance peak at the natural frequency of the firing pacemaker cells and then, when the noise dominates the signal, would decrease firing performance, thus giving rise to a resonance curve (Figure 6D). In the context of the stochastic resonance model, noise would have a positive role in signal processing. This effect could indeed be so efficient that a hypothetical SAN network consisting of only passive pacemaker cells, which only produce subthreshold oscillations, would be integrated to eventually produce suprathreshold network rhythm. This has recently been shown in a modeling study for the SAN.²²⁹ However, in the SAN, nonfiring cells with subthreshold oscillations (eg, inferior SAN) would be expected to be coupled to more periodically active SAN pacemaker cells that fire pacemaker potentials (eg, superior SAN). The noisy nonfiring SAN pacemaker cells would increase the strength and periodicity of tonically firing SAN pacemaker cells and, thereby, the robustness of pacemaker activity. In other words, random subthreshold voltage noise would have stabilizing antiarrhythmic effects on SAN pacemaker activity. Furthermore, all SAN cells are important in driving the system. However, the contribution of the 2 types of cells, that is, the noisy cells and the periodically oscillating cells, would be different. A loss of noisy nonfiring cells with subthreshold fluctuations in membrane potential would reduce the robustness of the system to synchronize and adapt. In contrast, the loss of periodically firing cells from the intrinsically oscillating cells would completely abolish SAN activity.

The resonance model could also explain how the superior SAN, which fires at a high frequency, and the inferior SAN, which fires at a lower frequency, interact.^{6,13} According to the model, most SAN pacemaker cells in the inferior region would generate stochastic subthreshold voltage fluctuations or rare single APs. These signals would only lead to periodic pacemaking when coupled to more periodically firing SAN pacemaker cells, that is, voltage oscillators of the superior SAN. Under these conditions, random subthreshold voltage fluctuations and APs are integrated by stochastic resonance to increase the

probability that superior SAN pacemaker cells reach the AP threshold. Like in dendritic integration in the brain, noisy SAN pacemaker cells would increase the strength and periodicity of tonically firing cells and the overall pacemaker activity of the SAN network. For this model to work, both are needed: the presence of heterogeneity and the presence of the inferior SAN. A recent study shows that loss of heterogeneity or the electrical separation of the inferior from the superior SAN will decrease HR and HR regularity.¹³

HCN CHANNELS IN DISEASE AND THERAPY

Robust pacemaking is central to cardiac physiology, and disturbances in this process give rise to cardiac disease. The most prominent disease of the SAN is sinus node dysfunction (SND), also known as sick sinus syndrome. SND is defined as a group of arrhythmias caused by malfunction of the SAN pacemaker process.^{84,230–233} These include bradycardia, sinus arrest, sinoatrial block, alternations of bradycardia and tachycardia known as tachybrady syndrome, and chronotropic incompetence.²³¹ Importantly, chronotropic incompetence is defined as the inability to adequately increase HR to meet elevated metabolic demands.^{46,48} This is reflected by not reaching the same maximum HR as healthy individuals during exercise, while the range of frequency regulation, albeit at lower absolute HRs, may be preserved. SND is generally considered to be an age-related pathology that develops secondary to degenerative fibrosis of the pacemaker tissue. However, there are other forms of SND, including the genetically caused idiopathic primary SND, and forms that arise secondary to cardiovascular or systemic disease. Typical symptoms of SND are palpitations, dizziness, presyncope, and syncope,^{230,232} but the disease can also occur asymptotically. Only patients with untreated symptomatic SND have a high risk of deterioration to cardiovascular events such as atrial fibrillation, heart failure, and systemic thromboembolism. This is also reflected by the finding that age-related SND and chronotropic incompetence are associated with an increased risk of cardiovascular death and overall mortality.⁸⁴ In a broader context, disturbances in HR regulation by the ANS generally play a significant role in the development and progression of cardiovascular disease. In support of this, there is a well-established link between ANS dysfunction (and subsequent HR dysregulation) and various cardiovascular diseases such as myocardial infarction, congestive heart failure, and arterial hypertension.²³⁴ In addition, pathological input from the ANS can potentially cause secondary SND,⁸⁴ and primary SND can be worsened by ANS imbalance.⁸⁴ Furthermore, bradycardia and SND can develop after cardiac transplantation.²³³ In hypertension, an increased HR will further increase blood

pressure, leading to the worsening of the disease and, as a consequence, a higher risk of myocardial infarction and stroke.²³⁵ Moreover, there is an important link between chronic heart failure (CHF) and SND⁸⁴; both diseases can arise as a consequence of the other, meaning that CHF can develop secondary to SND and vice versa. In this context, atrial fibrillation due to SND can lead to or worsen CHF. Furthermore, tachy-brady syndrome due to SND can have worsening effects in compensated CHF, possibly leading to decompensation and progression to terminal stages of the disease. Similarly, myocardial ischemia can be worsened by tachy-brady syndrome but can also be an important driver of SND. For example, acute stenosis or thrombosis of the SAN artery and myocardial infarction favor SND.⁸⁴ To date, the only definitive treatment option for SND is the implantation of an electronic pacemaker device.²³⁶

Several mutations in ion channels have been identified as the cause of familial forms of primary SND. For a comprehensive analysis of all the human mutations found to be causative of SND, please refer to references^{84,233,237}. Here, we specifically focus on SAN diseases caused by mutations in HCN4 (Table 4). Overall, HCN4 mutations have been linked to sinus bradycardia, chronotropic incompetence, inappropriate sinus tachycardia, and non-compaction cardiomyopathy. The link between changes in I_f and the HR of patients with associated HCN4 mutations has recently been confirmed *in silico*.²³⁸ Noncompaction cardiomyopathy is a congenital disease with not yet fully clarified pathogenesis. It is generally thought to arise from disturbed compaction of the trabeculated myocardium during embryogenesis, which takes place at around 5 to 8 weeks of gestation in humans.^{239–241} In line with this, there is evidence from mouse studies that HCN4 is expressed during early embryonic development in cardiac progenitors of the first heart field and is only later downregulated in the working myocardium.^{83,241–244} Accordingly, HCN4 could have an important signaling function in the normal compaction process, and dysfunction of HCN4 might interfere with molecular mechanisms required for cardiac development.^{239,241} This may cause hypertrabeculation that ultimately leads to noncompaction cardiomyopathy.²⁴¹

Given the important role of HCN channels in these and other physiological and pathophysiological conditions, great efforts have been made to explore the channels as targets for therapeutic intervention.^{245–247} Besides cardiac expression, HCN channels play important roles in neuronal excitability and are linked to diseases of the nervous system such as epilepsy, neuropathic pain, and affective disorders.^{58,246,248–250} Accordingly, several established anticonvulsant, analgesic, anesthetic, and antidepressant drugs have been shown to interact with HCN channels,^{246,248,249,251} which may account for at least part of their therapeutic effect. Because the expression profiles of the 4 HCN channel

isoforms vary between different tissues and cell types, there is ongoing work to identify subtype-specific compounds as potential drug candidates.^{250–254} For example, a series of brain-penetrant HCN1-specific inhibitors have recently been identified that enhance working memory while lacking cardiovascular side effects, qualifying them as possible candidates for the treatment of cognitive dysfunction in brain disorders.²⁵⁵ Moreover, there is ongoing research on peptides based on TRIP8b, an auxiliary subunit that regulates surface expression and modulates the cAMP sensitivity of HCN channels in the brain.^{256–259} This includes the development of small molecules targeting the TRIP8b-HCN interaction,²⁶⁰ as well as the design of shortened membrane-permeable versions of TRIP8b as tools for potential therapeutic use.²⁶¹ Given the crucial role of HCN channels in the development of neuronal and cardiac disease, the search for HCN-targeting drugs continues to be the subject of intensive research.^{262–266}

To date, the only clinically approved drug that specifically targets HCN channels is ivabradine.^{267–270} It does not cross the blood-brain barrier and is, therefore, used as a selective bradycardia-inducing agent.^{246,271} It is currently approved by the US Food and Drug Administration and the European Medicines Agency for the treatment of CHF with systolic dysfunction^{267,269,272,273} and the European Medicines Agency for the symptomatic treatment of chronic stable angina pectoris in patients with coronary artery disease.^{269,274–276} Ivabradine enters and blocks the pore of HCN channels from the intracellular side, thereby reducing I_f and decreasing SDD and the firing rate of pacemaker cells, allowing for a dose-dependent reduction in HR.^{277–280} It can access HCN4 only when the pore is opened by hyperpolarization.^{279,280} The resulting use dependency enables increased efficiency of ivabradine at higher HRs,^{280,281} which has been proven beneficial in patients with normal sinus rhythm at initial HRs of ≥ 70 –75 bpm.^{269,282,283} Interestingly, at the cellular level, the effects on SDD caused by blocking the pore of the channel (ie, slowdown of SDD²⁸⁰) are different from those caused by loss or blockade of CDR (ie, induction of nonfiring but normal SDD during firing mode²⁵). The reason for this apparent inconsistency could be that at therapeutic doses, only part of the channels are blocked, and only with further blockade, the cells would switch to the nonfiring mode. In support of this conclusion, even a partial block of I_f is sufficient to explain the clinically relevant HR-slowness effect of ivabradine.²⁸⁴ In fact, a clinically relevant ivabradine concentration of 3 μM slowed the spontaneous AP firing rate by 15% in isolated rabbit SAN pacemaker cells.²⁸⁴ Importantly, at a membrane potential of -60 mV, which roughly corresponds to the MDP, ivabradine (3 μM) reduced the I_f amplitude by 40%.²⁸⁴ However, in such experiments, repetitive activation/deactivation cycles were necessary to reach a substantial current

Table 4. Human HCN4 mutations causing cardiac disease

Human HCN4 mutations	HCN4 mutation	Clinical characteristics	Region of the channel affected	Effect on the channel/current
Cámara-Checa et al ³¹⁵	V240M	Inappropriate sinus tachycardia	HCN domain	Positive shift of $V_{0.5}$, increased current density, increased single-channel conductance, and faster activation kinetics
Macri et al ³¹⁶	P257S	Atrial fibrillation	N terminus	Reduced current density and channel conductance, and trafficking defective
Alonso-Fernandez-Gatta et al ³¹⁷	R375C	Noncompaction cardiomyopathy, sinus bradycardia, left atrial dilatation, and normal chronotropic competence	Voltage sensor (S4)	Negative shift of $V_{0.5}$, reduced current density and channel conductance, and slower activation kinetics
Moller et al ³¹⁸	R378C	Sinus bradycardia	Voltage sensor (S4)	Negative shift of $V_{0.5}$, Reduced current density, slower activation kinetics, faster deactivation kinetics, reduced expression of the channel, and trafficking defective
Ishikawa et al ²⁴⁴	R393H	Noncompaction cardiomyopathy, sinus bradycardia, atrial fibrillation, and dilated cardiomyopathy	Voltage sensor (S4)	Reduced current density and channel conductance, and smaller slope factor of the activation curves
Milano et al ²³⁹ and Verkerk and Wilders ³¹⁹	A414G	Noncompaction cardiomyopathy and sinus bradycardia	Loop between S4 and S5	Negative shift of $V_{0.5}$, reduced current density, slower activation kinetics, and faster deactivation kinetics
Nof et al ³²⁰ and Paszkowska et al ³²¹	G480R	Noncompaction cardiomyopathy, sinus bradycardia, normal chronotropic competence, and aortic dilation	Pore-forming loop between S5 and S6	Reduced current density and channel conductance, slower activation kinetics, and reduced expression of the channel
Milano et al ²³⁹ and Vermer et al ³²²	Y481H	Noncompaction cardiomyopathy, sinus bradycardia, and aortic dilation	Pore domain	Negative shift of $V_{0.5}$ and reduced current density
Milano et al, ²³⁹ Schweizer et al, ²⁴¹ Millat et al, ³²³ Ishikawa et al, ²⁴⁴ Hanania et al, ³²⁴ Paszkowska et al, ³²¹ and Brunet-Garcia et al ³²⁵	G482R	Noncompaction cardiomyopathy, sinus bradycardia, and aortic dilation	Pore-forming loop between S5 and S6	Negative shift of $V_{0.5}$, reduced current density and channel conductance, and defective ion permeation
Servatius et al ³²⁶	A485E/ I479V	Atrial fibrillation and noncompaction cardiomyopathy	Pore-forming loop between S5 and S6	Reduced current density and channel conductance
Laish-Farkash et al ³²⁷ and Paszkowska et al ³²¹	A485V	Noncompaction cardiomyopathy, sinus bradycardia, and normal chronotropic competence	Loop between the pore domain and S6	Negative shift of $V_{0.5}$, reduced current density and channel conductance, slower activation kinetics, and reduced expression of the channel
Biel et al ³²⁸	V492F	Brugada syndrome	S6	Negative shift of $V_{0.5}$, and reduced current density and channel conductance
Baruscotti et al ³²⁹	R524Q	Inappropriate sinus tachycardia	A' a-helix of the C-linker	Positive shift of $V_{0.5}$ and increased sensitivity to cAMP
Duhme et al ³³⁰	K530N	Atrial fibrillation and tachy-brady syndrome	A' helix of the C-linker	Negative shift of $V_{0.5}$ and slower activation kinetics
Moller et al ³¹⁸	R550H	Sinus bradycardia	C-linker	Reduced current density and reduced expression of the channel
Ueda et al ³³¹	D553N	Sinus bradycardia, QT prolongation, and polymorphic ventricular tachycardia	C-linker	Reduced current density, faster activation kinetics, slower deactivation kinetics, and trafficking defective
Schulze-Bahr et al ³³²	573X	Atrial fibrillation, sinus bradycardia, and chronotropic incompetence	Truncated C terminus before CNBD	Reduced current density and insensitive to cAMP
Wang et al ³³³	R666Q	Sinus bradycardia, QT prolongation, and ventricular tachycardia	CNBD	Reduced current density and channel conductance, no changes in cAMP sensitivity, and increased channel degradation
Milanesi et al ³³⁴	S672R	Sinus bradycardia	CNBD	Negative shift of $V_{0.5}$, faster deactivation kinetics, and normal response to cAMP

(Continued)

Table 4. Continued

Human HCN4 mutations	HCN4 mutation	Clinical characteristics	Region of the channel affected	Effect on the channel/current
Schweizer et al ¹³⁵ and Schweizer et al ²⁴¹	695X	Noncompaction cardiomyopathy, sinus bradycardia, ventricular premature beats, and normal chronotropic competence	Truncated CNBD	Insensitive to cAMP
Schweizer et al ²⁴¹	P883R	Noncompaction cardiomyopathy, sinus bradycardia, and atrial fibrillation	C terminus	Not investigated
Moller et al ³¹⁸	E1193Q	Sinus bradycardia	C terminus	Reduced current density, reduced expression of the channel, and trafficking defective

cAMP indicates cyclic adenosine monophosphate; CNBD, cyclic nucleotide-binding domain; HCN, hyperpolarization-activated cyclic nucleotide-gated cation channel; HCN4, hyperpolarization-activated cyclic nucleotide-gated cation channel isoform 4; and QT, time between the start of the Q wave and the end of the T wave in electrocardiogram recordings.

block, and there was only a little block (around 6%) observed during steady-state activation with a single test pulse to -100 mV.^{279,280} As there is evidence that HCN channels remain open throughout the pacemaker cycle,⁵⁹ the actual reduction in I_f under physiological conditions might be even smaller. Furthermore, part of the HR-reducing effect could also occur on the network level of the whole SAN due to an increased fraction of pacemaker cells entering the nonfiring mode. Successively increasing block larger than 40% would induce bradycardia and, in addition, HR fluctuations and sinus pauses. Eventually, a 100% block of HCN4 would be expected to completely stop the spontaneous beating of SAN cells. This conclusion is supported by results reported in studies using inducible knockout of HCN4 in adult mice, which resulted in a large fraction of quiescent isolated cells.^{73,74} Such a level of reduction in HCN4 activity is not possible with ivabradine because loss of selectivity will already occur at doses, which do not block 100% of HCN channels.^{285–287} Moreover, in addition to quantitative dose-dependent effects, there could be qualitative differences in the effects caused by reducing the current amplitude (knockout of the channel or blocking the pore with ivabradine) and by shifting the activation curve, that is, blocking or switching off CDR of the channel. This could be explained by the fact that different structural domains within the channel are targeted (pore region versus cyclic nucleotide-binding domain) and need to be further investigated in future studies. Importantly, such a qualitative difference should be considered in the development of future drugs that interfere with cAMP modulation of I_f (eg, TRIP8b-related molecules).

Given the limited treatment options available, different strategies have been used to develop biological pacemakers that could potentially replace the electronic devices currently used for the treatment of SND and other arrhythmias. For reviews and the most recent progress, please refer to references ^{288–292}. In line with the focus of this review, it is worth mentioning that

many of the approaches used to generate a biological pacemaker involve HCN channels. Some strategies are based on in situ injection of viral constructs of wild-type or mutated HCN2, HCN1, or chimeric (HCN2/12) genes in canine left atrium, left bundle branch, or rat subsidiary atrial pacemaker.^{70,77,293–296} Overexpression of solely the HCN channel induces spontaneous pacemaker activity at the site of injection. This fits well with the new mechanistic insights from native pacemaker cells that a certain level of I_f is important to maintain the firing mode and keep nonfiring at an appropriate balance. Other approaches involve genetically engineered cardiac or noncardiac cells to express HCN channels. Indeed, it has been shown that overexpression of HCN1 or HCN4 channels could modify ventricular myocyte monolayers and mesenchymal stem cells to become cardiac pacemaker cells.^{297,298} Transplantation of HCN2- or HCN4-mesenchymal stem cells induced stable firing activity in vivo for up to 6 weeks, displaying morphology adaptation to the site of injection.^{299–303} To date, the most promising approach to enhance pacemaker activity and autonomic response involves combining HCN channels with other genes, such as ADRB2 (beta[2]-adrenergic receptor), Ca²⁺-stimulated AC1, dominant-negative inward rectifier K⁺ channel (Kir2.1), or SkM1 (skeletal muscle Na⁺ channel 1).^{304–308} In particular, the HCN2/SkM1 gene hybrid approach achieved results that closely align with clinical requirements.^{290,304} Another promising approach to reprogram ventricular myocytes into pacemaker cells is the reexpression of transcription factors, such as Shox2, Tbx3, Tbx5, and Tbx18, which are physiologically involved in the differentiation of embryonic SAN cells.^{237,290,309} The expression of ≥ 1 of these transcription factors downregulates genes specific for the working myocardium and influences genes relevant for pacemaking.^{310–314} In view of the complexity of sinoatrial pacemaking and the differences in the various promising approaches to develop biological pacemakers, it will be interesting to see in which direction the field will progress in the future.

CONCLUSIONS

The chronotropic response is a complex physiological process by which HR is adapted to changing physical needs. The ANS densely innervates the SAN and regulates the membrane clock and calcium clock proteins to accelerate or decelerate the heart. Only recently, it has become more recognized that nonfiring or dormant pacemaker cells exist in the SAN and play an important role during the chronotropic response. Regulation of HCN4 by cAMP contributes to controlling the number of nonfiring cells rather than changing the frequency of firing cells. In this way, pacemaker channels do not contribute substantially to the frequency-increasing effect of the chronotropic response, while they do control other important aspects of the chronotropic effect, such as stabilization of basal HR and HR transitions, and also dampening of ANS input and limitation of maximal HR reduction by the vagal nerve. Dysfunction of this normally precise mechanism has important implications for a range of physiological and pathophysiological conditions, including the development and progression of cardiovascular disease.

ARTICLE INFORMATION

Affiliations

Institute of Cardiovascular Physiology and Pathophysiology, Biomedical Center Munich, Walter Brendel Centre of Experimental Medicine, Faculty of Medicine (K.H., C.P., C.W.-S.) and Department of Pharmacy, Center for Drug Research (M.B., S.F.), Ludwig-Maximilians-Universität München, Germany. German Centre for Cardiovascular Research (DZHK), Partner Site Munich Heart Alliance, Germany (M.B., S.F.).

Sources of Funding

This work was supported by the German Research Foundation (DFG) grants WA 2597/3-2, FE 1929/2-2, FE 1929/1-1, BI 484/5-2, SFB870 B05, and TRR152 P28.

Disclosures

None.

REFERENCES

- Billman GE. Heart rate variability - a historical perspective. *Front Physiol*. 2011;2:86. doi: 10.3389/fphys.2011.00086
- Keith A, Flack M. The form and nature of the muscular connections between the primary divisions of the vertebrate heart. *J Anat Physiol*. 1907;41:172-189.
- Boyett MR. 'And the beat goes on.' The cardiac conduction system: the wiring system of the heart. *Exp Physiol*. 2009;94:1035-1049. doi: 10.1113/expphysiol.2009.046920
- Hennis K, Rotzer RD, Piantoni C, Biel M, Wahl-Schott C, Fenske S. Speeding up the heart? Traditional and new perspectives on hcn4 function. *Front Physiol*. 2021;12:669029. doi: 10.3389/fphys.2021.669029
- Mangoni ME, Nargeot J. Genesis and regulation of the heart automaticity. *Physiol Rev*. 2008;88:919-982. doi: 10.1152/physrev.00018.2007
- Grainger N, Guarina L, Cudmore RH, Santana LF. The organization of the sinoatrial node microvasculature varies regionally to match local myocyte excitability. *Function (Oxf)*. 2021;2:zqab031. doi: 10.1093/function/zqab031
- Boyett MR, Honjo H, Kodama I. The sinoatrial node, a heterogeneous pacemaker structure. *Cardiovasc Res*. 2000;47:658-687. doi: 10.1016/s0008-6363(00)00135-8
- Schuessler RB, Boineau JP, Bromberg BI. Origin of the sinus impulse. *J Cardiovasc Electrophysiol*. 1996;7:263-274. doi: 10.1111/j.1540-8167.1996.tb00524.x
- Glukhov AV, Fedorov VV, Anderson ME, Mohler PJ, Efimov IR. Functional anatomy of the murine sinus node: high-resolution optical mapping of ankyrin-B heterozygous mice. *Am J Physiol Heart Circ Physiol*. 2010;299:H482-H491. doi: 10.1152/ajpheart.00756.2009
- Shibata N, Inada S, Mitsui K, Honjo H, Yamamoto M, Niwa R, Boyett MR, Kodama I. Pacemaker shift in the rabbit sinoatrial node in response to vagal nerve stimulation. *Exp Physiol*. 2001;86:177-184. doi: 10.1113/eph8602100
- Boineau JP, Schuessler RB, Roeske WR, Autry LJ, Miller CB, Wylds AC. Quantitative relation between sites of atrial impulse origin and cycle length. *Am J Physiol*. 1983;245:H781-H789. doi: 10.1152/ajpheart.1983.245.5.H781
- Fedorov VV, Glukhov AV, Chang R, Kostecky G, Aferol H, Hucker WJ, Wuskell JP, Loew LM, Schuessler RB, Moazzami N, et al. Optical mapping of the isolated coronary-perfused human sinus node. *J Am Coll Cardiol*. 2010;56:1386-1394. doi: 10.1016/j.jacc.2010.03.098
- Brennan JA, Chen Q, Gams A, Dyavanapalli J, Mendelowitz D, Peng W, Efimov IR. Evidence of superior and inferior sinoatrial nodes in the mammalian heart. *JACC Clin Electrophysiol*. 2020;6:1827-1840. doi: 10.1016/j.jacep.2020.09.012
- Bychkov R, Juhaszova M, Calvo-Rubio Barrera M, Donald LAH, Coletta C, Shumaker C, Moorman K, Sirenko ST, Maltsev AV, Sollott SJ, et al. The heart's pacemaker mimics brain cytoarchitecture and function: novel interstitial cells expose complexity of the san. *JACC Clin Electrophysiol*. 2022;8:1191-1215. doi: 10.1016/j.jacep.2022.07.003
- Chandler N, Aslanidi O, Buckley D, Inada S, Birchall S, Atkinson A, Kirk D, Monfredi O, Molenaar P, Anderson R, et al. Computer three-dimensional anatomical reconstruction of the human sinus node and a novel paranodal area. *Anat Rec (Hoboken)*. 2011;294:970-979. doi: 10.1002/ar.21379
- Chandler NJ, Greener ID, Tellez JO, Inada S, Musa H, Molenaar P, Difrancesco D, Baruscotti M, Longhi R, Anderson RH, et al. Molecular architecture of the human sinus node: insights into the function of the cardiac pacemaker. *Circulation*. 2009;119:1562-1575. doi: 10.1161/CIRCULATIONAHA.108.804369
- Monfredi O, Dobrzynski H, Mondal T, Boyett MR, Morris GM. The anatomy and physiology of the sinoatrial node—a contemporary review. *Pacing Clin Electrophysiol*. 2010;33:1392-1406. doi: 10.1111/j.1540-8159.2010.02838.x
- Soattin L, Borbas Z, Caldwell J, Prendergast B, Vohra A, Saeed Y, Hoschitzky A, Yanni J, Atkinson A, Logantha SJ, et al. Structural and functional properties of subsidiary atrial pacemakers in a goat model of sinus node disease. *Front Physiol*. 2021;12:592229. doi: 10.3389/fphys.2021.592229
- Choudhury M, Black N, Alghamdi A, D'Souza A, Wang R, Yanni J, Dobrzynski H, Kingston PA, Zhang H, Boyett MR, et al. Tbx18 overexpression enhances pacemaker function in a rat subsidiary atrial pacemaker model of sick sinus syndrome. *J Physiol*. 2018;596:6141-6155. doi: 10.1113/JP276508
- Morris GM, Boyett MR. Perspectives -- biological pacing, a clinical reality? *Ther Adv Cardiovasc Dis*. 2009;3:479-483. doi: 10.1177/1753944709345792
- Gray AL, Johnson TA, Ardell JL, Massari VJ. Parasympathetic control of the heart. II. A novel interganglionic intrinsic cardiac circuit mediates neural control of heart rate. *J Appl Physiol (1985)*. 2004;96:2273-2278. doi: 10.1152/jappphysiol.00616.2003
- Rozanski GJ, Lipsius SL, Randall WC, Jones SB. Alterations in subsidiary pacemaker function after prolonged subsidiary pacemaker dominance in the canine right atrium. *J Am Coll Cardiol*. 1984;4:535-542. doi: 10.1016/s0735-1097(84)80098-4
- Boineau JP, Canavan TE, Schuessler RB, Cain ME, Corr PB, Cox JL. Demonstration of a widely distributed atrial pacemaker complex in the human heart. *Circulation*. 1988;77:1221-1237. doi: 10.1161/01.cir.77.6.1221
- Bychkov R, Juhaszova M, Tsutsui K, Coletta C, Stern MD, Maltsev VA, Lakatta EG. Synchronized cardiac impulses emerge from heterogeneous local calcium signals within and among cells of pacemaker tissue. *JACC Clin Electrophysiol*. 2020;6:907-931. doi: 10.1016/j.jacep.2020.06.022
- Fenske S, Hennis K, Rotzer RD, Brox VF, Becirovic E, Scharr A, Gruner C, Ziegler T, Mehlfield V, Brennan J, et al. Camp-dependent regulation of hcn4 controls the tonic entrainment process in sinoatrial node pacemaker cells. *Nat Commun*. 2020;11:5555. doi: 10.1038/s41467-020-19304-9
- Kim MS, Maltsev AV, Monfredi O, Maltseva LA, Wirth A, Florio MC, Tsutsui K, Riordan DR, Parsons SP, Tagirova S, et al. Heterogeneity of calcium clock functions in dormant, dysrhythmically and rhythmically firing single pacemaker cells isolated from sa node. *Cell Calcium*. 2018;74:168-179. doi: 10.1016/j.ceca.2018.07.002
- Louradour J, Bortolotti O, Torre E, Bidaud I, Lamb N, Fernandez A, Le Guennec JY, Mangoni ME, Mesirca P. L-type Ca_v1.3 calcium channels are required for beta-adrenergic triggered automaticity

- in dormant mouse sinoatrial pacemaker cells. *Cells*. 2022;11:1114. doi: 10.3390/cells11071114
28. Tsutsui K, Monfredi OJ, Sirenko-Tagirova SG, Maltseva LA, Bychkov R, Kim MS, Ziman BD, Tarasov KV, Tarasova YS, Zhang J, et al. A coupled-clock system drives the automaticity of human sinoatrial nodal pacemaker cells. *Sci Signal*. 2018;11:eaap7608. doi: 10.1126/scisignal.aap7608
 29. Tsutsui K, Florio MC, Yang A, Wirth AN, Yang D, Kim MS, Ziman BD, Bychkov R, Monfredi OJ, Maltsev VA, et al. Camp-dependent signaling restores ap firing in dormant sa node cells via enhancement of surface membrane currents and calcium coupling. *Front Physiol*. 2021;12:596832. doi: 10.3389/fphys.2021.596832
 30. Cho HS, Takano M, Noma A. The electrophysiological properties of spontaneously beating pacemaker cells isolated from mouse sinoatrial node. *J Physiol*. 2003;550:169–180. doi: 10.1113/jphysiol.2003.040501
 31. Groenke S, Larson ED, Alber S, Zhang R, Lamp ST, Ren X, Nakano H, Jordan MC, Karagueuzian HS, Roos KP, et al. Complete atrial-specific knock-out of sodium-calcium exchange eliminates sinoatrial node pacemaker activity. *PLoS One*. 2013;8:e81633. doi: 10.1371/journal.pone.0081633
 32. Hennis K, Biel M, Wahl-Schott C, Fenske S. Beyond pacemaking: HCN channels in sinoatrial node function. *Prog Biophys Mol Biol*. 2021;166:51–60. doi: 10.1016/j.pbiomolbio.2021.03.004
 33. Hennis K, Biel M, Fenske S, Wahl-Schott C. Paradigm shift: new concepts for HCN4 function in cardiac pacemaking. *Pflugers Arch*. 2022;474:649–663. doi: 10.1007/s00424-022-02698-4
 34. Herring N, Kalla M, Paterson DJ. The autonomic nervous system and cardiac arrhythmias: current concepts and emerging therapies. *Nat Rev Cardiol*. 2019;16:707–726. doi: 10.1038/s41569-019-0221-2
 35. Mohanta SK, Yin C, Weber C, Godinho-Silva C, Veiga-Fernandes H, Xu QJ, Chang RB, Habenicht AJR. Cardiovascular brain circuits. *Circ Res*. 2023;132:1546–1565. doi: 10.1161/CIRCRESAHA.123.322791
 36. Wink J, van Delft R, Notenboom RGE, Wouters PF, DeRuiter MC, Plevier JWM, Jongbloed MRM. Human adult cardiac autonomic innervation: controversies in anatomical knowledge and relevance for cardiac neuromodulation. *Auton Neurosci*. 2020;227:102674. doi: 10.1016/j.autneu.2020.102674
 37. Abramovich-Sivan S, Akselrod S. A phase response curve based model: effect of vagal and sympathetic stimulation and interaction on a pacemaker cell. *J Theor Biol*. 1998;192:567–579. doi: 10.1006/jtbi.1998.0684
 38. Bernston GG, Bigger JT Jr, Eckberg DL, Grossman P, Kaufmann PG, Malik M, Nagaraja HN, Porges SW, Saul JP, Stone PH, et al. Heart rate variability: origins, methods, and interpretive caveats. *Psychophysiology*. 1997;34:623–648. doi: 10.1111/j.1469-8986.1997.tb02140.x
 39. McCraty R, Shaffer F. Heart rate variability: new perspectives on physiological mechanisms, assessment of self-regulatory capacity, and health risk. *Glob Adv Health Med*. 2015;4:46–61. doi: 10.7453/gahmj.2014.073
 40. Poirier P. Exercise, heart rate variability, and longevity: the cocoon mystery? *Circulation*. 2014;129:2085–2087. doi: 10.1161/CIRCULATIONAHA.114.009778
 41. Khan AA, Lip GYH, Shantsila A. Heart rate variability in atrial fibrillation: the balance between sympathetic and parasympathetic nervous system. *Eur J Clin Invest*. 2019;49:e13174. doi: 10.1111/eci.13174
 42. Spear JF, Moore EN. Influence of brief vagal and stellate nerve stimulation on pacemaker activity and conduction within the atrioventricular conduction system of the dog. *Circ Res*. 1973;32:27–41. doi: 10.1161/01.res.32.1.27
 43. Rajendran PS, Challis RC, Fowlkes CC, Hanna P, Tompkins JD, Jordan MC, Hiyari S, Gabris-Weber BA, Greenbaum A, Chan KY, et al. Identification of peripheral neural circuits that regulate heart rate using optogenetic and viral vector strategies. *Nat Commun*. 2019;10:1944. doi: 10.1038/s41467-019-09770-1
 44. Hanna P, Dacey MJ, Brennan J, Moss A, Robbins S, Achanta S, Biscola NP, Swid MA, Rajendran PS, Mori S, et al. Innervation and neuronal control of the mammalian sinoatrial node a comprehensive atlas. *Circ Res*. 2021;128:1279–1296. doi: 10.1161/CIRCRESAHA.120.318458
 45. Piantoni C, Carnevali L, Molla D, Barbuti A, DiFrancesco D, Bucci A, Baruscotti M. Age-related changes in cardiac autonomic modulation and heart rate variability in mice. *Front Neurosci*. 2021;15:617698. doi: 10.3389/fnins.2021.617698
 46. Brubaker PH, Kitzman DW. Chronotropic incompetence: causes, consequences, and management. *Circulation*. 2011;123:1010–1020. doi: 10.1161/CIRCULATIONAHA.110.940577
 47. Camm AJ, Fei L. Chronotropic incompetence—part I: normal regulation of the heart rate. *Clin Cardiol*. 1996;19:424–428. doi: 10.1002/clc.4960190518
 48. Zweerink A, van der Lingen ACJ, Handoko ML, van Rossum AC, Allaart CP. Chronotropic incompetence in chronic heart failure. *Circ Heart Fail*. 2018;11:e004969. doi: 10.1161/CIRCHEARTFAILURE.118.004969
 49. Milani-Nejad N, Janssen PM. Small and large animal models in cardiac contraction research: advantages and disadvantages. *Pharmacol Ther*. 2014;141:235–249. doi: 10.1016/j.pharmthera.2013.10.007
 50. Opthof T. Function and structure of the mouse sinus node: nothing you can see that isn't shown. *Cardiovasc Res*. 2001;52:1–4. doi: 10.1016/s0008-6363(01)00417-5
 51. MacDonald EA, Rose RA, Quinn TA. Neurohumoral control of sinoatrial node activity and heart rate: insight from experimental models and findings from humans. *Front Physiol*. 2020;11:170. doi: 10.3389/fphys.2020.00170
 52. Tomek J, Zaccolo M. Compartmentalized cAMP signalling and control of cardiac rhythm. *Philos Trans R Soc Lond B Biol Sci*. 2023;378:20220172. doi: 10.1098/rstb.2022.0172
 53. Maltsev VA, Lakatta EG. Dynamic interactions of an intracellular ca²⁺ clock and membrane ion channel clock underlie robust initiation and regulation of cardiac pacemaker function. *Cardiovasc Res*. 2008;77:274–284. doi: 10.1093/cvr/cvm058
 54. Capel RA, Terrar DA. The importance of ca(2+)-dependent mechanisms for the initiation of the heartbeat. *Front Physiol*. 2015;6:80. doi: 10.3389/fphys.2015.00080
 55. Joung B, Ogawa M, Lin SF, Chen PS. The calcium and voltage clocks in sinoatrial node automaticity. *Korean Circ J*. 2009;39:217–222. doi: 10.4070/kcj.2009.39.6.217
 56. Lakatta EG, Maltsev VA, Vinogradova TM. A coupled system of intracellular ca²⁺ clocks and surface membrane voltage clocks controls the timekeeping mechanism of the heart's pacemaker. *Circ Res*. 2010;106:659–673. doi: 10.1161/CIRCRESAHA.109.206078
 57. Donald L, Lakatta EG. What makes the sinoatrial node tick? A question not for the faint of heart. *Philos Trans R Soc Lond B Biol Sci*. 2023;378:20220180. doi: 10.1098/rstb.2022.0180
 58. Biel M, Wahl-Schott C, Michalakakis S, Zong X. Hyperpolarization-activated cation channels: from genes to function. *Physiol Rev*. 2009;89:847–885. doi: 10.1152/physrev.00029.2008
 59. Peters CH, Liu PW, Morotti S, Gantz SC, Grandi E, Bean BP, Proenza C. Bidirectional flow of the funny current (I_f) during the pacemaking cycle in murine sinoatrial node myocytes. *Proc Natl Acad Sci U S A*. 2021;118:e2104668118. doi: 10.1073/pnas.2104668118
 60. DiFrancesco D. Pacemaker mechanisms in cardiac tissue. *Annu Rev Physiol*. 1993;55:455–472. doi: 10.1146/annurev.ph.55.030193.002323
 61. DiFrancesco D, Ferroni A, Mazzanti M, Tromba C. Properties of the hyperpolarization-activated current (if) in cells isolated from the rabbit sino-atrial node. *J Physiol*. 1986;377:61–88. doi: 10.1113/jphysiol.1986.sp016177
 62. Biel M, Schneider A, Wahl C. Cardiac HCN channels: structure, function, and modulation. *Trends Cardiovasc Med*. 2002;12:206–212. doi: 10.1016/s1050-1738(02)00162-7
 63. Ludwig A, Zong X, Jeglitsch M, Hofmann F, Biel M. A family of hyperpolarization-activated mammalian cation channels. *Nature*. 1998;393:587–591. doi: 10.1038/31255
 64. DiFrancesco D, Tortora P. Direct activation of cardiac pacemaker channels by intracellular cyclic amp. *Nature*. 1991;351:145–147. doi: 10.1038/351145a0
 65. Herrmann S, Layh B, Ludwig A. Novel insights into the distribution of cardiac HCN channels: an expression study in the mouse heart. *J Mol Cell Cardiol*. 2011;51:997–1006. doi: 10.1016/j.jmcc.2011.09.005
 66. Liu J, Dobrzynski H, Yanni J, Boyett MR, Lei M. Organisation of the mouse sinoatrial node: structure and expression of HCN channels. *Cardiovasc Res*. 2007;73:729–738. doi: 10.1016/j.cardiores.2006.11.016
 67. Wahl-Schott C, Biel M. Hcn channels: structure, cellular regulation and physiological function. *Cell Mol Life Sci*. 2009;66:470–494. doi: 10.1007/s00018-008-8525-0
 68. Li N, Csepe TA, Hansen BJ, Dobrzynski H, Higgins RS, Kilic A, Mohler PJ, Janssen PM, Rosen MR, Biesiadecki BJ, et al. Molecular mapping of sinoatrial node HCN channel expression in the human heart. *Circ Arrhythm Electrophysiol*. 2015;8:1219–1227. doi: 10.1161/CIRCEP.115.003070
 69. Fenske S, Krause SC, Hassan SI, Becirovic E, Auer F, Bernard R, Kupatt C, Lange P, Ziegler T, Wotjak CT, et al. Sick sinus syndrome in HCN1-deficient mice. *Circulation*. 2013;128:2585–2594. doi: 10.1161/CIRCULATIONAHA.113.003712
 70. Morris GM, D'Souza A, Dobrzynski H, Lei M, Choudhury M, Billeter R, Kryukova Y, Robinson RB, Kingston PA, Boyett MR. Characterization of a right atrial subsidiary pacemaker and acceleration of the pacing rate by HCN over-expression. *Cardiovasc Res*. 2013;100:160–169. doi: 10.1093/cvr/cvt164
 71. Baruscotti M, Bucci A, Viscomi C, Mandelli G, Gonzalez G, Gneccchi-Rusconi T, Montano N, Casali KR, Micheloni S, Barbuti A, et al. Deep bradycardia and

- heart block caused by inducible cardiac-specific knockout of the pacemaker channel gene *Hcn4*. *Proc Natl Acad Sci U S A* 2011;108:1705–1710. doi: 10.1073/pnas.1010122108
72. Mesirca P, Alig J, Torrente AG, Muller JC, Marger L, Rollin A, Marquilly C, Vincent A, Dubel S, Bidaud I, et al. Cardiac arrhythmia induced by genetic silencing of 'funny' (f) channels is rescued by GIRK4 inactivation. *Nat Commun*. 2014;5:4664. doi: 10.1038/ncomms5664
 73. Herrmann S, Stieber J, Stockl G, Hofmann F, Ludwig A. *Hcn4* provides a 'depolarization reserve' and is not required for heart rate acceleration in mice. *EMBO J*. 2007;26:4423–4432. doi: 10.1038/sj.emboj.7601868
 74. Hoesl E, Stieber J, Herrmann S, Feil S, Tybl E, Hofmann F, Feil R, Ludwig A. Tamoxifen-inducible gene deletion in the cardiac conduction system. *J Mol Cell Cardiol*. 2008;45:62–69. doi: 10.1016/j.yjmcc.2008.04.008
 75. Kozasa Y, Nakashima N, Ito M, Ishikawa T, Kimoto H, Ushijima K, Makita N, Takano M. HCN4 pacemaker channels attenuate the parasympathetic response and stabilize the spontaneous firing of the sinoatrial node. *J Physiol*. 2018;596:809–825. doi: 10.1113/JP275303
 76. Alig J, Marger L, Mesirca P, Ehmke H, Mangoni ME, Isbrandt D. Control of heart rate by cAMP sensitivity of HCN channels. *Proc Natl Acad Sci U S A*. 2009;106:12189–12194. doi: 10.1073/pnas.0810332106
 77. Plotnikov AN, Bucchi A, Shlapakova I, Danilo P Jr, Brink PR, Robinson RB, Cohen IS, Rosen MR. HCN212-channel biological pacemakers manifesting ventricular tachyarrhythmias are responsive to treatment with I(f) blockade. *Heart Rhythm*. 2008;5:282–288. doi: 10.1016/j.hrthm.2007.09.028
 78. Shi W, Wymore R, Yu H, Wu J, Wymore RT, Pan Z, Robinson RB, Dixon JE, McKinnon D, Cohen IS. Distribution and prevalence of hyperpolarization-activated cation channel (HCN) mRNA expression in cardiac tissues. *Circ Res*. 1999;85:e1–e6. doi: 10.1161/01.res.85.1.e1
 79. Han W, Bao W, Wang Z, Nattel S. Comparison of ion-channel subunit expression in canine cardiac Purkinje fibers and ventricular muscle. *Circ Res*. 2002;91:790–797. doi: 10.1161/01.res.0000039534.18114.d9
 80. Marger L, Mesirca P, Alig J, Torrente A, Dubel S, Engeland B, Kanani S, Fontanaud P, Striessnig J, Shin HS, et al. Pacemaker activity and ionic currents in mouse atrioventricular node cells. *Channels (Austin)*. 2011;5:241–250. doi: 10.4161/chan.5.3.15264
 81. Marger L, Mesirca P, Alig J, Torrente A, Dubel S, Engeland B, Kanani S, Fontanaud P, Striessnig J, Shin HS, et al. Functional roles of $Ca_v(1.3)$, $Ca_v(3.1)$ and HCN channels in automaticity of mouse atrioventricular cells: insights into the atrioventricular pacemaker mechanism. *Channels (Austin)*. 2011;5:251–261. doi: 10.4161/chan.5.3.15266
 82. Milanesi R, Bucchi A, Baruscotti M. The genetic basis for inherited forms of sinoatrial dysfunction and atrioventricular node dysfunction. *J Interv Card Electrophysiol*. 2015;43:121–134. doi: 10.1007/s10840-015-9998-z
 83. Liang X, Wang G, Lin L, Lowe J, Zhang Q, Bu L, Chen Y, Chen J, Sun Y, Evans SM. HCN4 dynamically marks the first heart field and conduction system precursors. *Circ Res*. 2013;113:399–407. doi: 10.1161/circresaha.113.301588
 84. Mesirca P, Fedorov VV, Hund TJ, Torrente AG, Bidaud I, Mohler PJ, Mangoni ME. Pharmacologic approach to sinoatrial node dysfunction. *Annu Rev Pharmacol Toxicol*. 2021;61:757–778. doi: 10.1146/annurev-pharmtox-031120-115815
 85. Mesirca P, Torrente AG, Mangoni ME. T-type channels in the sino-atrial and atrioventricular pacemaker mechanism. *Pflügers Arch*. 2014;466:791–799. doi: 10.1007/s00424-014-1482-6
 86. Ono K, Iijima T. Pathophysiological significance of t-type Ca^{2+} channels: properties and functional roles of t-type Ca^{2+} channels in cardiac pacemaking. *J Pharmacol Sci*. 2005;99:197–204. doi: 10.1254/jphs.fmj05002x2
 87. Baumann L, Gerstner A, Zong X, Biel M, Wahl-Schott C. Functional characterization of the l-type Ca^{2+} channel $cav1.4\alpha1$ from mouse retina. *Invest Ophthalmol Vis Sci*. 2004;45:708–713. doi: 10.1167/iov.03-0937
 88. Mangoni ME, Couette B, Bourinot E, Platzer J, Reimer D, Striessnig J, Nargeot J. Functional role of l-type $cav1.3$ Ca^{2+} channels in cardiac pacemaker activity. *Proc Natl Acad Sci U S A*. 2003;100:5543–5548. doi: 10.1073/pnas.0935295100
 89. Mesirca P, Chemin J, Barrere C, Torre E, Gallot L, Monteil A, Bidaud I, Diochot S, Lazdunski M, Soong TW, et al. Selective blockade of $Ca_v1.2$ ($\alpha1c$) versus $Ca_v1.3$ ($\alpha1d$) l-type calcium channels by the black mamba toxin calciseptine. *Nat Commun*. 2024;15:54. doi: 10.1038/s41467-023-43502-w
 90. Maier SK, Westenbroek RE, Yamanushi TT, Dobrzynski H, Boyett MR, Catterall WA, Scheuer T. An unexpected requirement for brain-type sodium channels for control of heart rate in the mouse sinoatrial node. *Proc Natl Acad Sci U S A*. 2003;100:3507–3512. doi: 10.1073/pnas.2627986100
 91. Lei M, Jones SA, Liu J, Lancaster MK, Fung SS, Dobrzynski H, Camelliti P, Maier SK, Noble D, Boyett MR. Requirement of neuronal- and cardiac-type sodium channels for murine sinoatrial node pacemaking. *J Physiol*. 2004;559:835–848. doi: 10.1113/jphysiol.2004.068643
 92. Li N, Kalyanasundaram A, Hansen BJ, Artiga EJ, Sharma R, Abdulwahed SH, Helfrich KM, Rozenberg G, Wu PJ, Zakharkin S, et al. Impaired neuronal sodium channels cause intranodal conduction failure and reentrant arrhythmias in human sinoatrial node. *Nat Commun*. 2020;11:512. doi: 10.1038/s41467-019-14039-8
 93. Mitsuiye T, Shinagawa Y, Noma A. Sustained inward current during pacemaker depolarization in mammalian sinoatrial node cells. *Circ Res*. 2000;87:88–91. doi: 10.1161/01.res.87.2.88
 94. Toyoda F, Ding WG, Matsuura H. Heterogeneous functional expression of the sustained inward Na^+ current in guinea pig sinoatrial node cells. *Pflügers Arch*. 2018;470:481–490. doi: 10.1007/s00424-017-2091-y
 95. Shinagawa Y, Satoh H, Noma A. The sustained inward current and inward rectifier K^+ current in pacemaker cells dissociated from rat sinoatrial node. *J Physiol*. 2000;523(Pt 3):593–605. doi: 10.1111/j.1469-7793.2000.t01-2-00593.x
 96. Guo J, Ono K, Noma A. A sustained inward current activated at the diastolic potential range in rabbit sino-atrial node cells. *J Physiol*. 1995;483(Pt 1):1–13. doi: 10.1113/jphysiol.1995.sp020563
 97. Torrente AG, Mesirca P, Bidaud I, Mangoni ME. Channelopathies of voltage-gated l-type $cav1.3/\alpha_{1d}$ and t-type $cav3.1/\alpha_{1g}$ Ca^{2+} channels in dysfunction of heart automaticity. *Pflügers Arch*. 2020;472:817–830. doi: 10.1007/s00424-020-02421-1
 98. Toyoda F, Mesirca P, Dubel S, Ding WG, Striessnig J, Mangoni ME, Matsuura H. $Ca_v1.3$ l-type Ca^{2+} channel contributes to the heartbeat by generating a dihydropyridine-sensitive persistent Na^+ current. *Sci Rep*. 2017;7:7869. doi: 10.1038/s41598-017-08191-8
 99. Clark RB, Mangoni ME, Lueger A, Couette B, Nargeot J, Giles WR. A rapidly activating delayed rectifier K^+ current regulates pacemaker activity in adult mouse sinoatrial node cells. *Am J Physiol Heart Circ Physiol*. 2004;286:H1757–H1766. doi: 10.1152/ajpheart.00753.2003
 100. Temple J, Frias P, Rottman J, Yang T, Wu Y, Verheijck EE, Zhang W, Siprachanh C, Kanki H, Atkinson JB, et al. Atrial fibrillation in KCNE1-null mice. *Circ Res*. 2005;97:62–69. doi: 10.1161/01.RES.0000173047.42236.88
 101. Lei M, Honjo H, Kodama I, Boyett MR. Characterisation of the transient outward K^+ current in rabbit sinoatrial node cells. *Cardiovasc Res*. 2000;46:433–441. doi: 10.1016/s0008-6363(00)00036-5
 102. Uese K, Hagiwara N, Miyawaki T, Kasanuki H. Properties of the transient outward current in rabbit sino-atrial node cells. *J Mol Cell Cardiol*. 1999;31:1975–1984. doi: 10.1006/jmcc.1999.1028
 103. Wang Z, Feng J, Shi H, Pond A, Nerbonne JM, Nattel S. Potential molecular basis of different physiological properties of the transient outward K^+ current in rabbit and human atrial myocytes. *Circ Res*. 1999;84:551–561. doi: 10.1161/01.res.84.5.551
 104. Irisawa H, Brown HF, Giles W. Cardiac pacemaking in the sinoatrial node. *Physiol Rev*. 1993;73:197–227. doi: 10.1152/physrev.1993.73.1.197
 105. Wickman K, Krapivinsky G, Corey S, Kennedy M, Nemeč J, Medina I, Clapham DE. Structure, g protein activation, and functional relevance of the cardiac g protein-gated K^+ channel, IKACH. *Ann N Y Acad Sci*. 1999;868:386–398. doi: 10.1111/j.1749-6632.1999.tb11300.x
 106. Lei Q, Jones MB, Talley EM, Schrier AD, McIntire WE, Garrison JC, Bayliss DA. Activation and inhibition of g protein-coupled inwardly rectifying potassium (Kir3) channels by G protein beta gamma subunits. *Proc Natl Acad Sci U S A*. 2000;97:9771–9776. doi: 10.1073/pnas.97.17.9771
 107. Mesirca P, Marger L, Toyoda F, Rizzetto R, Audoubert M, Dubel S, Torrente AG, Difrancesco ML, Muller JC, Leoni AL, et al. The g-protein-gated K^+ channel, IKACH, is required for regulation of pacemaker activity and recovery of resting heart rate after sympathetic stimulation. *J Gen Physiol*. 2013;142:113–126. doi: 10.1085/jgp.201310996
 108. Wickman K, Nemeč J, Gendler SJ, Clapham DE. Abnormal heart rate regulation in GIRK4 knockout mice. *Neuron*. 1998;20:103–114. doi: 10.1016/s0896-6273(00)80438-9
 109. Fukuzaki K, Sato T, Miki T, Seino S, Nakaya H. Role of sarcolemmal ATP-sensitive K^+ channels in the regulation of sinoatrial node automaticity: an evaluation using Kir6.2-deficient mice. *J Physiol*. 2008;586:2767–2778. doi: 10.1113/jphysiol.2007.148932
 110. Aziz Q, Finlay M, Montaigne D, Ojake L, Li Y, Anderson N, Ludwig A, Tinker A. ATP-sensitive potassium channels in the sinoatrial node contribute to heart rate control and adaptation to hypoxia. *J Biol Chem*. 2018;293:8912–8921. doi: 10.1074/jbc.RA118.002775

111. Vedovato N, Rorsman O, Hennis K, Ashcroft FM, Proks P. Role of the C-terminus of sur in the differential regulation of β -cell and cardiac K_{ATP} channels by MgADP and metabolism. *J Physiol*. 2018;596:6205–6217. doi: 10.1113/JP276708
112. Noma A, Irisawa H. Contribution of an electrogenic sodium pump to the membrane potential in rabbit sinoatrial node cells. *Pflügers Arch*. 1975;358:289–301. doi: 10.1007/BF00580527
113. Sakai R, Hagiwara N, Matsuda N, Kassanuki H, Hosoda S. Sodium-potassium pump current in rabbit sino-atrial node cells. *J Physiol*. 1996;490 (Pt 1):51–62. doi: 10.1113/jphysiol.1996.sp021126
114. Xia XM, Fakler B, Rivard A, Wayman G, Johnson-Pais T, Keen JE, Ishii T, Hirschberg B, Bond CT, Lutsenko S, et al. Mechanism of calcium gating in small-conductance calcium-activated potassium channels. *Nature*. 1998;395:503–507. doi: 10.1038/26758
115. Fanger CM, Ghanshani S, Logsdon NJ, Rauer H, Kalman K, Zhou J, Beckingham K, Chandy KG, Cahalan MD, Aiyar J. Calmodulin mediates calcium-dependent activation of the intermediate conductance KCa channel, $IKCa1$. *J Biol Chem*. 1999;274:5746–5754. doi: 10.1074/jbc.274.9.5746
116. Schreiber M, Salkoff L. A novel calcium-sensing domain in the BK channel. *Biophys J*. 1997;73:1355–1363. doi: 10.1016/S0006-3495(97)78168-2
117. Xia XM, Zeng X, Lingle CJ. Multiple regulatory sites in large-conductance calcium-activated potassium channels. *Nature*. 2002;418:880–884. doi: 10.1038/nature00956
118. Chen WT, Chen YC, Lu YY, Yao YH, Huang JH, Lin YK, Chen SA, Chen YJ. Apamin modulates electrophysiological characteristics of the pulmonary vein and the sinoatrial node. *Eur J Clin Invest*. 2013;43:957–963. doi: 10.1111/eci.12125
119. Torrente AG, Zhang R, Wang H, Zaini A, Kim B, Yue X, Philipson KD, Goldhaber JL. Contribution of small conductance k^+ channels to sinoatrial node pacemaker activity: insights from atrial-specific Na^+/Ca^{2+} exchange knockout mice. *J Physiol*. 2017;595:3847–3865. doi: 10.1113/JP274249
120. Haron-Khoun S, Weisbrod D, Bueno H, Yadin D, Behar J, Peretz A, Binah O, Hochhauser E, Eldar M, Yaniv Y, et al. SK4 K^+ channels are therapeutic targets for the treatment of cardiac arrhythmias. *EMBO Mol Med*. 2017;9:415–429. doi: 10.15252/emmm.201606937
121. Lai MH, Wu Y, Gao Z, Anderson ME, Dalziel JE, Meredith AL. BK channels regulate sinoatrial node firing rate and cardiac pacing in vivo. *Am J Physiol Heart Circ Physiol*. 2014;307:H1327–H1338. doi: 10.1152/ajpheart.00354.2014
122. Weisbrod D. Small and intermediate calcium activated potassium channels in the heart: role and strategies in the treatment of cardiovascular diseases. *Front Physiol*. 2020;11:590534. doi: 10.3389/fphys.2020.590534
123. Torrente AG, Zhang R, Zaini A, Giani JF, Kang J, Lamp ST, Philipson KD, Goldhaber JL. Burst pacemaker activity of the sinoatrial node in sodium-calcium exchanger knockout mice. *Proc Natl Acad Sci U S A*. 2015;112:9769–9774. doi: 10.1073/pnas.1505670112
124. Herrmann S, Lipp P, Wiesen K, Stieber J, Nguyen H, Kaiser E, Ludwig A. The cardiac sodium-calcium exchanger NCX1 is a key player in the initiation and maintenance of a stable heart rhythm. *Cardiovasc Res*. 2013;99:780–788. doi: 10.1093/cvr/cvt154
125. Baartscheer A, Schumacher CA, Coronel R, Fiolet JW. The driving force of the Na/Ca -exchanger during metabolic inhibition. *Front Physiol*. 2011;2:10. doi: 10.3389/fphys.2011.00010
126. Bers DM, Christensen DM, Nguyen TX. Can Ca entry via $Na-Ca$ exchange directly activate cardiac muscle contraction? *J Mol Cell Cardiol*. 1988;20:405–414. doi: 10.1016/s0022-2828(88)80132-9
127. Hof T, Chaigne S, Recalde A, Salle L, Brette F, Guinamard R. Transient receptor potential channels in cardiac health and disease. *Nat Rev Cardiol*. 2019;16:344–360. doi: 10.1038/s41569-018-0145-2
128. Ju YK, Chu Y, Chaulet H, Lai D, Gervasio OL, Graham RM, Cannell MB, Allen DG. Store-operated Ca^{2+} influx and expression of TRPC genes in mouse sinoatrial node. *Circ Res*. 2007;100:1605–1614. doi: 10.1161/CIRCRESAHA.107.152181
129. Wen H, Gwathmey JK, Xie LH. Role of transient receptor potential canonical channels in heart physiology and pathophysiology. *Front Cardiovasc Med*. 2020;7:24. doi: 10.3389/fcvm.2020.00024
130. Demion M, Bois P, Launay P, Guinamard R. TRPM4, a Ca^{2+} -activated non-selective cation channel in mouse sino-atrial node cells. *Cardiovasc Res*. 2007;73:531–538. doi: 10.1016/j.cardiores.2006.11.023
131. Guinamard R, Bouvagnet P, Hof T, Liu H, Simard C, Salle L. TRPM4 in cardiac electrical activity. *Cardiovasc Res*. 2015;108:21–30. doi: 10.1093/cvr/cvt213
132. Hof T, Simard C, Rouet R, Salle L, Guinamard R. Implication of the TRPM4 nonselective cation channel in mammalian sinus rhythm. *Heart Rhythm*. 2013;10:1683–1689. doi: 10.1016/j.hrthm.2013.08.014
133. Sah R, Mesirca P, Van den Boogert M, Rosen J, Mably J, Mangoni ME, Clapham DE. Ion channel-kinase TRPM7 is required for maintaining cardiac automaticity. *Proc Natl Acad Sci U S A*. 2013;110:E3037–E3046. doi: 10.1073/pnas.1311865110
134. Quinn TA, Kohl P. Cardiac mechano-electric coupling: acute effects of mechanical stimulation on heart rate and rhythm. *Physiol Rev*. 2021;101:37–92. doi: 10.1152/physrev.00036.2019
135. MacDonald EA, Madl J, Greiner J, Ramadan AF, Wells SM, Torrente AG, Kohl P, Rog-Zielinska EA, Quinn TA. Sinoatrial node structure, mechanics, electrophysiology and the chronotropic response to stretch in rabbit and mouse. *Front Physiol*. 2020;11:809. doi: 10.3389/fphys.2020.00809
136. Arbel Ganon L, Eid R, Hamra M, Yaniv Y. The mechano-electric feedback mediates the dual effect of stretch in mouse sinoatrial tissue. *Journal of Molecular and Cellular Cardiology Plus*. 2023;5. doi: 10.1016/j.jmccpl.2023.100042
137. Cooper RJ, Kohl P. Species- and preparation-dependence of stretch effects on sino-atrial node pacemaking. *Ann N Y Acad Sci*. 2005;1047:324–335. doi: 10.1196/annals.1341.029
138. Blinks JR. Positive chronotropic effect of increasing right atrial pressure in the isolated mammalian heart. *Am J Physiol*. 1956;186:299–303. doi: 10.1152/ajplegacy.1956.186.2.299
139. Eijsbouts SC, Majidi M, van Zandvoort M, Allestie MA. Effects of acute atrial dilation on heterogeneity in conduction in the isolated rabbit heart. *J Cardiovasc Electrophysiol*. 2003;14:269–278. doi: 10.1046/j.1540-8167.2003.02280.x
140. Han S, Wilson SJ, Bolter CP. Tertiapin-Q removes a mechanosensitive component of muscarinic control of the sinoatrial pacemaker in the rat. *Clin Exp Pharmacol Physiol*. 2010;37:900–904. doi: 10.1111/j.1440-1681.2010.05408.x
141. Rossberg F, Seim H, Strack E. Chronotropic effects of the reversed carboxyl (RC) analogue of acetylcholine (beta-homobetaine methylester) at defined intraluminal pressures on isolated right rabbit atria. *Res Exp Med (Berl)*. 1985;185:139–144. doi: 10.1007/BF01854899
142. Wilson SJ, Bolter CP. Do cardiac neurons play a role in the intrinsic control of heart rate in the rat? *Exp Physiol*. 2002;87:675–682. doi: 10.1113/eph8702364
143. Cooper RJ, Lei M, Cheng LX, Kohl P. Selected contribution: axial stretch increases spontaneous pacemaker activity in rabbit isolated sinoatrial node cells. *J Appl Physiol (1985)*. 2000;89:2099–2104. doi: 10.1152/jappl.2000.89.5.2099
144. Turner D, Kang C, Mesirca P, Hong J, Mangoni ME, Glukhov AV, Sah R. Electrophysiological and molecular mechanisms of sinoatrial node mechanosensitivity. *Front Cardiovasc Med*. 2021;8:662410. doi: 10.3389/fcvm.2021.662410
145. Peyronnet R, Nerbonne JM, Kohl P. Cardiac mechano-gated ion channels and arrhythmias. *Circ Res*. 2016;118:311–329. doi: 10.1161/CIRCRESAHA.115.305043
146. Calloe K, Elmedy P, Olesen SP, Jorgensen NK, Grunnet M. Hypoosmotic cell swelling as a novel mechanism for modulation of cloned HCN2 channels. *Biophys J*. 2005;89:2159–2169. doi: 10.1529/biophysj.105.063792
147. Lin W, Laitko U, Juranka PF, Morris CE. Dual stretch responses of mHCN2 pacemaker channels: accelerated activation, accelerated deactivation. *Biophys J*. 2007;92:1559–1572. doi: 10.1529/biophysj.106.092478
148. Baumgarten CM, Deng W, Raucis FJ. 27 cell volume-sensitive ion channels and transporters in cardiac myocytes. In: Kohl P, Sachs F, Franz MR, eds. *Cardiac Mechano-Electric Coupling and Arrhythmias*. Oxford University Press; 2011:27–34.
149. Bolter CP, Wilson SJ. Influence of right atrial pressure on the cardiac pacemaker response to vagal stimulation. *Am J Physiol*. 1999;276:R1112–R1117. doi: 10.1152/ajpregu.1999.276.4.R1112
150. Wilson SJ, Bolter CP. Interaction of the autonomic nervous system with intrinsic cardiac rate regulation in the guinea-pig, cavia porcellus. *Comp Biochem Physiol A Mol Integr Physiol*. 2001;130:723–730. doi: 10.1016/s1095-6433(01)00404-4
151. Bogdanov KY, Vinogradova TM, Lakatta EG. Sinoatrial nodal cell ryanodine receptor and $Na(+)-Ca(2+)$ exchanger: molecular partners in pacemaker regulation. *Circ Res*. 2001;88:1254–1258. doi: 10.1161/hh1201.092095
152. Rigg L, Heath BM, Cui Y, Terrar DA. Localisation and functional significance of ryanodine receptors during beta-adrenoceptor stimulation in the guinea-pig sino-atrial node. *Cardiovasc Res*. 2000;48:254–264. doi: 10.1016/s0008-6363(00)00153-x
153. Vinogradova TM, Zhou YY, Maltsev V, Lyashkov A, Stern M, Lakatta EG. Rhythmic ryanodine receptor Ca^{2+} releases during diastolic depolarization of sinoatrial pacemaker cells do not require membrane depolarization. *Circ Res*. 2004;94:802–809. doi: 10.1161/01.RES.0000122045.55331.0F

154. Baudot M, Torre E, Bidaud I, Louradour J, Torrente AG, Fossier L, Talssi L, Nargeot J, Barrere-Lemaire S, Mesirca P, et al. Concomitant genetic ablation of L-type $\text{Ca}_v1.3$ (α_{1D}) and T-type $\text{Ca}_v3.1$ (α_{1E}) Ca^{2+} channels disrupts heart automaticity. *Sci Rep*. 2020;10:18906. doi: 10.1038/s41598-020-76049-7
155. Chen B, Wu Y, Mohler PJ, Anderson ME, Song LS. Local control of Ca^{2+} -induced Ca^{2+} release in mouse sinoatrial node cells. *J Mol Cell Cardiol*. 2009;47:706–715. doi: 10.1016/j.jmcc.2009.07.007
156. Torrente AG, Mesirca P, Neco P, Rizzetto R, Dubel S, Barrere C, Sinegger-Brauns M, Striessnig J, Richard S, Nargeot J, et al. L-type $\text{Ca}_v1.3$ channels regulate ryanodine receptor-dependent Ca^{2+} release during sinoatrial node pacemaker activity. *Cardiovasc Res*. 2016;109:451–461. doi: 10.1093/cvr/cvw006
157. Vinogradova TM, Lyashkov AE, Zhu W, Ruknudin AM, Sirenko S, Yang D, Deo S, Barlow M, Johnson S, Caffrey JL, et al. High basal protein kinase a-dependent phosphorylation drives rhythmic internal Ca^{2+} store oscillations and spontaneous beating of cardiac pacemaker cells. *Circ Res*. 2006;98:505–514. doi: 10.1161/01.RES.0000204575.94040.d1
158. Tagirova Sirenko S, Tsutsui K, Tarasov KV, Yang D, Wirth AN, Maltsev VA, Ziman BD, Yaniv Y, Lakatta EG. Self-similar synchronization of calcium and membrane potential transitions during action potential cycles predict heart rate across species. *JACC Clin Electrophysiol*. 2021;7:1331–1344. doi: 10.1016/j.jacep.2021.02.016
159. Vinogradova TM, Brochet DX, Sirenko S, Li Y, Spurgeon H, Lakatta EG. Sarcoplasmic reticulum Ca^{2+} pumping kinetics regulates timing of local Ca^{2+} releases and spontaneous beating rate of rabbit sinoatrial node pacemaker cells. *Circ Res*. 2010;107:767–775. doi: 10.1161/CIRCRESAHA.110.220517
160. Vinogradova TM, Tagirova Sirenko S, Lakatta EG. Unique Ca^{2+} -cycling protein abundance and regulation sustains local Ca^{2+} releases and spontaneous firing of rabbit sinoatrial node cells. *Int J Mol Sci*. 2018;19:2173. doi: 10.3390/ijms19082173
161. Toth N, Loewe A, Szlovak J, Kohajda Z, Bitay G, Levijoki J, Papp JG, Varro A, Nagy N. The reverse mode of the $\text{Na}^+/\text{Ca}^{2+}$ exchanger contributes to the pacemaker mechanism in rabbit sinus node cells. *Sci Rep*. 2022;12:21830. doi: 10.1038/s41598-022-25574-8
162. Capel RA, Bose SJ, Collins TP, Rajasundaram S, Ayagama T, Zaccolo M, Burton RB, Terrar DA. IP_3 -mediated Ca^{2+} release regulates atrial Ca^{2+} transients and pacemaker function by stimulation of adenylyl cyclases. *Am J Physiol Heart Circ Physiol*. 2021;320:H95–H107. doi: 10.1152/ajpheart.00380.2020
163. Ju YK, Liu J, Lee BH, Lai D, Woodcock EA, Lei M, Cannell MB, Allen DG. Distribution and functional role of inositol 1,4,5-trisphosphate receptors in mouse sinoatrial node. *Circ Res*. 2011;109:848–857. doi: 10.1161/CIRCRESAHA.111.243824
164. Kapoor N, Tran A, Kang J, Zhang R, Philipson KD, Goldhaber JL. Regulation of calcium clock-mediated pacemaking by inositol-1,4,5-trisphosphate receptors in mouse sinoatrial nodal cells. *J Physiol*. 2015;593:2649–2663. doi: 10.1113/JP270082
165. Glukhov AV, Kalyanasundaram A, Lou Q, Hage LT, Hansen BJ, Belevych AE, Mohler PJ, Knollmann BC, Periasamy M, Gyorke S, et al. Calsequestrin 2 deletion causes sinoatrial node dysfunction and atrial arrhythmias associated with altered sarcoplasmic reticulum calcium cycling and degenerative fibrosis within the mouse atrial pacemaker complex1. *Eur Heart J*. 2015;36:686–697. doi: 10.1093/eurheartj/eh452
166. MacDonald EA, Quinn TA. What keeps us ticking? Sinoatrial node mechanosensitivity: the grandfather clock of cardiac rhythm. *Biophys Rev*. 2021;13:707–716. doi: 10.1007/s12551-021-00831-8
167. Linscheid N, Logantha S, Poulsen PC, Zhang S, Schrolkamp M, Egerod KL, Thompson JJ, Kitmitto A, Galli G, Humphries MJ, et al. Quantitative proteomics and single-nucleus transcriptomics of the sinus node elucidates the foundation of cardiac pacemaking. *Nat Commun*. 2019;10:2889. doi: 10.1038/s41467-019-10709-9
168. Nakayama T, Kurachi Y, Noma A, Irisawa H. Action potential and membrane currents of single pacemaker cells of the rabbit heart. *Pflügers Arch*. 1984;402:248–257. doi: 10.1007/BF00585507
169. Ophof T, de Jonge B, Masson-Pevet M, Jongsma HJ, Bouman LN. Functional and morphological organization of the cat sinoatrial node. *J Mol Cell Cardiol*. 1986;18:1015–1031. doi: 10.1016/s0022-2828(86)80290-5
170. Fan JS, Palade P. Perforated patch recording with beta-escin. *Pflügers Arch*. 1998;436:1021–1023. doi: 10.1007/pl00008086
171. Ishibashi H, Moorhouse AJ, Nabekura J. Perforated whole-cell patch-clamp technique: a user's guide. *Patch clamp techniques*. 2012;436:71–83. doi: 10.1007/978-4-431-53993-3_4
172. Harzheim D, Pfeiffer KH, Fabritz L, Kremmer E, Buch T, Waisman A, Kirchhof P, Kaupp UB, Seifert R. Cardiac pacemaker function of HCN4 channels in mice is confined to embryonic development and requires cyclic AMP. *EMBO J*. 2008;27:692–703. doi: 10.1038/emboj.2008.3
173. Ren L, Thai PN, Gopireddy RR, Timofeyev V, Ledford HA, Woltz RL, Park S, Puglisi JL, Moreno CM, Santana LF, et al. Adenylyl cyclase isoform 1 contributes to sinoatrial node automaticity via functional microdomains. *JCI Insight*. 2022;7:e162602. doi: 10.1172/jci.insight.162602
174. Vinogradova TM, Zhou YY, Bogdanov KY, Yang D, Kuschel M, Cheng H, Xiao RP. Sinoatrial node pacemaker activity requires Ca^{2+} /calmodulin-dependent protein kinase II activation. *Circ Res*. 2000;87:760–767. doi: 10.1161/01.res.87.9.760
175. Brown HF, DiFrancesco D, Noble SJ. How does adrenaline accelerate the heart? *Nature*. 1979;280:235–236. doi: 10.1038/280235a0
176. Zagotta WN, Olivier NB, Black KD, Young EC, Olson R, Gouaux E. Structural basis for modulation and agonist specificity of HCN pacemaker channels. *Nature*. 2003;425:200–205. doi: 10.1038/nature01922
177. Peters CH, Rickert C, Morotti S, Grandi E, Aronow KA, Beam KG, Proenza C. The funny current I_f is essential for the fight-or-flight response in cardiac pacemaker cells. *J Gen Physiol*. 2022;154:e202213193. doi: 10.1085/jgp.202213193
178. Stieber J, Herrmann S, Feil S, Loster J, Feil R, Biel M, Hofmann F, Ludwig A. The hyperpolarization-activated channel HCN4 is required for the generation of pacemaker action potentials in the embryonic heart. *Proc Natl Acad Sci USA*. 2003;100:15235–15240. doi: 10.1073/pnas.2434235100
179. Behar J, Ganesan A, Zhang J, Yaniv Y. The autonomic nervous system regulates the heart rate through cAMP-PKA dependent and independent coupled-clock pacemaker cell mechanisms. *Front Physiol*. 2016;7:419. doi: 10.3389/fphys.2016.00419
180. Li Y, Wang F, Zhang X, Qi Z, Tang M, Szeto C, Li Y, Zhang H, Chen X. β -adrenergic stimulation increases $\text{Ca}_v3.1$ activity in cardiac myocytes through protein kinase A. *PLoS One*. 2012;7:e39965. doi: 10.1371/journal.pone.0039965
181. Zhang Y, Jiang X, Snutch TP, Tao J. Modulation of low-voltage-activated T-type Ca^{2+} channels. *Biochim Biophys Acta*. 2013;1828:1550–1559. doi: 10.1016/j.bbamem.2012.08.032
182. Zaveri S, Srivastava U, Qu YS, Chahine M, Boutjdir M. Pathophysiology of $\text{Ca}_v1.3$ L-type calcium channels in the heart. *Front Physiol*. 2023;14:1144069. doi: 10.3389/fphys.2023.1144069
183. Keef KD, Hume JR, Zhong J. Regulation of cardiac and smooth muscle Ca^{2+} channels ($\text{Ca}_v1.2a,b$) by protein kinases. *Am J Physiol Cell Physiol*. 2001;281:C1743–C1756. doi: 10.1152/ajpcell.2001.281.6.C1743
184. van der Heyden MA, Wijnhoven TJ, Ophof T. Molecular aspects of adrenergic modulation of cardiac L-type Ca^{2+} channels. *Cardiovasc Res*. 2005;65:28–39. doi: 10.1016/j.cardiores.2004.09.028
185. Abriel H. Roles and regulation of the cardiac sodium channel $\text{Na}_v1.5$: recent insights from experimental studies. *Cardiovasc Res*. 2007;76:381–389. doi: 10.1016/j.cardiores.2007.07.019
186. Iqbal SM, Lemmens-Gruber R. Phosphorylation of cardiac voltage-gated sodium channel: potential players with multiple dimensions. *Acta Physiol (Oxf)*. 2019;225:e13210. doi: 10.1111/apha.13210
187. Shan J, Kushnir A, Betzenhauser MJ, Reiken S, Li J, Lehnart SE, Lindegger N, Mongillo M, Mohler PJ, Marks AR. Phosphorylation of the ryanodine receptor mediates the cardiac fight or flight response in mice. *J Clin Invest*. 2010;120:4388–4398. doi: 10.1172/JCI32726
188. MacLennan DH, Kranias EG. Phospholamban: a crucial regulator of cardiac contractility. *Nat Rev Mol Cell Biol*. 2003;4:566–577. doi: 10.1038/nrm1151
189. Gao J, Cohen IS, Mathias RT, Baldo GJ. Regulation of the beta-stimulation of the Na^+/K^+ pump current in guinea-pig ventricular myocytes by a cAMP-dependent PKA pathway. *J Physiol*. 1994;477(Pt 3):373–380. doi: 10.1113/jphysiol.1994.sp020199
190. Lei M, Brown HF, Terrar DA. Modulation of delayed rectifier potassium current, i_K , by isoprenaline in rabbit isolated pacemaker cells. *Exp Physiol*. 2000;85:27–35. doi: 10.1017/s0958067000019151
191. Aziz Q, Li Y, Tinker A. Potassium channels in the sinoatrial node and their role in heart rate control. *Channels*. 2018;12:356–366. doi: 10.1080/19336950.2018.1532255
192. Liu G, Papa A, Katchman AN, Zakharov SI, Roybal D, Hennessey JA, Kushner J, Yang L, Chen BX, Kushnir A, et al. Mechanism of adrenergic $\text{Ca}_v1.2$ stimulation revealed by proximity proteomics. *Nature*. 2020;577:695–700. doi: 10.1038/s41586-020-1947-z

193. Levitan BM, Ahern BM, Aloysius A, Brown L, Wen Y, Andres DA, Satin J. Rad-GTPase contributes to heart rate via L-type calcium channel regulation. *J Mol Cell Cardiol.* 2021;154:60–69. doi: 10.1016/j.jmcc.2021.01.005
194. Papa A, Zakharov SI, Katchman AN, Kushner JS, Chen BX, Yang L, Liu G, Jimenez AS, Eisert RJ, Bradshaw GA, et al. Rad regulation of ca(v)1.2 channels controls cardiac fight-or-flight response. *Nat Cardiovasc Res.* 2022;1:1022–1038. doi: 10.1038/s44161-022-00157-y
195. Grimm M, Brown JH. Beta-adrenergic receptor signaling in the heart: role of CaMKII. *J Mol Cell Cardiol.* 2010;48:322–330. doi: 10.1016/j.jmcc.2009.10.016
196. Wu Y, Anderson ME. CaMKII in sinoatrial node physiology and dysfunction. *Front Pharmacol.* 2014;5:48. doi: 10.3389/fphar.2014.00048
197. Wu Y, Gao Z, Chen B, Koval OM, Singh MV, Guan X, Hund TJ, Kutschke W, Sarma S, Grumbach IM, et al. Calmodulin kinase ii is required for fight or flight sinoatrial node physiology. *Proc Natl Acad Sci U S A.* 2009;106:5972–5977. doi: 10.1073/pnas.0806422106
198. Li Y, Sirenko S, Riordon DR, Yang D, Spurgeon H, Lakatta EG, Vinogradova TM. CaMKII-dependent phosphorylation regulates basal cardiac pacemaker function via modulation of local Ca²⁺ releases. *Am J Physiol Heart Circ Physiol.* 2016;311:H532–H544. doi: 10.1152/ajpheart.00765.2015
199. Narayanan N, Xu A. Phosphorylation and regulation of the Ca(2+)-pumping ATPase in cardiac sarcoplasmic reticulum by calcium/calmodulin-dependent protein kinase. *Basic Res Cardiol.* 1997;92:25–35. doi: 10.1007/BF00794065
200. Bogdanov KY, Maltsev VA, Vinogradova TM, Lyashkov AE, Spurgeon HA, Stern MD, Lakatta EG. Membrane potential fluctuations resulting from submembrane Ca²⁺ releases in rabbit sinoatrial nodal cells impart an exponential phase to the late diastolic depolarization that controls their chronotropic state. *Circ Res.* 2006;99:979–987. doi: 10.1161/01.RES.0000247933.66532.0b
201. Maltsev VA, Lakatta EG. Synergism of coupled subsarcolemmal Ca²⁺ clocks and sarcolemmal voltage clocks confers robust and flexible pacemaker function in a novel pacemaker cell model. *Am J Physiol Heart Circ Physiol.* 2009;296:H594–H615. doi: 10.1152/ajpheart.01118.2008
202. Mattick P, Parrington J, Oda E, Simpson A, Collins T, Terrar D. Ca²⁺-stimulated adenylyl cyclase isoform AC1 is preferentially expressed in guinea-pig sino-atrial node cells and modulates the I(f) pacemaker current. *J Physiol.* 2007;582:1195–1203. doi: 10.1113/jphysiol.2007.133439
203. Robinson RB, Dun W, Boyden PA. Autonomic modulation of sinoatrial node: role of pacemaker current and calcium sensitive adenylyl cyclase isoforms. *Prog Biophys Mol Biol.* 2021;166:22–28. doi: 10.1016/j.pbiomolbio.2020.08.004
204. Azene EM, Xue T, Marban E, Tomaselli GF, Li RA. Non-equilibrium behavior of hcn channels: insights into the role of hcn channels in native and engineered pacemakers. *Cardiovasc Res.* 2005;67:263–273. doi: 10.1016/j.cardiores.2005.03.006
205. Elinder F, Mannikko R, Pandey S, Larsson HP. Mode shifts in the voltage gating of the mouse and human HCN2 and HCN4 channels. *J Physiol.* 2006;575:417–431. doi: 10.1113/jphysiol.2006.110437
206. Mannikko R, Pandey S, Larsson HP, Elinder F. Hysteresis in the voltage dependence of hcn channels: conversion between two modes affects pacemaker properties. *J Gen Physiol.* 2005;125:305–326. doi: 10.1085/jgp.200409130
207. Villalba-Galea CA. Hysteresis in voltage-gated channels. *Channels (Austin).* 2017;11:140–155. doi: 10.1080/19336950.2016.1243190
208. Xiao YF, Chandler N, Dobrzynski H, Richardson ES, Tenbroek EM, Wilhelm JJ, Sharma V, Varghese A, Boyett MR, Iuzzo PA, et al. Hysteresis in human HCN4 channels: a crucial feature potentially affecting sinoatrial node pacemaking. *Sheng Li Xue Bao.* 2010;62:1–13.
209. Ho SY, Sanchez-Quintana D. Anatomy and pathology of the sinus node. *J Interv Card Electrophysiol.* 2016;46:3–8. doi: 10.1007/s10840-015-0049-6
210. Verheijck EE, Wilders R, Bouman LN. Atrio-sinus interaction demonstrated by blockade of the rapid delayed rectifier current. *Circulation.* 2002;105:880–885. doi: 10.1161/hc0702.104128
211. Pauza DH, Rysevaite K, Inokaitis H, Jokubauskas M, Pauza AG, Brack KE, Pauziene N. Innervation of sinoatrial nodal cardiomyocytes in mouse. A combined approach using immunofluorescent and electron microscopy. *J Mol Cell Cardiol.* 2014;75:188–197. doi: 10.1016/j.jmcc.2014.07.016
212. Camelliti P, Green CR, LeGrice I, Kohl P. Fibroblast network in rabbit sinoatrial node: structural and functional identification of homogeneous and heterogeneous cell coupling. *Circ Res.* 2004;94:828–835. doi: 10.1161/01.RES.0000122382.19400.14
213. Hulsmans M, Clauss S, Xiao L, Aguirre AD, King KR, Hanley A, Hucker WJ, Wulfers EM, Seemann G, Courties G, et al. Macrophages facilitate electrical conduction in the heart. *Cell.* 2017;169:510–522.e20. doi: 10.1016/j.cell.2017.03.050
214. Grainger N, Santana LF. The central brain of the heart: the sinoatrial node. *JACC Clin Electrophysiol.* 2022;8:1216–1218. doi: 10.1016/j.jacep.2022.08.016
215. Zhou B. Sinoatrial node pacemaker cells: cardiomyocyte-or neuron-like cells? *Protein Cell.* 2021;12:518–519. doi: 10.1007/s13238-021-00827-w
216. Liang D, Xue Z, Xue J, Xie D, Xiong K, Zhou H, Zhang F, Su X, Wang G, Zou Q, et al. Sinoatrial node pacemaker cells share dominant biological properties with glutamatergic neurons. *Protein Cell.* 2021;12:545–556. doi: 10.1007/s13238-020-00820-9
217. Boyett MR, Inada S, Yoo S, Li J, Liu J, Tellez J, Greener ID, Honjo H, Billeter R, Lei M, et al. Connexins in the sinoatrial and atrioventricular nodes. *Adv Cardiol.* 2006;42:175–197. doi: 10.1159/000092569
218. Kohl P, Kamkin AG, Kiseleva IS, Noble D. Mechanosensitive fibroblasts in the sino-atrial node region of rat heart: interaction with cardiomyocytes and possible role. *Exp Physiol.* 1994;79:943–956. doi: 10.1113/expphysiol.1994.sp003819
219. Jalife J. Mutual entrainment and electrical coupling as mechanisms for synchronous firing of rabbit sino-atrial pace-maker cells. *J Physiol.* 1984;356:221–243. doi: 10.1113/jphysiol.1984.sp015461
220. Jalife J, Moe GK. Phasic effects of vagal stimulation on pacemaker activity of the isolated sinus node of the young cat. *Circ Res.* 1979;45:595–608. doi: 10.1161/01.res.45.5.595
221. Michaels DC, Matyas EP, Jalife J. Mechanisms of sinoatrial pacemaker synchronization: a new hypothesis. *Circ Res.* 1987;61:704–714. doi: 10.1161/01.res.61.5.704
222. Michaels DC, Matyas EP, Jalife J. Dynamic interactions and mutual synchronization of sinoatrial node pacemaker cells. A mathematical model. *Circ Res.* 1986;58:706–720. doi: 10.1161/01.res.58.5.706
223. Verheijck EE, Wilders R, Joyner RW, Golod DA, Kumar R, Jongasma HJ, Bouman LN, van Ginneken AC. Pacemaker synchronization of electrically coupled rabbit sinoatrial node cells. *J Gen Physiol.* 1998;111:95–112. doi: 10.1085/jgp.111.1.95
224. Wahl-Schott C, Fenske S, Biel M. Hcn channels: new roles in sinoatrial node function. *Curr Opin Pharmacol.* 2014;15:83–90. doi: 10.1016/j.coph.2013.12.005
225. Fedorov VV, Hucker WJ, Dobrzynski H, Rosenshtraukh LV, Efimov IR. Postganglionic nerve stimulation induces temporal inhibition of excitability in rabbit sinoatrial node. *Am J Physiol Heart Circ Physiol.* 2006;291:H612–H623. doi: 10.1152/ajpheart.00022.2006
226. Li N, Hansen BJ, Csepe TA, Zhao J, Ignozzi AJ, Sul LV, Zakharkin SO, Kalyanasundaram A, Davis JP, Biesiadecki BJ, et al. Redundant and diverse intranodal pacemakers and conduction pathways protect the human sinoatrial node from failure. *Sci Transl Med.* 2017;9:eam5607. doi: 10.1126/scitranslmed.aam5607
227. Clancy CE, Santana LF. Evolving discovery of the origin of the heartbeat: a new perspective on sinus rhythm. *JACC Clin Electrophysiol.* 2020;6:932–934. doi: 10.1016/j.jacep.2020.07.002
228. Grainger N, Santana LF. The inferior sinoatrial node suffers the most during heart failure. *JACC Clin Electrophysiol.* 2022;8:1354–1356. doi: 10.1016/j.jacep.2022.09.001
229. Maltsev VA, Stern MD. The paradigm shift: heartbeat initiation without “the pacemaker cell”. *Front Physiol.* 2022;13:1090162. doi: 10.3389/fphys.2022.1090162
230. De Ponti R, Marazzato J, Bagliani G, Leonelli FM, Padeletti L. Sick sinus syndrome. *Card Electrophysiol Clin.* 2018;10:183–195. doi: 10.1016/j.ccep.2018.02.002
231. Dobrzynski H, Boyett MR, Anderson RH. New insights into pacemaker activity: promoting understanding of sick sinus syndrome. *Circulation.* 2007;115:1921–1932. doi: 10.1161/CIRCULATIONAHA.106.616011
232. Hawks MK, Paul MLB, Malu OO. Sinus node dysfunction. *Am Fam Physician.* 2021;104:179–185.
233. Wallace MJ, El Refaey M, Mesirca P, Hund TJ, Mangoni ME, Mohler RJ. Genetic complexity of sinoatrial node dysfunction. *Front Genet.* 2021;12:654925. doi: 10.3389/fgene.2021.654925
234. Goldberger JJ, Arora R, Buckley U, Shivkumar K. Autonomic nervous system dysfunction: JACC focus seminar. *J Am Coll Cardiol.* 2019;73:1189–1206. doi: 10.1016/j.jacc.2018.12.064
235. Cierpka-Kmiec K, Hering DT. The hidden cardiovascular risk factor in uncomplicated arterial hypertension. *Cardiol J.* 2020;27:857–867. doi: 10.5603/CJ.a.2019.0021
236. Kusumoto FM, Schoenfeld MH, Barrett C, Edgerton JR, Ellenbogen KA, Gold MR, Goldschlager NF, Hamilton RM, Joglar JA, Kim RJ, et al. 2018

- ACC/AHA/HRS guideline on the evaluation and management of patients with bradycardia and cardiac conduction delay: a report of the American College of Cardiology/American Heart Association Task Force on Clinical Practice Guidelines and the Heart Rhythm Society. *J Am Coll Cardiol*. 2019;74:e51–e156. doi: 10.1016/j.jacc.2018.10.044
237. van der Maarel LE, Postma AV, Christoffels VM. Genetics of sinoatrial node function and heart rate disorders. *Dis Model Mech*. 2023;16:dmm050101. doi: 10.1242/dmm.050101
238. Verkerk AO, Wilders R. The action potential clamp technique as a tool for risk stratification of sinus bradycardia due to loss-of-function mutations in HCN4: an in silico exploration based on in vitro and in vivo data. *Biomedicines*. 2023;11:2447. doi: 10.3390/biomedicines11092447
239. Milano A, Vermeer AM, Lodder EM, Barc J, Verkerk AO, Postma AV, van der Bilt IA, Baars MJ, van Haelst PL, Caliskan K, et al. HCN4 mutations in multiple families with bradycardia and left ventricular non-compaction cardiomyopathy. *J Am Coll Cardiol*. 2014;64:745–756. doi: 10.1016/j.jacc.2014.05.045
240. Sedmera D, Pexieder T, Vuillemin M, Thompson RP, Anderson RH. Developmental patterning of the myocardium. *Anat Rec*. 2000;258:319–337. doi: 10.1002/(SICI)1097-0185(20000401)258:4<319::AID-AR1>3.0.CO;2-O
241. Schweizer PA, Schroter J, Greiner S, Haas J, Yampolsky P, Mereles D, Buss SJ, Seyler C, Bruehl C, Draguhn A, et al. The symptom complex of familial sinus node dysfunction and myocardial noncompaction is associated with mutations in the HCN4 channel. *J Am Coll Cardiol*. 2014;64:757–767. doi: 10.1016/j.jacc.2014.06.1155
242. Schweizer PA, Yampolsky P, Malik R, Thomas D, Zehelein J, Katus HA, Koenen M. Transcription profiling of HCN-channel isoatypes throughout mouse cardiac development. *Basic Res Cardiol*. 2009;104:621–629. doi: 10.1007/s00395-009-0031-5
243. Spater D, Abramczuk MK, Buac K, Zangi L, Stachel MW, Clarke J, Sahara M, Ludwig A, Chien KR. A HCN4+ cardiomyogenic progenitor derived from the first heart field and human pluripotent stem cells. *Nat Cell Biol*. 2013;15:1098–1106. doi: 10.1038/ncb2824
244. Ishikawa T, Ohno S, Murakami T, Yoshida K, Mishima H, Fukuoka T, Kimoto H, Sakamoto R, Ohkusa T, Aiba T, et al. Sick sinus syndrome with hcn4 mutations shows early onset and frequent association with atrial fibrillation and left ventricular noncompaction. *Heart Rhythm*. 2017;14:717–724. doi: 10.1016/j.hrthm.2017.01.020
245. Balducci V, Credi C, Sacconi L, Romanelli MN, Sartiani L, Cerbai E. The HCN channel as a pharmacological target: why, where, and how to block it. *Prog Biophys Mol Biol*. 2021;166:173–181. doi: 10.1016/j.pbiomolbio.2021.07.010
246. Postea O, Biel M. Exploring HCN channels as novel drug targets. *Nat Rev Drug Discov*. 2011;10:903–914. doi: 10.1038/nrd3576
247. Santoro B, Shah MM. Hyperpolarization-activated cyclic nucleotide-gated channels as drug targets for neurological disorders. *Annu Rev Pharmacol Toxicol*. 2020;60:109–131. doi: 10.1146/annurev-pharmtox-010919-023356
248. Ku SM, Han MH. HCN channel targets for novel antidepressant treatment. *Neurotherapeutics*. 2017;14:698–715. doi: 10.1007/s13311-017-0538-7
249. Ramirez D, Zuniga R, Concha G, Zuniga L. HCN channels: new therapeutic targets for pain treatment. *Molecules*. 2018;23:2094. doi: 10.3390/molecules23092094
250. Kharouf Q, Phillips AM, Bleakley LE, Morrisroe E, Oyrer J, Jia L, Ludwig A, Jin L, Nicolazzo JA, Cerbai E, et al. The hyperpolarization-activated cyclic nucleotide-gated 4 channel as a potential anti-seizure drug target. *Br J Pharmacol*. 2020;177:3712–3729. doi: 10.1111/bph.15088
251. Novella Romanelli M, Sartiani L, Masi A, Mannaioni G, Manetti D, Mugelli A, Cerbai E. HCN channels modulators: the need for selectivity. *Curr Top Med Chem*. 2016;16:1764–1791. doi: 10.2174/1568026616999160315130832
252. Chen SJ, Xu Y, Liang YM, Cao Y, Lv JY, Pang JX, Zhou PZ. Identification and characterization of a series of novel hcn channel inhibitors. *Acta Pharmacol Sin*. 2019;40:746–754. doi: 10.1038/s41401-018-0162-z
253. Dini L, Del Lungo M, Resta F, Melchiorre M, Spinelli V, Di Cesare Mannelli L, Ghelardini C, Laurino A, Sartiani L, Coppini R, et al. Selective blockade of HCN1/HCN2 channels as a potential pharmacological strategy against pain. *Front Pharmacol*. 2018;9:1252. doi: 10.3389/fphar.2018.01252
254. Kharouf Q, Pinares-Garcia P, Romanelli MN, Reid CA. Testing broad-spectrum and isoform-preferring HCN channel blockers for anti-convulsant properties in mice. *Epilepsy Res*. 2020;168:106484. doi: 10.1016/j.eplepsyres.2020.106484
255. Harde E, Hierl M, Weber M, Waiz D, Wylter R, Wach JY, Haab R, Gundlfinger A, He W, Schneider P, et al. Selective and brain-penetrant hcn1 inhibitors reveal links between synaptic integration, cortical function, and working memory. *Cell Chem Biol*. 2023;31:577–592.e23. doi: 10.1016/j.chembiol.2023.11.004
256. Han Y, Lyman KA, Foote KM, Chetkovich DM. The structure and function of TRIP8b, an auxiliary subunit of hyperpolarization-activated cyclic-nucleotide gated channels. *Channels*. 2020;14:110–122. doi: 10.1080/19336950.2020.1740501
257. Saponaro A, Pauleta SR, Cantini F, Matzapetakis M, Hammann C, Donadoni C, Hu L, Thiel G, Banci L, Santoro B, et al. Structural basis for the mutual antagonism of cAMP and TRIP8b in regulating HCN channel function. *Proc Natl Acad Sci U S A*. 2014;111:14577–14582. doi: 10.1073/pnas.1410389111
258. Peters CH, Singh RK, Bankston JR, Proenza C. Regulation of HCN channels by protein interactions. *Front Physiol*. 2022;13:928507. doi: 10.3389/fphys.2022.928507
259. Santoro B, Wainger BJ, Siegelbaum SA. Regulation of HCN channel surface expression by a novel C-terminal protein-protein interaction. *J Neurosci*. 2004;24:10750–10762. doi: 10.1523/JNEUROSCI.3300-04.2004
260. Han Y, Iyama ID, Clutter MR, Mishra RK, Lyman KA, Zhou C, Michailidis I, Xia MY, Sharma H, Luan CH, et al. Discovery of a small-molecule inhibitor of the TRIP8b-HCN interaction with efficacy in neurons. *J Biol Chem*. 2022;298:102069. doi: 10.1016/j.jbc.2022.102069
261. Saponaro A, Cantini F, Porro A, Bucchi A, DiFrancesco D, Maione V, Donadoni C, Introini B, Mesirca P, Mangoni ME, et al. A synthetic peptide that prevents cAMP regulation in mammalian hyperpolarization-activated cyclic nucleotide-gated (HCN) channels. *Elife*. 2018;7:e35753. doi: 10.7554/eLife.35753
262. Chen M, Wu Q. Roles and mechanisms of natural drugs on sinus node dysfunction. *Biomed Pharmacother*. 2023;164:114777. doi: 10.1016/j.biopha.2023.114777
263. Depuydt AS, Peigneur S, Tytgat JR. Hcn channels in the heart. *Curr Cardiol Rev*. 2022;18:e040222200836. doi: 10.2174/1573403X18666220204142436
264. Liu R, Li J, Liu Y, Peng J, Guan X. The effect of astragaloside on pacemaker current and the cytoskeleton in rabbit sinoatrial node cells under the ischemia and reperfusion condition. *Front Pharmacol*. 2018;9:551. doi: 10.3389/fphar.2018.00551
265. Piantoni C, Paina M, Molla D, Liu S, Bertoli G, Jiang H, Wang Y, Wang Y, Wang Y, DiFrancesco D, et al. Chinese natural compound decreases pacemaker regulation of f-channels. *Elife*. 2022;11:e75119. doi: 10.7554/eLife.75119
266. Zhang JC, Xie XT, Chen Q, Zou T, Hong-Lin W, Zhu C, Dong Y, Ye L, Li Y, Zhu PL. The effect of forskolin on membrane clock and calcium clock in the hypoxic/reoxygenation of sinoatrial node cells and its mechanism. *Pharmacol Rep*. 2020;72:1706–1716. doi: 10.1007/s43440-020-00094-2
267. Chaudhary R, Garg J, Krishnamoorthy P, Shah N, Lian G, Martinez MW, Freudenberger RI. Heart failure and beyond. *J Cardiovasc Pharmacol Ther*. 2016;21:335–343. doi: 10.1177/1074248415624157
268. Iness AN, Shah KM, Kukreja RC. Physiological effects of ivabradine in heart failure and beyond. *Mol Cell Biochem*. 2023. doi: 10.1007/s11010-023-04862-5
269. Koruth JS, Lala A, Pinney S, Reddy VY, Dukkupati SR. The clinical use of ivabradine. *J Am Coll Cardiol*. 2017;70:1777–1784. doi: 10.1016/j.jacc.2017.08.038
270. Psotka MA, Teerlink JR. Ivabradine: role in the chronic heart failure armamentarium. *Circulation*. 2016;133:2066–2075. doi: 10.1161/CIRCULATIONAHA.115.018094
271. Savelieva I, Camm AJ. I f inhibition with ivabradine: electrophysiological effects and safety. *Drug Saf*. 2008;31:95–107. doi: 10.2165/00002018-200831020-00001
272. Chen C, Kaur G, Mehta PK, Morrone D, Godoy LC, Bangalore S, Sidhu MS. Ivabradine in cardiovascular disease management revisited: a review. *Cardiovasc Drugs Ther*. 2021;35:1045–1056. doi: 10.1007/s10557-020-07124-4
273. Das D, Savarese G, Dahlstrom U, Fu M, Howlett J, Ezekowitz JA, Lund LH. Ivabradine in heart failure: the representativeness of SHIFT (Systolic Heart Failure Treatment With the If Inhibitor Ivabradine Trial) in a broad population of patients with chronic heart failure. *Circ Heart Fail*. 2017;10:e004112. doi: 10.1161/CIRCHEARTFAILURE.117.004112
274. Ide T, Ohtani K, Higo T, Tanaka M, Kawasaki Y, Tsutsui H. Ivabradine for the treatment of cardiovascular diseases. *Circ J*. 2019;83:252–260. doi: 10.1253/circj.CJ-18-1184
275. Knuuti J, Wijns W, Saraste A, Capodanno D, Barbato E, Funck-Brentano C, Prescott E, Storey RF, Deaton C, Cuisset T, et al. 2019 ESC guidelines for the diagnosis and management of chronic coronary syndromes. *Eur Heart J*. 2020;41:407–477. doi: 10.1093/eurheartj/ehz425

276. Task Force M, Montalescot G, Sechtem U, Achenbach S, Andreotti F, Arden C, Budaj A, Bugiardini R, Crea F, Cuisset T, et al. 2013 ESC guidelines on the management of stable coronary artery disease: the task force on the management of stable coronary artery disease of the European Society of Cardiology. *Eur Heart J*. 2013;34:2949–3003. doi: 10.1093/eurheartj/ehd296
277. Bucchi A, Barbuti A, Baruscotti M, DiFrancesco D. Heart rate reduction via selective ‘funny’ channel blockers. *Curr Opin Pharmacol*. 2007;7:208–213. doi: 10.1016/j.coph.2006.09.005
278. Bucchi A, Baruscotti M, Robinson RB, DiFrancesco D. Modulation of rate by autonomic agonists in san cells involves changes in diastolic depolarization and the pacemaker current. *J Mol Cell Cardiol*. 2007;43:39–48. doi: 10.1016/j.yjmcc.2007.04.017
279. Bucchi A, Tognati A, Milanese R, Baruscotti M, DiFrancesco D. Properties of ivabradine-induced block of hcn1 and hcn4 pacemaker channels. *J Physiol*. 2006;572:335–346. doi: 10.1113/jphysiol.2005.100776
280. Bucchi A, Baruscotti M, DiFrancesco D. Current-dependent block of rabbit sino-atrial node I(f) channels by ivabradine. *J Gen Physiol*. 2002;120:1–13. doi: 10.1085/jgp.20028593
281. Thollon C, Bedut S, Villeneuve N, Coge F, Piffard L, Guillaumin JP, Brunel-Jacquemin C, Chomarat P, Boutin JA, Peglion JL, et al. Use-dependent inhibition of hHCN4 by ivabradine and relationship with reduction in pacemaker activity. *Br J Pharmacol*. 2007;150:37–46. doi: 10.1038/sj.bjp.0706940
282. Fox K, Ford I, Steg PG, Tendera M, Ferrari R, Investigators B. Ivabradine for patients with stable coronary artery disease and left-ventricular systolic dysfunction (beautiful): a randomised, double-blind, placebo-controlled trial. *Lancet*. 2008;372:807–816. doi: 10.1016/S0140-6736(08)61170-8
283. Swedberg K, Komajda M, Bohm M, Borer JS, Ford I, Dubost-Brama A, Lerebours G, Tavazzi L, Investigators S. Ivabradine and outcomes in chronic heart failure (SHIFT): a randomised placebo-controlled study. *Lancet*. 2010;376:875–885. doi: 10.1016/S0140-6736(10)61198-1
284. Yaniv Y, Maltsev VA, Ziman BD, Spurgeon HA, Lakatta EG. The ‘funny’ current (I_f) inhibition by ivabradine at membrane potentials encompassing spontaneous depolarization in pacemaker cells. *Molecules*. 2012;17:8241–8254. doi: 10.3390/molecules17078241
285. Haechl N, Ebner J, Hilber K, Todt H, Koenig X. Pharmacological profile of the bradycardic agent ivabradine on human cardiac ion channels. *Cell Physiol Biochem*. 2019;53:36–48. doi: 10.33594/000000119
286. Lees-Miller JP, Guo J, Wang Y, Perissinotti LL, Noskov SY, Duff HJ. Ivabradine prolongs phase 3 of cardiac repolarization and blocks the hERG1 (KCNH2) current over a concentration-range overlapping with that required to block HCN4. *J Mol Cell Cardiol*. 2015;85:71–78. doi: 10.1016/j.yjmcc.2015.05.009
287. Melgari D, Brack KE, Zhang C, Zhang Y, El Harchi A, Mitcheson JS, Dempsey CE, Ng GA, Hancox JC. hERG potassium channel blockade by the HCN channel inhibitor bradycardic agent ivabradine. *J Am Heart Assoc*. 2015;4:e001813. doi: 10.1161/JAHA.115.001813
288. Karimi T, Pan Z, Potaman VN, Alt EU. Conversion of unmodified stem cells to pacemaker cells by overexpression of key developmental genes. *Cells*. 2023;12:1381. doi: 10.3390/cells12101381
289. Komosa ER, Wolfson DW, Bressan M, Cho HC, Ogle BM. Implementing biological pacemakers: design criteria for successful. *Circ Arrhythm Electrophysiol*. 2021;14:e009957. doi: 10.1161/CIRCEP.121.009957
290. Liu CM, Chen YC, Hu YF. Harnessing cell reprogramming for cardiac biological pacing. *J Biomed Sci*. 2023;30:74. doi: 10.1186/s12929-023-00970-y
291. Naumova N, Iop L. Bioengineering the cardiac conduction system: advances in cellular, gene, and tissue engineering for heart rhythm regeneration. *Front Bioeng Biotechnol*. 2021;9:673477. doi: 10.3389/fbioe.2021.673477
292. Zhang W, Wang F, Yin L, Tang Y, Wang X, Huang C. Cadherin-5 facilitated the differentiation of human induced pluripotent stem cells into sinoatrial node-like pacemaker cells by regulating beta-catenin. *J Cell Physiol*. 2024;239:212–226. doi: 10.1002/jcp.31161
293. Bucchi A, Plotnikov AN, Shlapakova I, Danilo P Jr, Kryukova Y, Qu J, Lu Z, Liu H, Pan Z, Potapova I, et al. Wild-type and mutant HCN channels in a tandem biological-electronic cardiac pacemaker. *Circulation*. 2006;114:992–999. doi: 10.1161/CIRCULATIONAHA.106.617613
294. Plotnikov AN, Sosunov EA, Qu J, Shlapakova IN, Anyukhovsky EP, Liu L, Janse MJ, Brink PR, Cohen IS, Robinson RB, et al. Biological pacemaker implanted in canine left bundle branch provides ventricular escape rhythms that have physiologically acceptable rates. *Circulation*. 2004;109:506–512. doi: 10.1161/01.CIR.0000114527.10764.CC
295. Qu J, Plotnikov AN, Danilo P Jr, Shlapakova I, Cohen IS, Robinson RB, Rosen MR. Expression and function of a biological pacemaker in canine heart. *Circulation*. 2003;107:1106–1109. doi: 10.1161/01.cir.0000059939.97249.2c
296. Tse HF, Xue T, Lau CP, Siu CW, Wang K, Zhang QY, Tomaselli GF, Akar FG, Li RA. Bioartificial sinus node constructed via in vivo gene transfer of an engineered pacemaker HCN channel reduces the dependence on electronic pacemaker in a sick-sinus syndrome model. *Circulation*. 2006;114:1000–1011. doi: 10.1161/circulationaha.106.615385
297. Boink GJ, Verkerk AO, van Amersfoort SC, Tasseron SJ, van der Rijt R, Bakker D, Linnenbank AC, van der Meulen J, de Bakker JM, Seppen J, et al. Engineering physiologically controlled pacemaker cells with lentiviral HCN4 gene transfer. *J Gene Med*. 2008;10:487–497. doi: 10.1002/jgm.1172
298. Zhou YF, Yang XJ, Li HX, Han LH, Jiang WP. Genetically-engineered mesenchymal stem cells transfected with human HCN1 gene to create cardiac pacemaker cells. *J Int Med Res*. 2013;41:1570–1576. doi: 10.1177/0300060513501123
299. Cho HC, Kashiwakura Y, Marban E. Creation of a biological pacemaker by cell fusion. *Circ Res*. 2007;100:1112–1115. doi: 10.1161/01.RES.0000265845.04439.78
300. Lu W, Yaoming N, Boli R, Jun C, Changhai Z, Yang Z, Zhiyuan S. mHCN4 genetically modified canine mesenchymal stem cells provide biological pacemaking function in complete dogs with atrioventricular block. *Pacing Clin Electrophysiol*. 2013;36:1138–1149. doi: 10.1111/pace.12154
301. Nong Y, Zhang C, Wei L, Zhang Z, Cheng J, Wen L, Song Z. In situ investigation of allografted mouse HCN4 gene-transfected rat bone marrow mesenchymal stromal cells with the use of patch-clamp recording of ventricular slices. *Cytotherapy*. 2013;15:905–919. doi: 10.1016/j.jcyt.2013.03.010
302. Zhang Z, Song Z, Cheng J, Nong Y, Wei L, Zhang C. The integration and functional evaluation of rabbit pacing cells transplanted into the left ventricular free wall. *Int J Med Sci*. 2012;9:513–520. doi: 10.7150/ijms.4971
303. Plotnikov AN, Shlapakova I, Szabolcs MJ, Danilo P Jr, Lorell BH, Potapova IA, Lu Z, Rosen AB, Mathias RT, Brink PR, et al. Xenografted adult human mesenchymal stem cells provide a platform for sustained biological pacemaker function in canine heart. *Circulation*. 2007;116:706–713. doi: 10.1161/CIRCULATIONAHA.107.703231
304. Boink GJ, Duan L, Nearing BD, Shlapakova IN, Sosunov EA, Anyukhovsky EP, Bobkov E, Kryukova Y, Ozgen N, Danilo P Jr, et al. HCN2/SKM1 gene transfer into canine left bundle branch induces stable, autonomously responsive biological pacing at physiological heart rates. *J Am Coll Cardiol*. 2013;61:1192–1201. doi: 10.1016/j.jacc.2012.12.031
305. Boink GJ, Nearing BD, Shlapakova IN, Duan L, Kryukova Y, Bobkov E, Tan HL, Cohen IS, Danilo P Jr, Robinson RB, et al. Ca²⁺-stimulated adenylyl cyclase AC1 generates efficient biological pacing as single gene therapy and in combination with HCN2. *Circulation*. 2012;126:528–536. doi: 10.1161/CIRCULATIONAHA.111.083584
306. Cingolani E, Yee K, Shehata M, Chugh SS, Marban E, Cho HC. Biological pacemaker created by percutaneous gene delivery via venous catheters in a porcine model of complete heart block. *Heart Rhythm*. 2012;9:1310–1318. doi: 10.1016/j.hrthm.2012.04.020
307. Piron J, Quang KL, Briec F, Amirault JC, Leoni AL, Desigaux L, Escande D, Pitard B, Charpentier F. Biological pacemaker engineered by nonviral gene transfer in a mouse model of complete atrioventricular block. *Mol Ther*. 2008;16:1937–1943. doi: 10.1038/mt.2008.209
308. Vegh AMD, Verkerk AO, Cocera Ortega L, Wang J, Geerts D, Klerk M, Lodder K, Nobel R, Tijssen AJ, Devalla HD, et al. Toward biological pacing by cellular delivery of Hcn2/SKM1. *Front Physiol*. 2020;11:588679. doi: 10.3389/fphys.2020.58867
309. Raghunathan S, Islas JF, Mistretta B, Iyer D, Shi L, Gunaratne PH, Ko G, Schwartz RJ, McConnell BK. Conversion of human cardiac progenitor cells into cardiac pacemaker-like cells. *J Mol Cell Cardiol*. 2020;138:12–22. doi: 10.1016/j.yjmcc.2019.09.015
310. Bakker ML, Boink GJ, Boukens BJ, Verkerk AO, van den Boogaard M, den Haan AD, Hoogaars WM, Buermans HP, de Bakker JM, Seppen J, et al. T-box transcription factor TBX3 reprogrammes mature cardiac myocytes into pacemaker-like cells. *Cardiovasc Res*. 2012;94:439–449. doi: 10.1093/cvr/cvs120
311. Frank DU, Carter KL, Thomas KR, Burr RM, Bakker ML, Coetzee WA, Tristani-Firouzi M, Bamshad MJ, Christoffels VM, Moon AM. Lethal arrhythmias in Tbx3-deficient mice reveal extreme dosage sensitivity of cardiac conduction system function and homeostasis. *Proc Natl Acad Sci U S A*. 2012;109:E154–E163. doi: 10.1073/pnas.1115165109
312. Kapoor N, Galang G, Marban E, Cho HC. Transcriptional suppression of connexin43 by TBX18 undermines cell-cell electrical coupling in postnatal cardiomyocytes. *J Biol Chem*. 2011;286:14073–14079. doi: 10.1074/jbc.M110.185298

313. Kapoor N, Liang W, Marban E, Cho HC. Direct conversion of quiescent cardiomyocytes to pacemaker cells by expression of Tbx18. *Nat Biotechnol*. 2013;31:54–62. doi: 10.1038/nbt.2465
314. Sanchez L, Mesquita T, Zhang R, Liao K, Rogers R, Lin YN, Miguel-Dos-Santos R, Akhmerov A, Li L, Nawaz A, et al. MicroRNA-dependent suppression of biological pacemaker activity induced by TBX18. *Cell Rep Med*. 2022;3:100871. doi: 10.1016/j.xcrm.2022.100871
315. Cámara-Checa A, Perin F, Rubio-Alarcón M, Dago M, Crespo-García T, Rapún J, Marín M, Cebrián J, Gómez R, Bermúdez-Jiménez F, et al. A gain-of-function HCN4 mutant in the HCN domain is responsible for inappropriate sinus tachycardia in a Spanish family. *Proc Natl Acad Sci U S A*. 2023;120:e2305135120. doi: 10.1073/pnas.2305135120
316. Macri V, Mahida SN, Zhang ML, Sinner MF, Dolmatova EV, Tucker NR, McLellan M, Shea MA, Milan DJ, Lunetta KL, et al. A novel trafficking-defective hcn4 mutation is associated with early-onset atrial fibrillation. *Heart Rhythm*. 2014;11:1055–1062. doi: 10.1016/j.hrthm.2014.03.002
317. Alonso-Fernandez-Gatta M, Gallego-Delgado M, Caballero R, Villacorta E, Diaz-Pelaez E, Garcia-Berroca LB, Crespo-Garcia T, Plata-Izquierdo B, Marcos-Vadillo E, Garcia-Cuenllas L, et al. A rare HCN4 variant with combined sinus bradycardia, left atrial dilatation, and hypertrabeculation/left ventricular noncompaction phenotype. *Rev Esp Cardiol (Engl Ed)*. 2021;74:781–789. doi: 10.1016/j.rec.2020.06.019
318. Moller M, Silbernagel N, Wrobel E, Stallmayer B, Amedonu E, Rinne S, Peischard S, Meuth SG, Wunsch B, Strutz-Seebohm N, et al. In vitro analyses of novel HCN4 gene mutations. *Cell Physiol Biochem*. 2018;49:1197–1207. doi: 10.1159/000493301
319. Verkerk AO, Wilders R. Functional characterization of the A414G loss-of-function mutation in HCN4 associated with sinus bradycardia. *Cardiogenetics*. 2023;13:117–134. doi: 10.3390/cardiogenetics13030012
320. Nof E, Luria D, Brass D, Marek D, Lahat H, Reznik-Wolf H, Pras E, Dascal N, Eldar M, Glikson M. Point mutation in the hcn4 cardiac ion channel pore affecting synthesis, trafficking, and functional expression is associated with familial asymptomatic sinus bradycardia. *Circulation*. 2007;116:463–470. doi: 10.1161/CIRCULATIONAHA.107.706887
321. Paszkowska A, Piekutowska-Abramczuk D, Ciara E, Mirecka-Rola A, Brzezinska M, Wicher D, Kostrzewa G, Sarnecki J, Ziolkowska L. Clinical presentation of left ventricular noncompaction cardiomyopathy and bradycardia in three families carrying HCN4 pathogenic variants. *Genes (Basel)*. 2022;13:477. doi: 10.3390/genes13030477
322. Vermeer AMC, Lodder EM, Thomas D, Duijkers FAM, Marcelis C, van Gorselen EOF, Fortner P, Buss SJ, Mereles D, Katus HA, et al. Dilatation of the aorta ascendens forms part of the clinical spectrum of HCN4 mutations. *J Am Coll Cardiol*. 2016;67:2313–2315. doi: 10.1016/j.jacc.2016.01.086
323. Millat G, Janin A, de Tauriac O, Roux A, Dauphin C. HCN4 mutation as a molecular explanation on patients with bradycardia and non-compaction cardiomyopathy. *Eur J Med Genet*. 2015;58:439–442. doi: 10.1016/j.ejmg.2015.06.004
324. Hanania HL, Regalado ES, Guo DC, Xu L, Demo E, Sallee D, Milewicz DM. Do HCN4 variants predispose to thoracic aortic aneurysms and dissections? *Circ Genom Precis Med*. 2019;12:e002626. doi: 10.1161/CIRCGEN.119.002626
325. Brunet-Garcia L, Odori A, Fell H, Field E, Roberts AM, Starling L, Kaski JP, Cervi E. Noncompaction cardiomyopathy, sick sinus disease, and aortic dilatation: too much for a single diagnosis? *JACC Case Rep*. 2022;4:287–293. doi: 10.1016/j.jaccas.2022.01.013
326. Servatius H, Porro A, Pless SA, Schaller A, Asatryan B, Tanner H, de Marchi SF, Roten L, Seiler J, Haeberlin A, et al. Phenotypic spectrum of hcn4 mutations: a clinical case. *Circ Genom Precis Med*. 2018;11:e002033. doi: 10.1161/CIRCGEN.117.002033
327. Laish-Farkash A, Glikson M, Brass D, Marek-Yagel D, Pras E, Dascal N, Antzelevitch C, Nof E, Reznik H, Eldar M, et al. A novel mutation in the HCN4 gene causes symptomatic sinus bradycardia in Moroccan Jews. *J Cardiovasc Electrophysiol*. 2010;21:1365–1372. doi: 10.1111/j.1540-8167.2010.01844.x
328. Biel S, Aquila M, Hertel B, Berthold A, Neumann T, DiFrancesco D, Moroni A, Thiel G, Kaufenstein S. Mutation in S6 domain of HCN4 channel in patient with suspected Brugada syndrome modifies channel function. *Pflugers Arch*. 2016;468:1663–1671. doi: 10.1007/s00424-016-1870-1
329. Baruscotti M, Bucchi A, Milanese R, Paina M, Barbuti A, Gnecci-Ruscione T, Bianco E, Vitali-Serdoz L, Cappato R, DiFrancesco D. A gain-of-function mutation in the cardiac pacemaker HCN4 channel increasing cAMP sensitivity is associated with familial inappropriate sinus tachycardia. *Eur Heart J*. 2017;38:280–288. doi: 10.1093/eurheartj/ehv582
330. Duhme N, Schweizer PA, Thomas D, Becker R, Schroter J, Barends TR, Schlichting I, Draguhn A, Bruehl C, Katus HA, et al. Altered HCN4 channel C-linker interaction is associated with familial tachycardia-bradycardia syndrome and atrial fibrillation. *Eur Heart J*. 2013;34:2768–2775. doi: 10.1093/eurheartj/ehs391
331. Ueda K, Nakamura K, Hayashi T, Inagaki N, Takahashi M, Arimura T, Morita H, Higashiesato Y, Hirano Y, Yasunami M, et al. Functional characterization of a trafficking-defective HCN4 mutation, D553N, associated with cardiac arrhythmia. *J Biol Chem*. 2004;279:27194–27198. doi: 10.1074/jbc.M311953200
332. Schulze-Bahr E, Neu A, Friederich P, Kaupp UB, Breithardt G, Pongs O, Isbrandt D. Pacemaker channel dysfunction in a patient with sinus node disease. *J Clin Invest*. 2003;111:1537–1545. doi: 10.1172/JCI16387
333. Wang H, Wu T, Huang Z, Huang J, Geng Z, Cui B, Yan Y, Zhang Y, Wang Y. Channel HCN4 mutation R666Q associated with sporadic arrhythmia decreases channel electrophysiological function and increases protein degradation. *J Biol Chem*. 2022;298:102599. doi: 10.1016/j.jbc.2022.102599
334. Milanese R, Baruscotti M, Gnecci-Ruscione T, DiFrancesco D. Familial sinus bradycardia associated with a mutation in the cardiac pacemaker channel. *N Engl J Med*. 2006;354:151–157. doi: 10.1056/NEJMoa052475
335. Schweizer PA, Duhme N, Thomas D, Becker R, Zehelein J, Draguhn A, Bruehl C, Katus HA, Koenen M. cAMP sensitivity of HCN pacemaker channels determines basal heart rate but is not critical for autonomic rate control. *Circ Arrhythm Electrophysiol*. 2010;3:542–552. doi: 10.1161/CIRCEP.110.949768
336. Fabbri A, Fantini M, Wilders R, Severi S. Computational analysis of the human sinus node action potential: model development and effects of mutations. *J Physiol*. 2017;595:2365–2396. doi: 10.1113/JP273259
337. van der Groen O, Tang MF, Wenderoth N, Mattingley JB. Stochastic resonance enhances the rate of evidence accumulation during combined brain stimulation and perceptual decision-making. *PLoS Comput Biol*. 2018;14:e1006301. doi: 10.1371/journal.pcbi.1006301